VOL. II

This work was performed for the Jet Propulsion Laboratory, California Institute of Technology, sponsored by the National Aeronautics and Space Administration under Contract NAS7-100.

ANALYSIS OF POTENTIAL SECONDARY EXPERIMENTS FOR A SOLAR-THERMIONIC FLIGHT TEST VEHICLE

Prepared for

California Institute of Technology
Jet Propulsion Laboratory
4800 Oak Grove Drive
Pasadena, California
Attention: Mr. J. L. Flatley

Contract No. 951162

EOS Report 6761-Final 1 November 1965

VOLUME II — SCIENCE EXPERIMENTS CATALOG

Prepared by Staff
Program Management and Systems Engineering

Approved by

J. Neustein, Manager
PROGRAM MANAGEMENT AND SYSTEMS ENGINEERING

ELECTRO-OPTICAL SYSTEMS, INC. - PASADENA, CALIFORNIA
A Subsidiary of Xerox Corporation

CONTENTS

I	ASTRONOMY	5
	I-A Ultraviolet and Infrared Emission of Stars	8
	I-B Mapping of Galactic Structure in the IR and UV	11
	I-C 0.75 to 1.5 Mc Galactic Radio Noise	16
II	SOLAR PHYSICS	20
	II-A Ultraviolet Imaging of Solar Flares	21
	II-B Search for Solar Neutrons	25
	II-C Detection of Low Energy Solar Gamma Radiation	31
	II-D Solar Coronagraph	37
	II-E Study of Temporal Variations in Solar Ultraviolet Emissions	40
	II-F Infrared Emission From the Sun	50
	II-G Search for Characteristic X-Ray From the Sun	53
	II-H Monitoring of Solar X-Ray Emissions in the Region of 0.2 to 24 Kev	59
	II-I Extreme Ultraviolet Spectrum of the Sun	68
	II-J Profile of Solar Lyman α	73
III	PARTICLES AND FIELDS	75
	III-A Spectra of Galactic Electrons	78
	III-B Study of Earth's Albedo Neutrons	83
	III-C Intensity and Abundance of the Light and Medium Nuclei in Galactic Cosmic Radiation	89
	III-D Trapped Particle Experiment	95
	III-E Detection of High Energy Galactic Gamma Radiation	101
	III-F Proton Dosimeter	107
	III-G Search for Key Galactic Gamma Radiations	116
	III-H Spectrum and Flux of High Energy Galactic Protons	121

CONTENTS (cont'd)

III-I	Low Energy Proton Spectrometry and Differentially [illegible] Solar [illegible]	127
III-J	Satellite Charging and Discharging Characteristics	134
III-K	Ionization Chamber Experiment	139
IV	PLANETARY ATMOSPHERES	145
IV-A	Measurements of Earth Ultraviolet Radiation Flux	146
V	IONOSPHERES AND RADIO PHYSICS	150
V-A	Topside Sounder	152
V-B	Investigation of the Compositions of the Upper Ionosphere	156
VI	PLANETOLOGY	162
VI-A	Photon Emission From Dark Areas of the Moon	163
VI-B	Earth Albedo	165
VI-C	Ultraviolet and Infrared Lunar [illegible]	168
VI-D	Physical Analysis of Micrometeoroids	171
VI-E	Effect of Hypervelocity Impacts on Structural Surfaces	177
VI-F	Chemical Analysis of Carbonaceous Meteoroids	186
VII	BIOSCIENCE	194

1. INTRODUCTION

This volume contains a description of representative science experiments selected because of scoring high in the following areas:

1. Scientific interest
2. Adds new scientific knowledge
3. Compatible with specified missions
4. Compatible with JPL spacecraft

The selected science experiments are divided into the appropriate disciplines and listed in Table I. Several of the experiments were interdisciplinary in nature and these are cataloged under the area in which they provide the most useful information.

Due to the sun orientation of the spacecraft and the types of orbits specified, the science experiments are more numerous in the solar physics and particle and fields disciplines.

To reach this final catalog approximately 100 science experiments were reviewed. The experiments not included in the catalog were dropped for various reasons. Among these were:

1. Bioscience experiments - all required environmental control and data handling beyond the capabilities of the vehicle.
2. Astronomy experiments - many required pointing accuracies beyond the capability of the vehicle or required large aperture detectors not compatible with vehicle configuration.
3. All disciplines: size, weight, power, and data handling requirements exceeded vehicle capabilities.
4. All disciplines: scored poorly on scientific need or experiment is presently being flown.

All experiments, in order to be contained in this catalog, were required to be new or provide more detailed measurements of scientific areas.

TABLE I

LIST OF SCIENCE EXPERIMENTS CONTAINED IN CATALOG

Discipline	Experiments
I Astronomy	I-A Ultraviolet and Infrared Emission of Stars (D. G. Marlow)
	I-B Mapping of Galactic Structure in Infrared and Ultraviolet (D. G. Marlow)
	I-C 0.75 to 10 Mc Galactic Radio Noise (R. Hertel)
II Solar Physics	II-A Ultraviolet Imaging of Solar Flares (D. G. Marlow)
	II-B Search for Solar Neutrons (C. Black)
	II-C Detection of Low Energy Gamma Radiation (C. Black)
	II-D Solar Coronigraph (D. G. Marlow)
	II-E Study of Temporal Variations in Solar Ultraviolet Emissions (W. T. Holm)
	II-F Infrared Emission from the Sun (D. G. Marlow)
	II-G Search for Characteristic X-Ray Emissions from the Sun (C. Black)
	II-H Monitoring of Solar X-Ray Emissions in the Region of 0.2 to 24 keV (C. Black)
	II-I Extreme Ultraviolet Spectrum of the Sun (L. M. Snyder)
	II-J Profile of Solar Lyman Alpha (R. Anderson)
III Particles and Fields	
	III-A Spectra of Galactic Electrons (R. Hertel)
	III-B Study of Earth's Albedo Neutrons (C. Black/ J. H. Mullins)
	III-C Intensity and Anisotropy of Light Ions Trapped and Accelerated in Galactic Cosmic Ray Interactions (R. Hertel)

TABLE I (contd)

Discipline	Experiments
	III-D Trapped Particle Experiment (A. Y. Yahiku)
	III-E Detection of High-Energy Galactic Gamma Radiation (C. Black)
	III-F Proton Dosimeter (R. Hertel)
	III-G Search for Key Galactic Gamma Radiation (C. Black)
	III-H Spectrum and Flux of High-Energy Galactic Protons (T. T. Samaras)
	III-I Low-Energy Proton Spectrometry with Differentially Shielded Solar Cells (D. Moss)
	III-J Satellite Charging and Discharging Characteristics (R. Hertel)
	III-K Ionization Chamber Experiment (T. T. Samaras)
IV Planetary Atmospheres	
	IV-A Measurements of Earth Ultraviolet Radiation Flux (D. G. Marlow)
V Ionospheres and Radio Physics	
	V-A Topside Sounder (R. Hertel)
	V-B Investigation of the Composition of the Upper Atmosphere (R. Hertel)
VI Planetology	VI-A Photon Emission from the Dark Areas of the Moon (D. G. Marlow)
	VI-B Earth Albedo (D. G. Marlow)
	VI-C Ultraviolet and Infrared Lunar Albedo (D. G. Marlow)
	VI-D Physical Analysis of Micrometeoroids (L. M. Snyder)
	VI-E Effect of Hypervelocity Impacts on Structural Surfaces (L. M. Snyder)
	VI-F Chemical Analysis of Cosmic Meteoroids (L. M. Snyder)

Therefore, not included in the catalog are numerous known experiments which have been flown on previous satellites. Several of these experiments are attractive scientifically for inclusion on the JPL spacecraft, because of the variety of missions and the ability of the spacecraft to carry several directly related (or indirectly related) experiments at the same time. A summary of previously flown scientific experiments is contained in the Space Measurements Survey for Defense Atomic Support Agency compiled by Electro-Optical Systems, Inc. The reader is referred to this document as a source for additional experiments which could be accommodated by the JPL spacecraft. A copy of the Space Measurements Survey is available in the JPL Library for reference.

I

ASTRONOMY

1. BACKGROUND

The astronomy discipline is intended to extend the ground based observational techniques of astronomers to the study of celestial objects from positions above the earth's atmosphere and, therefore, under conditions free from the absorption or scattering effects of the atmosphere. Depending on the wavelength, astronomical observations in space must be made from altitudes ranging from a minimum of 100,000 feet for the visible and infrared wavelengths to altitudes of at least several thousand kilometers for observations in the long-wave radio wavelengths.

2. PLANETARY, STELLAR, AND GALACTIC ASTRONOMY

2.1 Ultraviolet and Infrared Astronomy

Many stars and all planets and emission nebulae emit a large fraction of their energy in wavelengths which cannot be observed readily from the earth's surface. Thus, astronomers have been forced to make extensive extrapolations to estimate both the total energy emitted by astronomical bodies and that portion absorbed by interstellar material. In many cases they have been forced to hypothesize conditions in stellar and planetary atmospheres without any means of checking these hypotheses. Some typical examples of problems are discussed briefly.

Dust between the stars reddens the light reaching the earth. This phenomenon is the result of the greater penetration of red wavelength light through the dust particles accompanied by the greater absorption and scattering of blue wavelength light by the dust. Dust grains also polarize the light received from the stars. Although interstellar dust comprises a major fraction of the mass in the universe, astronomers are not yet agreed as to its exact nature since many types

of material could give rise to the optical effects observed between 3000Å and 10,000Å. Observations in the ultraviolet region will be particularly important in establishing the nature of the interstellar particles, while observations in the infrared region will lead to an improvement in our estimates of total interstellar absorption.

In recent years astronomers have made numerous observations of the intensity of the brightest stars in the wavelengths between 1000Å and 3000Å. These observations have already indicated that the understanding of stellar atmospheres is sufficiently poor that one cannot explain why stars emit as little radiation as they do in this spectral region. Equally puzzling is the fact that stars which look nearly identical in wavelengths penetrating to the ground seem to differ greatly from one another in ultraviolet wavelengths. Neither of these effects is understood sufficiently, and more data must be obtained in order to understand the problem. Photometric and broadband spectrophotometric observations also contain data which will help to extend the stellar reddening law to the ultraviolet.

The brightness in the long wave radio region of the galactic halo and of most radio sources increases with increasing wavelength throughout the region in which the earth's ionosphere begins to prevent earth-based observations. For various reasons, resulting both from the physical characteristics of the sources and from the characteristics of the intervening interstellar and interplanetary media, the intensity cannot continue to increase indefinitely. Data collected from a Journeyman rocket flight indicate that a maximum of intensity may occur near a wavelength of 300 meters.

2.2 Visible and Short Wave Radio Region

Observations in this portion of the spectrum will be useful for the study of planets, of emission nebulae, of close double stars, the possible detection of planetary companions to nearby stars, and studies of crowded star fields such as those found in clusters and distant galaxies.

This requires very high resolution photographic and television systems to be flown. Due to the lack of adequate data storage, experiments requiring high density data storage, such as high resolution imaging devices, were excluded from consideration in this study.

3. GRAVITATION ASTRONOMY

The deduction of satellite and space probe trajectories have led to the development of new techniques in gravitational astronomy. Satellites have also proven exceedingly useful for mapping the gravitational field of the earth and they are becoming increasingly useful for establishing the relative positions of geographical locations on the earth. Although many satellites have been used for such studies, starting with VANGUARD I, ANNA IB was the first satellite especially designed to study geodesy. Additional satellites in different inclinations and altitudes are necessary for the complete mapping of the earth, both geographically and gravitationally. (Refer to Engineering Experiments, Volume III, Section 2 - Laser Experiment, for additional information in support of this gravitational astronomy.)

EXPERIMENT I-A

ULTRAVIOLET AND INFRARED EMISSION OF STARS

1. DESCRIPTION OF EXPERIMENT

The purpose of this experiment is to measure the ultraviolet and infrared energy flux of bright stars located near the ecliptic. Earth-based measurements of stellar spectra are limited by the atmosphere to the region 3000 Å to about 2.5μ, although there are some long-wave windows beyond 2.5μ through which some information can be obtained.

Measurements extending into the UV and IR regions could greatly improve our knowledge of stellar physics, even if only broad-band spectra could be obtained, such as could be measured with a system of photometers and fillers.

2. DESCRIPTION OF INSTRUMENTATION

The instrument consists basically of two energy collection systems, each provided with a suitable detector. For the UV system, the collector would be a sapphire lens which would transmit wavelengths greater than ~1450 Å. The detector would be a solar-blind CsTe photomultiplier with a sapphire window, sensitive only to wavelengths < 3000 Å.

In order to cover a wide spectrum in the IR it would be best to use reflective optics, e.g., a gold surfaced Newtonian system and a wide-band detector such as a vacuum thermocouple or a bolometer. In this system a filter is required to remove the visual and UV energy.

Figure 1-1 is a sketch of the proposed instrument. In the UV telescope, the objective lens forms an image of the star in the plane of the field stop, which has an opening determined by the desired field of view. The field lens images the objective lens onto the photocathode in order to avoid the highly localized illumination that would exist if the star were imaged on the cathode.

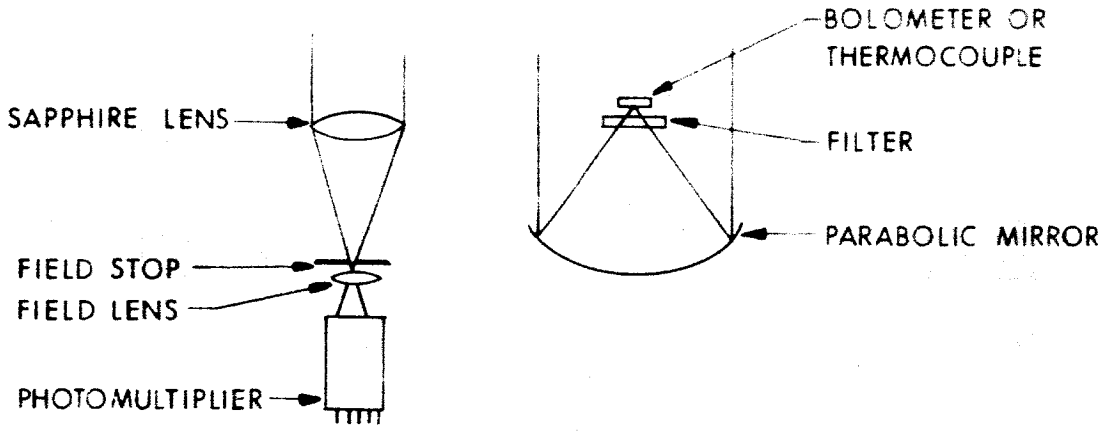
SAPPHIRE LENS
FIELD STOP
FIELD LENS
PHOTOMULTIPLIER
BOLOMETER OR
THERMOCOUPLE
FILTER
PARABOLIC MIRROR

[illegible]

The IR system is a simple parabolic mirror which images the star, through a filter, onto the thermal detector.

The two optical systems would be combined in a single package which would be mounted on the satellite with its optic axis at some angle θ to the spin axis. Twice each revolution of the satellite the optic axis would cross the ecliptic and, since the axis is constrained to point always at the sun, in the course of a year the instrument would scan a full circle in celestial longitude. A study would have to be made to determine the maximum value of θ ($\pi/2 \geq \theta > 0$) compatible with the light-collecting system.

3. INSTRUMENT SPECIFICATIONS

Dimensions: Optics and detectors in a package 4" x 8" x 6"
Electronics package, 2" x 4" x 6"

Weight: Optics; 3 lbs; electronics, 1 lb

Electrical: Power ~ 2 watts at 28 volts

Mag. interference: Not susceptible; shielded as needed to protect other systems.

Data Rate: 10 bits/sec continuous

Thermal: -20°C to $+60^{\circ}$C

Mounting: Optics preferred mounting is 90 degrees with respect to sunline; optics secondary mounting position is 180 degrees from the sun

Preferred Mission: 1000 nautical miles modified sun-synchronous

EXPERIMENT I-B

MAPPING OF GALACTIC STRUCTURE IN THE IR AND UV

1. DESCRIPTION OF EXPERIMENT

The structure of the galaxy has been mapped in exhaustive detail in the visual spectrum, but because of the opacity of the earth's atmosphere, little is known about galactic radiation in the UV and IR regions.

The proposed experiment would map the gross features of the galaxy in these hitherto inaccessible wavelengths, and any especially interesting areas discovered would then be selected for more detailed study on later missions.

2. DESCRIPTION OF INSTRUMENT

The galactic survey instrument would consist of two optical systems, one for the UV and one for the IR, each provided with a linear array of detectors to give reasonably good one-coordinate resolution. The resolution in the orthogonal direction would be provided by the scanning motion resulting from the rotation of the satellite. Each optical system will have a 90° field of view and is mounted on the satellite facing away from the sun, as shown in Fig. I-2. During one revolution of the satellite, one half of the celestial sphere will be scanned. In six months, the whole sphere will be mapped, assuming that the spin vector is kept pointed at the sun.

In addition to galactic radiation, the system receives energy from the earth during a part of each revolution and, between first and last quarters, from the moon. The detector system could be disabled at these times, or the data can be collected and subsequently rejected, a much simpler procedure. Because of the enormously greater luminosity of the earth and moon compared with any galactic feature, there will be no doubt concerning the identity of the data to be rejected.

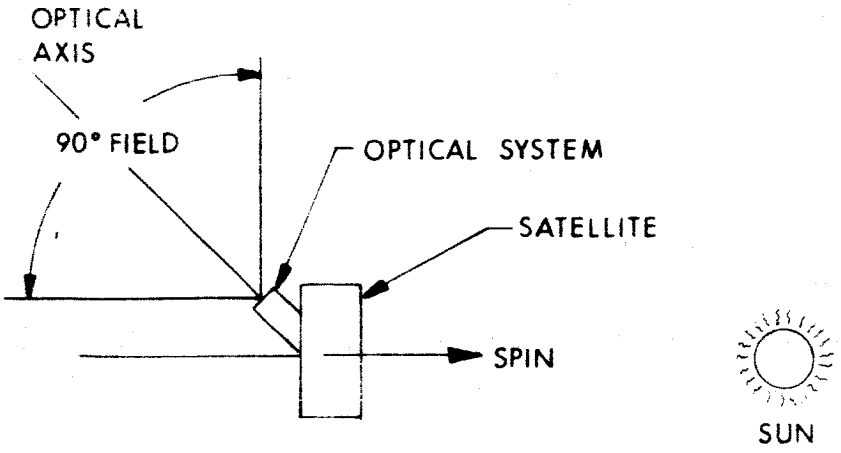

FIG. 1-2 SCANNING GEOMETRY OF GALACTIC SURVEY INSTRUMENT

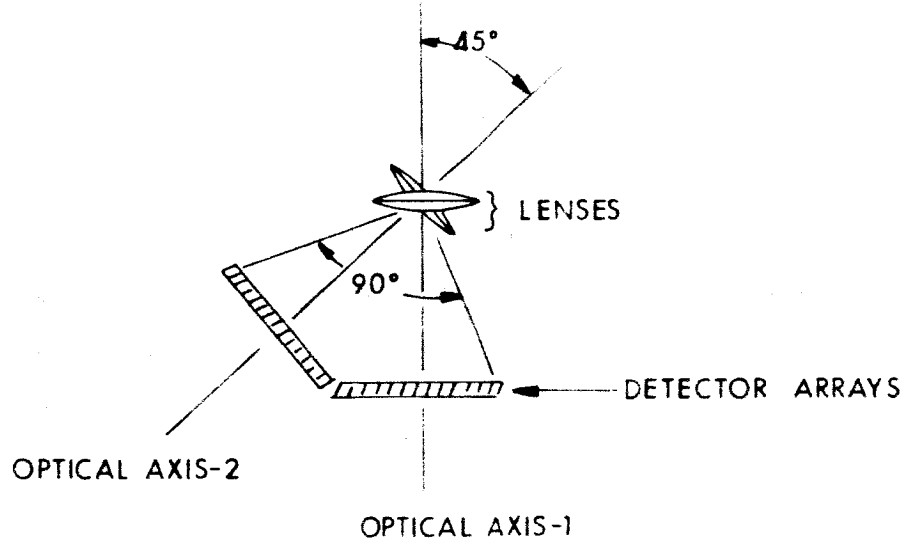

FIG. - OPTICAL SYSTEM FOR 90° FIELD OF VIEW

It is not possible to have adequate image quality over a 90° field with a simple optical system; hence, each system will consist of two subsystems covering 45°, Fig. 1-3. There will therefore be 4 lenses altogether, 2 for the UV and 2 for the IR.

The UV lenses will be of fused silica, which transmits to ~ 1800 Å, and the IR lenses of Irtran glass which will transmit to ~ 3μ. No attempt will be made to obtain spectral resolution other than by observing the broad UV and IR bands determined by the choice of lenses and detectors.

The UV detectors are EOS UV-sensitive silicon sensors, which can be made in array form if desired, by photoetching. They have a very stable responsivity and will need no in-flight calibration. The IR sensors will be multi-element arrays of PbS. These sensors do not have a stable responsivity and must be periodically calibrated by a simple system utilizing a rugged, undervolted tungsten lamp. Fig. 1-4.

The number of detector elements in each array depends, of course, on the degree of resolution desired. For a preliminary survey, it is not necessary to strive for fine detail, nor is it feasible in a simple, lightweight, low power experiment. If, for example, the resolution element were 1 square degree, the entire celestial sphere would be represented by 4.13×10^4 elements. A 2° square element would divide the sky into 1.04×10^4 parts and there would only be 45 detector elements for each spectral band.

Because of the slow rotation rate of the satellite, it will be feasible to read the detector elements sequentially, with a concomitant saving in electronic components.

3. INSTRUMENT SPECIFICATIONS

Dimensions:	Optical system - 8" x 10" x 12"	
	Electronics - 2" x 4" x 6"	
Weight:	Optics - 3 lbs.	
	Electronics - 1 lb	

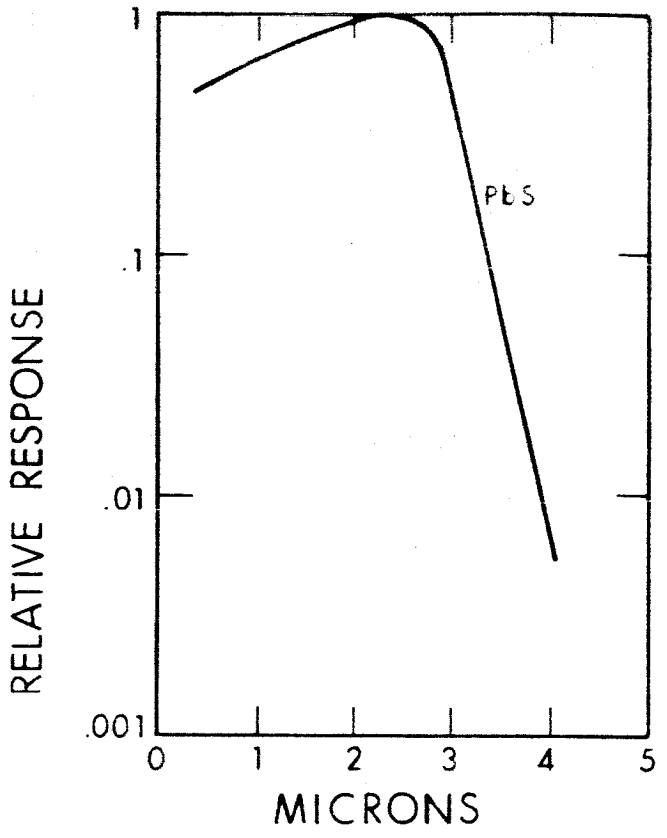
RELATIVE RESPONSE
1
.1
.01
.001
PbS
0
1
2
3
4
5
MICRONS

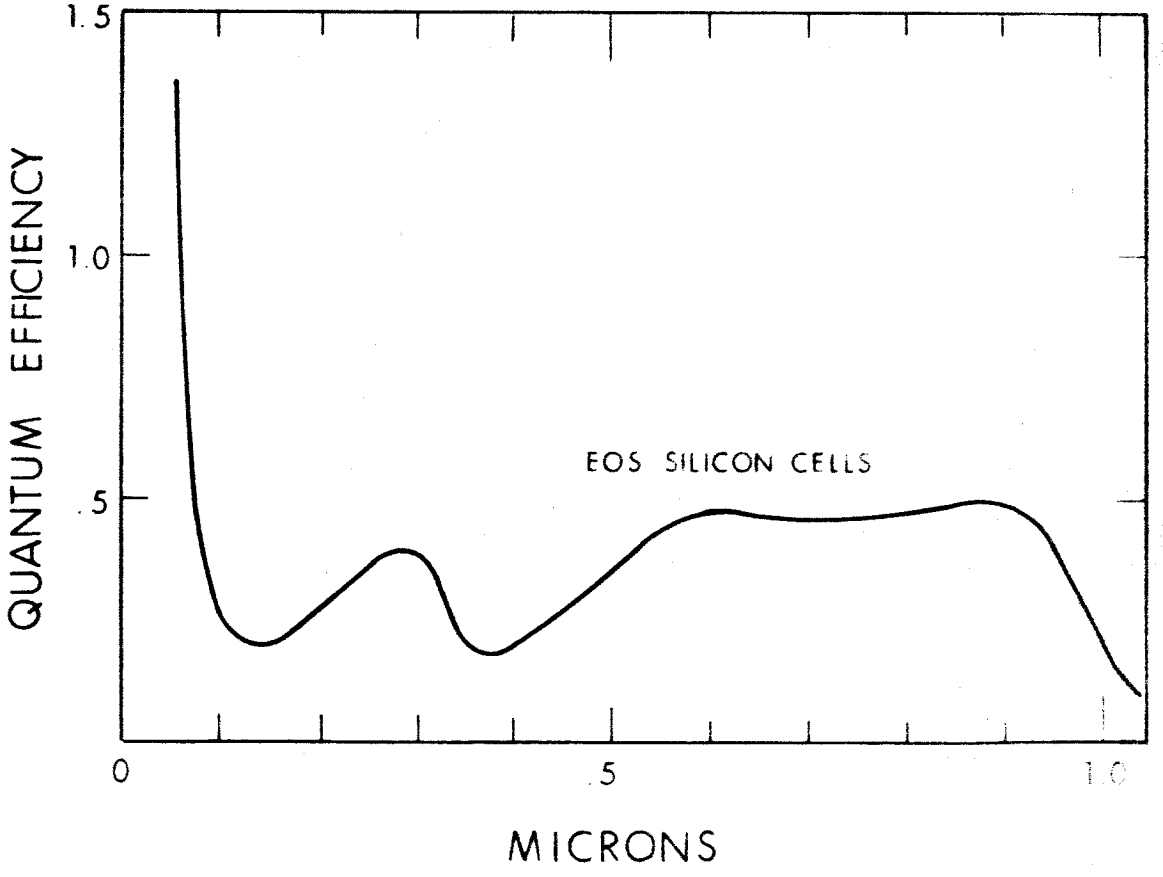
QUANTUM EFFICIENCY
1.5
1.0
.5
EOS SILICON CELLS
0
.5
1.0
MICRONS

619527

Power:	2 watts at 28 volts
Circuits:	Commutator, amplifier, programmer, calibration, power supply
Thermal:	$-20^{\circ}C$ to $+60^{\circ}C$
Data:	50 bits/sec continuous
Mounting:	Preferred mounting of optics is 90 degrees with respect to sun line

Preferred Mission: 1000 nautical mile modified sun synchronous

EXPERIMENT I-C

0.75 TO 10 Mc GALACTIC RADIO NOISE

1. DESCRIPTION OF EXPERIMENT

The great success of ground-based radio astronomy has resulted recently in efforts to extend the frequency range of galactic radio emission measurements below the $f_o F_2$ cutoff frequency introduced by ionospheric absorption. Depending on various factors, the maximum electron density of the ionosphere varies from about 5×10^5 cm^{-3} to 5×10^6 cm^{-3}, corresponding to plasma frequencies from about 6 to 20 Mc; on rare occasions the plasma frequency may drop below 20 Mc. A ground-based radio receiver operating at frequencies below the plasma frequency is hampered by the great attenuation suffered by the waves in penetrating the ionosphere, both as to sensitivity and in reconstructing the incident energy spectrum. Several rocket- and satellite-borne receivers[1&2] have been flown; in the 1 - 5 Mc region their results do not agree with ground-based measurements[3]. Reasons suggested for the discrepancies have been improper correction for ionospheric effects in the case of ground-based measurements and the difficulty of calculating antenna efficiencies for the rocket and satellite measurements (which were carried out at 1000 km or below).

The experiment proposed here would make galactic radio noise measurements in the 1 - 10 Mc frequency range from a highly eccentric orbit extending to a region of negligible electron density (25,000 miles) so as to circumvent both of these problems. A 100-foot dipole antenna is proposed for the

---

1. D. Walshe, F. T. Haddock, and D. H. Schulte, Univ. Michigan, Radioastronomy Rep. (June 1963).
2. T. R. Hartz, Nature 203, 173 (1963).
3. G.R.A. Ellis, Nature 204, 171 (1964).

experiment, although in later versions an antenna with greater directivity would be desirable. For reasons of economy and efficiency in spacecraft weight utilization it is proposed that the experiment be combined with a topside sounder experiment, which uses a similar antenna and receiver.

While the use of a dipole antenna will result in limited spatial resolution, frequency resolution will be held to about 50 cps in order to observe any spectral irregularities which may be present and to keep receiver noise at a minimum.

2. DESCRIPTION OF INSTRUMENT

Figure 1-5 shows a block diagram of the proposed galactic radio noise receiver. The instrument is basically a phase-sensitive or lock-in amplifier which is electronically tuned from 1 to 10 Mc by a saw-tooth sweep generator. The received signal is first amplified by a relatively broad-band (0.5 Mc) tuned preamplifier, then multiplied by a sample of the frequency to be measured. The output of the multiplier is passed through a low-pass filter which controls the bandwidth of the system. In this way very narrow bandwidths may be achieved without the necessity for critical, high-Q amplifiers. If desired, several parallel output filters may be used to obtain simultaneous measurements with different bandwidths. At the end of each sweep a standard noise generator is switched into the preamplifier input for calibration purposes.

The antenna proposed is an extendable tubular dipole of the type used on the satellite alouette.

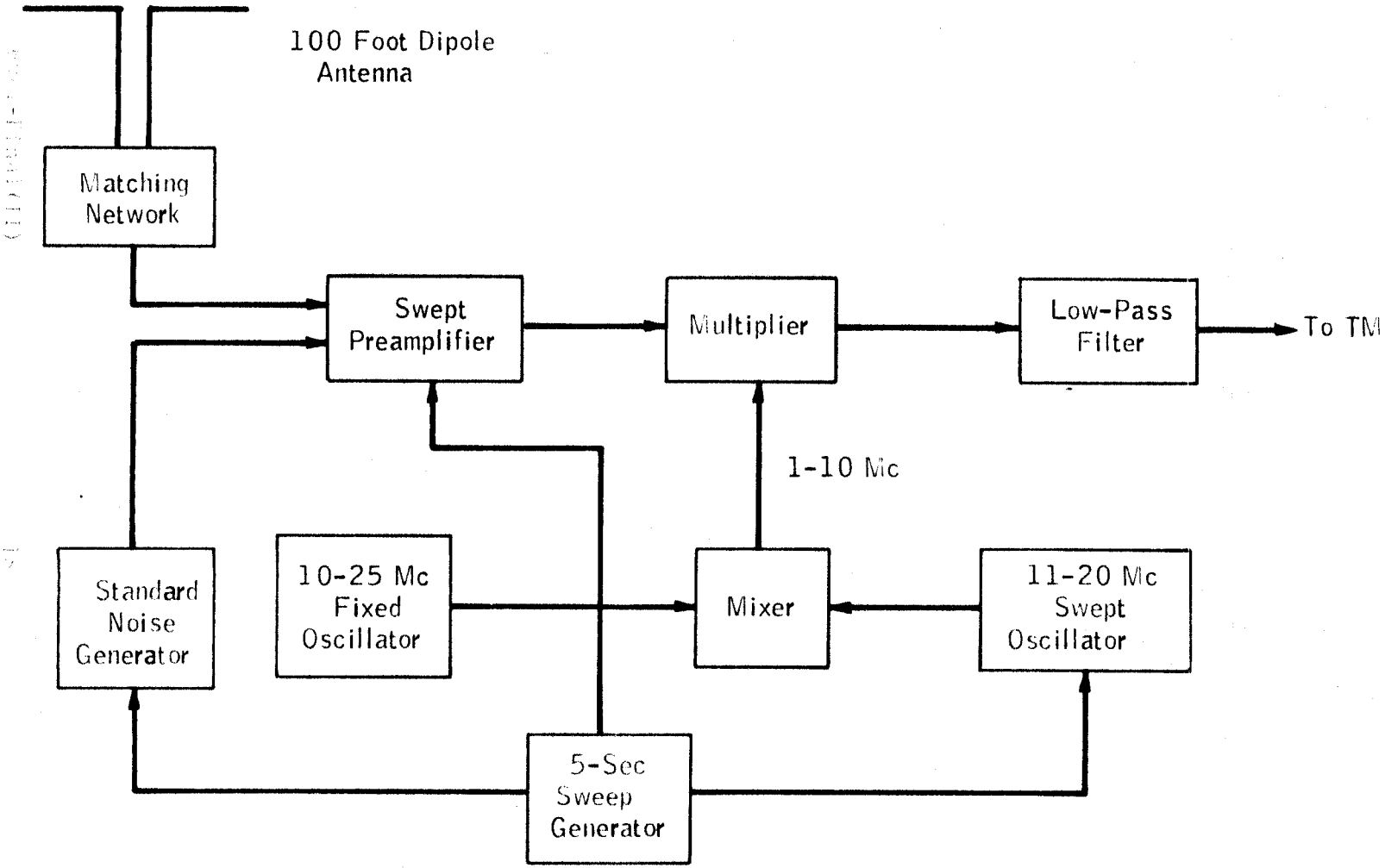

FIG. 1-1 BLOCK DIAGRAM OF 1-10 Mc NOISE RECEIVER

3. INSTRUMENT SPECIFICATIONS

Dimensions:	10" x 8" x 6" electronics plus two erectable booms
Weight:	10 lbs
Power:	3 watts at 28 volts
Thermal:	$-20^{\circ}C$ to $+60^{\circ}C$
Data:	200 bits/sec
Mounting:	Extendable dipoles mounted 180 degrees apart
Preferred Orbit:	High, elliptical 200-nautical mile - 25,000-nautical mile

II

SOLAR PHYSICS

1. BACKGROUND

The primary objectives of the solar physics discipline are:

1. To advance the understanding of the sun's constitution and behavior
2. To clarify the physical processes by which the sun influences the earth.

Since the sun is the nearest star, it offers an opportunity to acquire knowledge of astrophysical phenomena, and to test theories. It is the only star where direct observation of structural features like sunspots or prominences can be observed, and the only one near enough to permit the study of its x-ray, gamma-ray, or radio emission. However, the earth's atmosphere is nearly or completely opaque to solar radiation at wavelengths shorter than about 2 mμ. In order to study the solar ultraviolet light, or x- or gamma-rays, it is necessary to carry the instruments above the atmosphere.

The solar radiations are subject to dynamic, unpredictable, transient variations which produce responses on earth and the near earth vicinity, which are often violent. As an example of the changing solar phenomena, the x-ray emission of a chromospheric flare usually varies in close step with its brightness in visible hydrogen radiation. Even when the visible sun is notably active, there persists some flux of x-rays, in proportion to the calcium facular area. Unanticipated pulses of x-ray emission were detected, which have not yet been identified with known visible light phenomena. Experiment data also indicates an increase in net solar Lyman-alpha emission during a solar flare. Solar flares also influence the Van Allen belts, Aurora, ionosphere, and the earth's magnetosphere. Therefore, the major questions in this area concern discovering and explaining the sun-earth relation on a dynamic basis.

EXPERIMENT II-A

ULTRAVIOLET IMAGING OF SOLAR FLARES

1. DESCRIPTION OF EXPERIMENT

The goal of this experiment is to form a rough image of the solar disc in the ultraviolet in order to locate flares and study their UV emissions uniquely.

A great many ultraviolet spectrograms of the sun have been photographed by rocket-borne spectrographs, but the instruments have been non-imaging and have thus recorded the total-sun spectrum, rather than that from any particular region.

Since a knowledge of the ultraviolet emissions from flares is essential to a complete understanding of the mechanisms underlying their genesis and development, and since atmospheric absorption severely restricts the ultraviolet capabilities of earth-based coronagraphs, the addition of a coronagraph or equivalent aboard a solar-oriented satellite is extremely desirable. The instrument described in the following paragraphs has been designed for a vehicle with limited telemetry capabilities and thus represents a compromise with regard to spectral and imaging resolution. It will, nevertheless, provide a wealth of valuable information not previously available to astrophysicists by permitting these radiations to be monitored with moderate resolution over a relatively long period of time.

2. DESCRIPTION OF INSTRUMENT

The detector consists of linear arrays of EOS UV-sensitive silicon detectors formed on single chips by photomasking techniques. A lens or mirror optical system forms an image of the sun which, by a scanning motion, is rotated across the detector arrays.

Each element scans a narrow band running across the image. The resolution in the direction perpendicular to the scan is $1/n$, where n is the number of detector elements. In the scanning direction, the resolution would depend on the scanning speed and the speed of response of each detector and its amplifier system.

The scanning motion is provided by the rotation of the satellite about the solar vector. Figure 2-1 shows conceptually how the scanning would be performed. One end of the detector array is centered on the spin axis, which also passes through the center of the image. As the satellite turns, the array swings around the spin axis so that each detector sweeps a circular band concentric with the image center.

Each detector element is 0.004 inch wide, measured along the array, and is separated from its neighbors by 0.001 inch gaps, making a total element width of 0.005 inch. The length of each element (i.e., overall array width) is 0.04 inch. The radius of the image is given by 0.005 n inches, where n = number of annular bands included in the disc. For example, if n = 20, the image diameter would have to be less than 2 x 0.005 x 20 = 0.20 inch. Since the sun's angular diameter (including the larger flares) is about 0.01 radians, a focal length of 0.2/0.01 = 20 inches would be required. The optical system would not necessarily be this long. It could be shortened by folding the optical path or by using the telephoto principle (e.g., a Cassegrain system in the case of reflective optics).

Spectral resolution is obtained by placing an interference filter, designed to transmit only a selected band of frequencies in the UV region, over each detector array. By having several radially disposed arrays of detectors, each with a different filter, information in different spectral bands is obtained.

The electronic circuitry consists of an amplifier for each detector element or, if the spin rate is sufficiently slow, one amplifier per array sequentially scanning the elements of that array. A power converter and a programmer to control the scanning of the amplifier outputs completes the system.

3. INSTRUMENT SPECIFICATIONS: (Fig. 2-2)

Dimensions:	Optical system - 6-inch diameter by 12-inch length
	Electronics - 1 by 2 by 4 inches
Weight:	~ 5 lbs
Power:	~ 5 watts

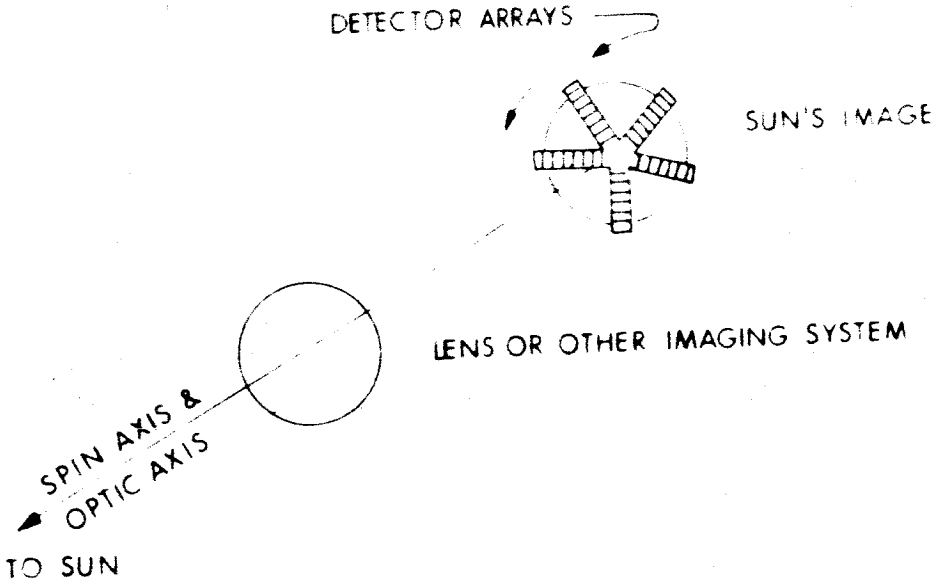

FIG. 2-1 SCANNING OPERATION

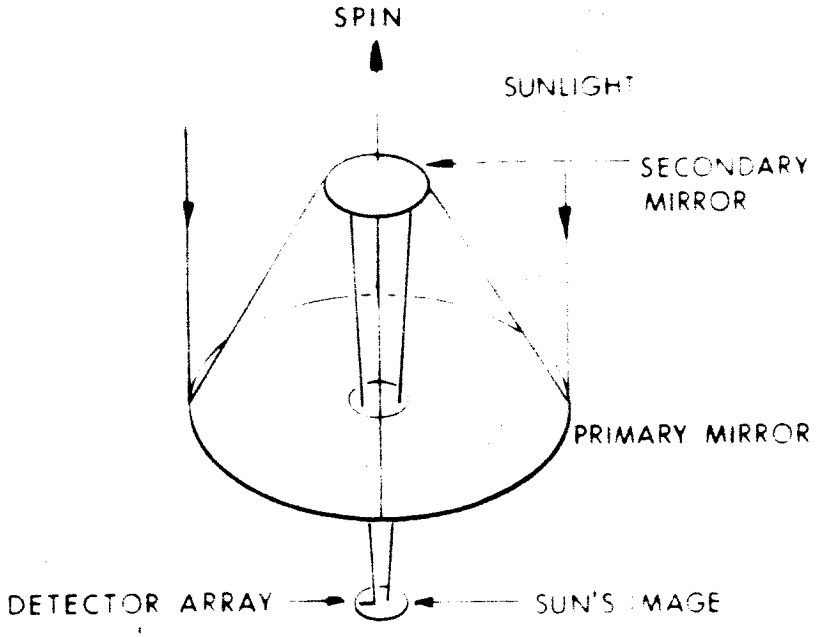

FIG. 2-2 INSTRUMENT SCHEMATIC

Output: 20 parallel outputs; analog 0 to 5V.

Magnetic interference: Not susceptible; shielded to prevent disturbance in other systems.

Data Output: 100 bits/sec (depends on number of parallel channels) continuous.

Thermal: $-50^{\circ}C$ to $+50^{\circ}C$.

Mounting: Sun-oriented.

Preferred Orbit: 1000 nautical miles modified sun-synchronous for long interupted look. Either mission B or C would be suitable except for shadow.

EXPERIMENT II-B

SEARCH FOR SOLAR NEUTRONS

1. DESCRIPTION OF EXPERIMENT

The following experiment has been designed to investigate the solar neutron output. The production of neutrons in the sun is a process which is expected on theoretical grounds. Little data is presently available for a study of the particle reactions at the solar surface which would be sufficiently energetic to produce neutrons. Reactions which yield neutrons (and gamma rays) are probably induced by protons which have been accelerated by the magnetic fields available during solar flare activity. The energies of such protons are sometimes as high as 10^9 electron volts. Such energies are more than sufficient to produce neutron reactions. Neutron production from proton bombardment of helium, for instance, is significantly large at 25 million electron volts.

Even during normal solar activity, surface turbulence and the associated small scale magnetic field variations could accelerate protons to energies of many million electron volts. Since little has been done to determine the abundance of such reactions, a study is needed of neutrons emanating from the sun during minimum and average solar activity to give solar investigators a better understanding of the field and particle energies available during normal, as well as active, periods. Neutron energies are very important in such a study, since they relate directly to the energy of the reacting protons. Spectrometric measurements are, therefore, very desirable.

Neutrons produced in the sun's atmosphere during flare activity will give information regarding flare mechanism and energy not obtainable from the study of solar flare proton spectra. Solar flare protons are diverted from isotropic propagation from their source by the sun's magnetic field and are probably anisotropic from local fields at their point of origin. The anisotropy is strongly energy-dependent so that measurements made of intensity and spectra of protons lack information

regarding time and sequence of flare events. If good spectral information is obtained for neutron emissions occurring during flare activity, the variations in neutron intensity and energy could be related to the sequence of flare development; neutron propagation is more nearly isotropic, being altered only by scattering in the solar atmosphere.

Since the lifetime of a neutron is on the order of 10^3 seconds, only neutrons having high energies will, in general, reach the earth before decaying. For instance, the decay "length" for a [illegible] MeV neutron is approximately the distance from the earth to the sun and so only 63 percent of the initial flux from the sun would arrive here. The percent of 10 MeV and 1 MeV neutrons arriving at earth would be 3.5 percent and 0.14 percent, respectively. Thus, it is seen that spectral information from solar flares must be processed to account for time of flight and lifetime to obtain the solar flare neutron signature, if such exists. It is also obvious that low energy neutrons, if present in solar reactions, will be relatively undetectable at earth distance.

The measurement of solar neutron flux will require constant surveillance, i.e., satellite orientation to the sun, since the earth is also a source of high-energy neutrons which are a by-product of high-energy cosmic ray interactions with our atmosphere. This requirement for orientation, of course, infers directional sensitivity of the detector to neutrons. Since the flux from a normal sun is on the order of 0.02 neutrons/cm^2-sec, the earth's albedo neutrons with a flux of 0.1 neutrons/cm^2-sec could interfere considerably.

Since little is known concerning the neutron fluxes during solar flares except that they should be of the order of the earth's equatorial albedo, one must assume that small fluxes must be measured to some significance and that dynamic range be as large as possible. Background from charged particles must certainly be considered, since solar flare protons, Van Allen radiation, and cosmic radiation will create considerable

interference which cannot be eliminated by any directional properties of the detector. These sources of interference must be handled by anti-coincidence techniques, since for all practical purposes the energies deposited in neutron detectors by these particles are of the order of those expected from the solar flare neutrons.

2. DESCRIPTION OF INSTRUMENTATION

The detector which is proposed for this experiment is essentially a proton range spectrometer with a hydrogenous converter plate which yields a proton for each interacting neutron by a recoil interaction. The proton is then collected by one of a series of solid-state detectors which determine its recoil energy. Protons reaching these detectors are representative of the energies of the colliding neutrons, since such processes are predominately forward scattering. Figure 2-3 shows the general configuration of the device.

The basic problems are several. The n-p collision is not, in general, a total conversion process, and thus only a lower limit to the neutron energy can be obtained. Also, the directionality is limited by the fact that the recoil proton cannot go backward. However, at higher energies, the relativistic kinematics tend to favor the forward angles for the collision process (essentially a charge-exchange collision with small momentum transfer), and the directionality is improved. The other problem is that the hydrogenous radiator also usually contains carbon, and the n-carbon reactions are more complicated and less directional. Another problem concerns efficiency. The n-p cross section at higher energy gets relatively small ($\sim$ 0.1 barn) so that the conversion efficiency becomes poor. A converter that would allow the passage of a 50 MeV proton would have a conversion efficiency of only about 2 percent.

Such problems notwithstanding, the following instrument constitutes a good beginning toward a satisfactory detector.

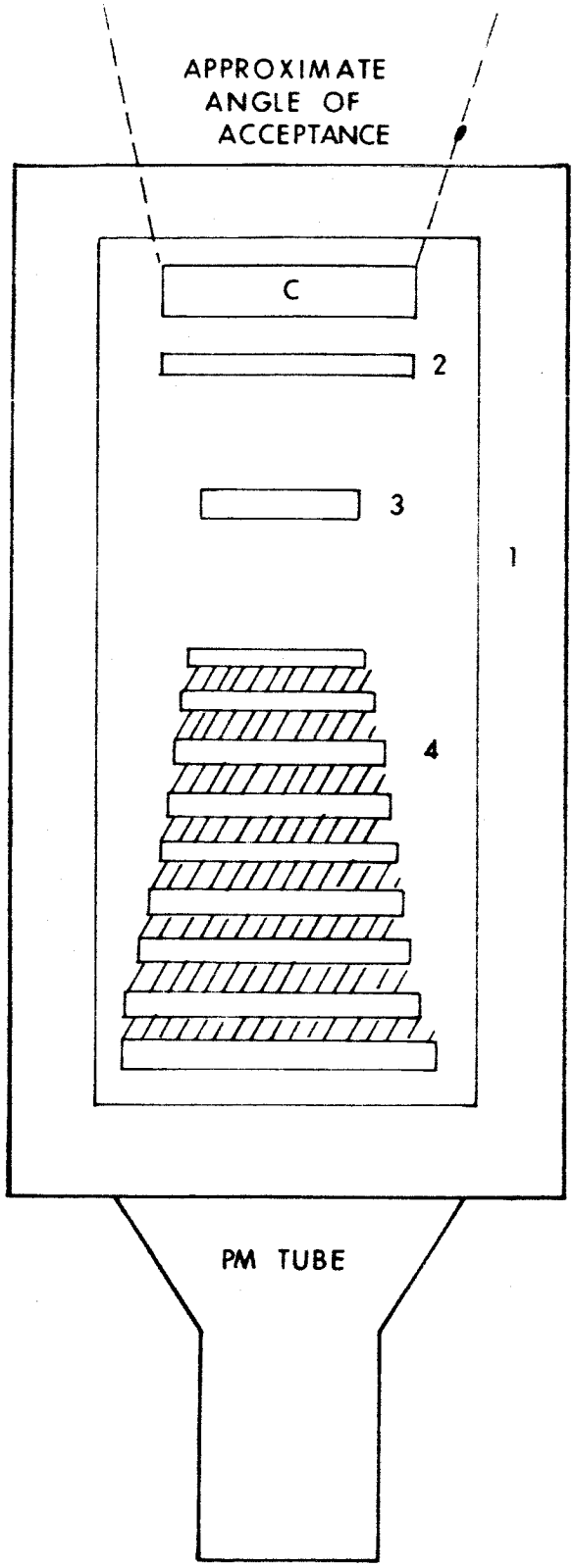

FIG. 2-3 SECTOR 2 DETECTOR

Description of Neutron Detector

Referring to Fig. 2-3 note that:

1 - is a plastic scintillator, totally enclosing the detector and used to provide anticoincidence isolation from charged-particle background.

2 - is a solid-state dE/dX counter

3 - is a second solid-state dE/dX counter

4 - is a copper absorber-solid-state detector sandwich, which is a proton telescope with maximum range of about 300 MeV protons.

C - is CH_2 converter-detector operation.

The scintillator (1) vetoes all entering charged particles. A neutron enters C, knocking out a proton, which triggers 2, 3, and 4 to distinguish protons from electrons, thus eliminating counts due to gamma conversion. The proton telescope, in conjunction with 2 and 3, gives the proton energy (range and identification).

If desired, the in-line assembly can be covered with a layer of lead to convert gammas, thus vetoing them. (This would add considerable weight, however.)

The above device will measure neutrons, put a lower limit on their energy, and measure directions crudely, i.e., about $\pm 45^{\circ}$, but enough to identify the sun as the source rather than the earth.

3. INSTRUMENT SPECIFICATIONS

Dimensions:

Optics:	6" diameter x 12" long
Electronics:	1" x 6" x 7"
Weight:	~ 8 pounds
Power:	5 watts at 28 volts

Thermal:	$-30^{\circ}C$ to $+65^{\circ}C$
Data:	10 bits/sec continuous
Mounting:	Sun-oriented
Preferred Orbit:	Any orbit; 1000 nautical mile modified sun synchronous has long look at sun.

EXPERIMENT II-C

DETECTION OF LOW ENERGY SOLAR GAMMA RADIATION

1. DESCRIPTION OF EXPERIMENT

The detection of solar gamma-radiation in the region of 0.1 to 3 MeV and the determination of the photon energy distribution during solar flare periods and normal quiet periods is recently of great interest. The search for radiation in this interval will yield information indicating the possibility or extent of occurrence of several nuclear reactions in the sun's atmosphere which could produce low-energy gamma radiation. Such reactions that could produce fluxes detectable at earth distance are:

1. Positron annihilation radiation at an energy of 0.511 MeV;
2. Deuterium formation through neutron /proton capture reactions producing gammas at 2.23 Mev;
3. Bremsstrahlung produced by relativistic electrons in the solar atmosphere.

Data on this region of photon energies would aid in evaluating models of solar flare mechanisms since most studies of flare emission have been directed toward the thermal x-ray regions.

A number of experiments[1,2,3] have observed bremsstrahlung radiation during solar flares. These observations were made in the energy range below 0.1 MeV and only with gross energy analysis, and extrapolation of this data to higher energies would be of questionable validity.

Estimates of photon fluxes in this region (0.1 to 3 MeV) indicate that 0.1 to 0.01 photons/cm^2/sec may be expected.[1,2,4,5] Detection of photon fluxes in this range demands relatively high performance from the detector used and long observation times. Solar oriented satellites would be required to provide the constant viewing of the sun necessary to assure significant data during flares.

2. DESCRIPTION OF INSTRUMENTATION

In order to reduce background from galactic gamma radiation, atmospherically produced gammas, solar flare protons, and earth's trapped radiation, the detection instrument must have fairly good directional properties. Techniques generally employed for reducing background include the use of shielding external to the detector, and anticoincidence arrangements. Generally speaking, shielding techniques are difficult to design and often bremsstrahlung is produced by the charged particle component of the background. This is especially a problem in thin shielding with high Z materials. Anticoincidence techniques offer greater background reduction for weight optimization but suffer from the problem of gross angular resolution. Since only moderate angular resolution is necessary in this application, such a technique is reasonable, especially in terms of weight.

The detector suggested for this experiment is a CsI(Tl) crystal, 1 inch in diameter by 2 inches long, inserted into a well bored into a large CsI(Tl) crystal and viewed by a 1-inch-diameter photomultiplier tube such as an RCA C7151D, as shown in Fig. 2-4. The large crystal is viewed by four similar tubes, the outputs of which are added and operated in anticoincidence with the output of the central detector. Cesium iodide is chosen for this application because of its collection efficiency for gammas and greater physical ruggedness. A compromise exists in the placement of the phototube, i.e., in the acceptance aperture; however, it is desirable to maintain the greatest amount of shielding coverage possible to reduce the large background of charged particles. The phototube, however, should provide shielding for low-energy charged particles and electrons on the order of 1 MeV of energy. The angular response of this assembly will depend upon the geometry chosen for the outer scintillator (Fig. 2-5).

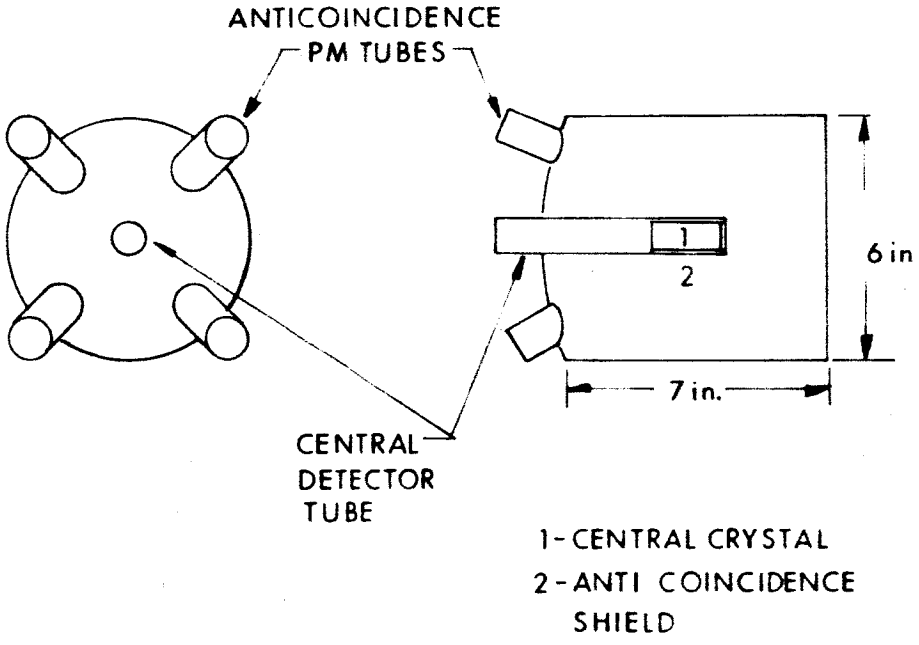

FIG. 2-4 ANTICOINCIDENCE PM TUBES

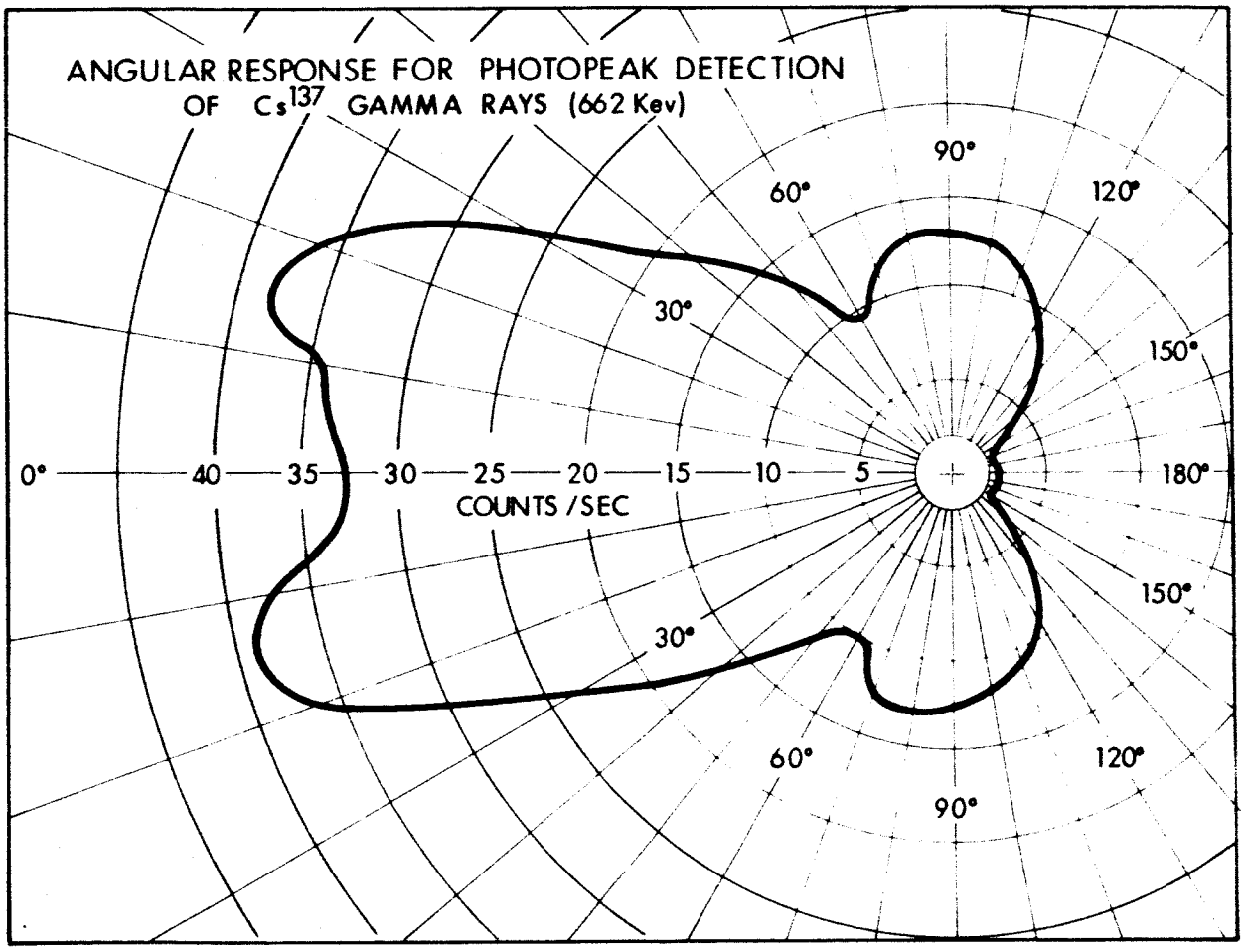

FIG. 2-5 ANGULAR RESPONSE FOR PHOTOPEAK DETECTION OF Cs 137 GAMMA RAYS (662 Kev). Data was taken for 40 minutes at each point with a 50μ C source at distance of 24 inches from the central crystal.

A crystal of approximately 7-inch length by 6-inch diameter will have about 1 steradian of solid angle at half-maximum response, with background reduction to the sides by a factor of 3 and to the rear by a factor of 10. This reduction can be improved by increasing the cesium iodide shield dimensions at the expense of weight. The weight of the detector as described is approximately 3 lbs

The anticoincidence shield rejects high-energy charged particles either by absorption or anticoincidence, background gammas by absorption. In addition, it reduces that Compton continuum which is common to the central detector and the anticoincidence shield to a value which is only one-fourth of that seen with a bare central crystal. Energy resolution with this spectrometer crystal arrangement is on the order of 25 percent, full width at half maximum of the energy spectrum of an 0.5 Mev gamma source.

The detector is used with a pulse-height analyzer with an appropriate number (e.g., 64) of channels. Data from each channel is accumulated for a period of time suitable to the experiment and shifted to a buffer for processing and transmittal. The dead time should be short to ensure no loss of data during high count-rate periods (solar flares). Sufficient time base should be provided to accumulate significant counts in each channel and reduce the percent of data lost in the time base switching process.

The electronic circuitry in general is comprised of the following:

Preamplifiers	Storage Buffer
Pulse-shaping Amplifiers	Commutators
Discriminators	High-voltage Power Converters
Coincidence Circuits	Low-voltage Power Converters
Accumulators	Voltage Dividers

3. INSTRUMENT SPECIFICATIONS

Dimensions:	6" dia. x 12"
Weight:	15 pounds
Power:	2 watts at 28 volts
Thermal:	$-20^{\circ}C$ to $+65^{\circ}C$
Data:	5 bits/sec continuous
Mounting:	Must view sun directly and continuously
Preferred Orbit:	1000 nautical mile modified sun synchronous

REFERENCES

[1] Morrison, P., "On Gamma-Ray Astronomy," Nuovo Cimento, 7, pp. 858-865 (1958)

[2] Peterson, L. E., and Winckler, J. R., "Gamma Ray Burst from a Solar Flare," J. Geophys. Res., 64, pp. 697-708 (1959)

[3] Winckler, J. R., "Observation of a Solar Bremsstrahlung Burst at 1926 UT, 11 August 1960," J. Geophys. Res., 66, pp. 316-320 (1961)

[4] Peterson, L. E., and Howard, R. L., "Gamma Ray Astronomy in Space in the 50 keV to 3 MeV Region," Joint Nuclear Instrumentation Symposium, 6 Sep 1961

[5] Frost, K. J., and Ruthe, E. D., "Detector for Low Energy Gamma Ray Experiment," IRE Transactions on Nuclear Science, Vol. NS-9, No. 3, Jun 1962

EXPERIMENT II-D

SOLAR CORONAGRAPH

1. DESCRIPTION OF EXPERIMENT

The purpose of this experiment is to study the solar corona over a wide spectrum, unimpeded by the earth's atmosphere. Observations from the ground, whether by coronagraph or by solar eclipse, are limited to an uninterrupted spectral range of about 3000Å to 1.2..

The proposed instrument would not be spectrally limited in principle except by the availability of detectors and filters. Three spectral bands would be covered: $\lambda <$ 3000Å, 4000Å $< \lambda <$ 1., and 1. $< \lambda <$ 3.5..

2. INSTRUMENT DESCRIPTION

1. Optical System and Detectors

The optical system would be a small Cassegrain telescope which would form an image of the sun on the focal plane. The optical axis would be parallel to the sun-directed spin vector of the satellite, so that the image would rotate relative to the satellite coordinates. The image of the solar disc would pass through a hole and be absorbed in a cavity, leaving only the image of the corona on the focal plane (Fig. 2-6). Three linear detector arrays would extend radially outward from the hole and as the image rotated, each detector element would scan a circular band concentric with the sun's center.

For the UV and visual arrays, EOS UV-sensitive silicon detectors would be used. The elements are formed on a single chip of silicon by photo-etching techniques and are .005 inch wide measured along the array and about .04 inch long, measured across the array. An identical geometry would be used for the IR array which, however, would be made of PbS cells.

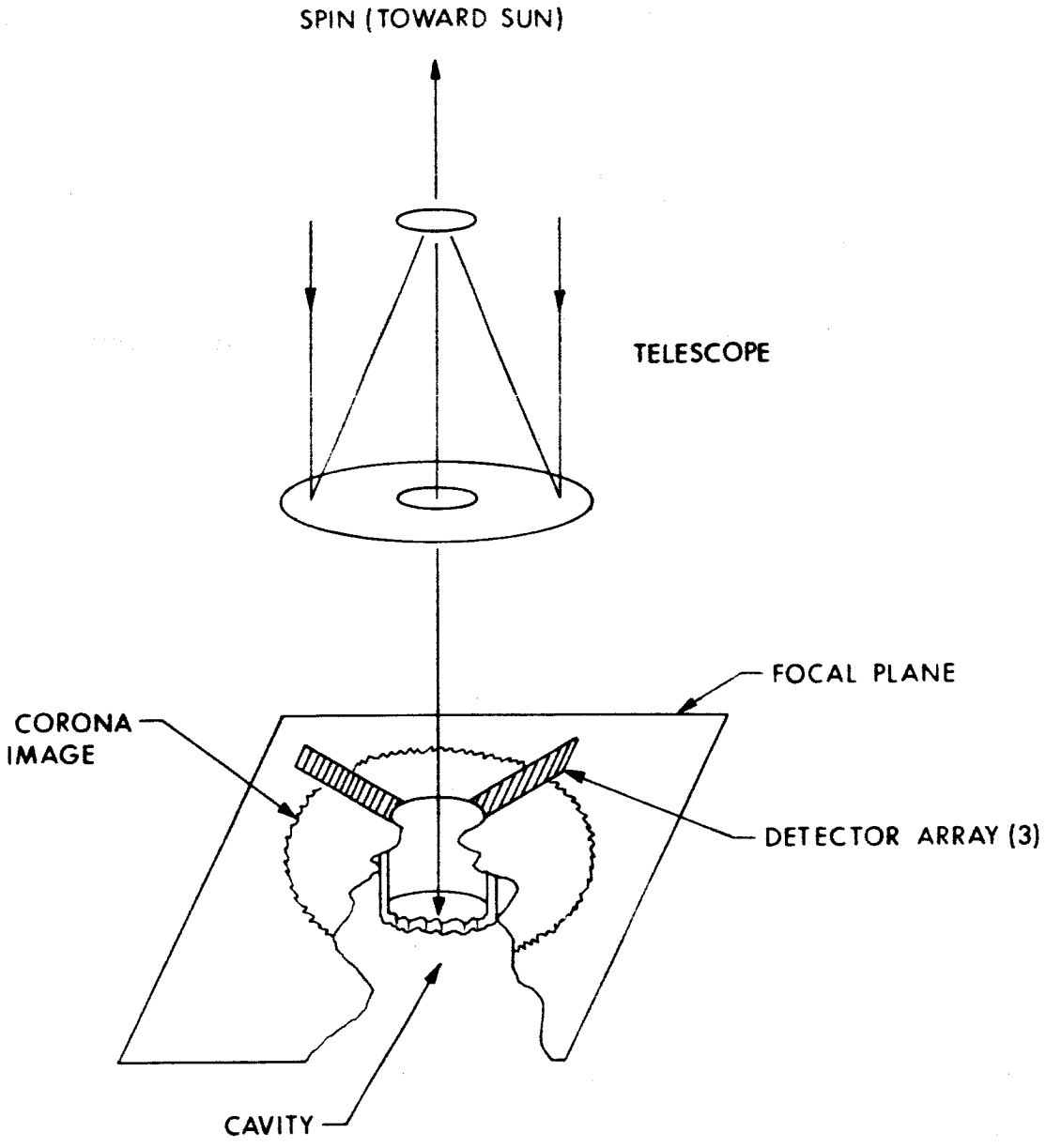

FIG. 2-6 CONCEPTUAL SKETCH OF CORONAGRAPH

The ECS detector is sensitive to wavelengths < 3000Å and to wavelengths between 4000Å and 10000Å, hence it can be used both as a UV and a visual detector. It is difficult to filter out the visual spectrum, leaving only the UV, but the opposite process is easy, hence, the UV energy would be found by a subtraction process. One silicon detector would receive unfiltered light and would therefore measure the sum UV + Vis. The other detector would receive light from which the UV had been removed by a simple absorption filter and would measure the visual energy only. From the two outputs, the UV energy could be computed. The PbS array would receive light of wavelengths > 1μ only, for which it is easy to find filters.

2. Electronics

Owing to the large number of detector elements, 20 per array, it is more economical to sample the detectors repetitively rather than to attempt to telemeter or store all outputs in parallel.

The basic electronic system would therefore consist of a commutator, an amplifier, a programmer, and a power converter.

3. INSTRUMENT SPECIFICATIONS

Dimensions: Optical system - 6 in. dia. x 12 in. long
Electronics: 1 x 2 x 4 inches

Weight ~ 5 lbs

Power ~ 5 watts

Data: 20 channels; 6 bits/second continuously

Magnetic interference: Not susceptible. Shielded to protect other circuits.

Thermal: -20°C to +65°C

Mounting: Must view sun directly and continuously

Preferred Orbit: 1000 nautical mile modified sun synchronous

EXPERIMENT II-E

STUDY OF TEMPORAL VARIATIONS IN SOLAR ULTRAVIOLET EMISSIONS

1. DESCRIPTION OF EXPERIMENT

This experiment has as its objective the detection of temporal variations in the ultraviolet output of the sun. Comparisons of these variations with independently obtained data on solar activity should reveal interesting correlations with practical as well as theoretical value.

The sun is a dynamic entity - rotating about its axis with a latitude-dependent period, subject to violet turbulence and storms, developing prominences and flares, emitting vast fluxes of charged-particle radiation in addition to an extremely broad spectrum of electromagnetic radiations. Fortunately for man and other terrestrial life forms, the atmosphere absorbs a large fraction of these radiations. Unfortunately for the earth-bound scientist, the sun must accordingly be observed through a narrow "window" comprised mainly of the visible and near-ultraviolet regions of the spectrum. Sounding rockets and balloons, and instrumented earth-orbiting satellites of growing sophistication are circumventing this atmospheric window, but the data are still fragmentary and in particular need to be supplemented with extended measurements which will reveal both periodic and random fluctuations in the solar output. Such information will be of great value in providing a deeper insight into the mechanisms and processes underlying the sun's behavior.

Man's interest in the sun is not exclusively academic. The absorption of solar radiations which restricts the astrophysicist so severely results in the production of ozone in the upper layers of the atmosphere and in other photochemical reactions. The outer regions of the atmosphere are strongly ionized, and tremendous quantities of heat are dumped into that part of the atmosphere facing the sun. Changes in the solar output in one portion of the spectrum can significantly alter the atmospheric absorption in other spectral regions because of intermediate factors.

Meteorologists in particular are interested in these processes since they have profound influences on the weather. Radio communications similarly show a close relationship to the vagaries of solar activity because of the effects on the propagation of radio waves which result from changes in the structure of the ionosphere. Other considerations could be cited.

2. DESCRIPTION OF INSTRUMENTATION

The solar ultraviolet spectrum is divided into five unequal bands, the limits of which are determined by the sensitivity of the detectors and the characteristics of their associated filters. A two-coordinate solar aspect sensor is also provided to permit conversion of the sensor outputs to equivalent outputs for normal illumination. The radiation sensors are sampled sequentially by a commutator, permitting a single amplifier to be used for all energy bands. A reserve amplifier will automatically assume the function of the primary amplifier should the latter fail. In addition, housekeeping sensors are included for monitoring critical temperatures and voltages. A simplified block diagram of the instrument is shown in Fig. 2-7, and a sketch showing the external outline of the instrument in Fig. 2-8.

The sensors are vacuum photodiodes with cathodes chosen to cover the appropriate spectral ranges. Their characteristics are summarized in Table II-1, below.

TABLE II-1

SENSOR CHARACTERISTICS AND FILTER SPECIFICATIONS

Sensor	Eff. λ	$\Delta\lambda$	Cathode	Filter	ASCOP No.
P_1	2600 Å	600 Å	CsTe	Sapphire, fused SiO_2, Calcite	540F-05
P_2	2100	450	CsI	Sapphire, fused SiO_2, ADP	540G-05
P_3	1800	300	CuI	Sapphire, fused SiO_2	540H-05
P_4	1600	150	RbI	Sapphire	540K-05
P_5	~ 1 to 1400		W	None	549-4011A

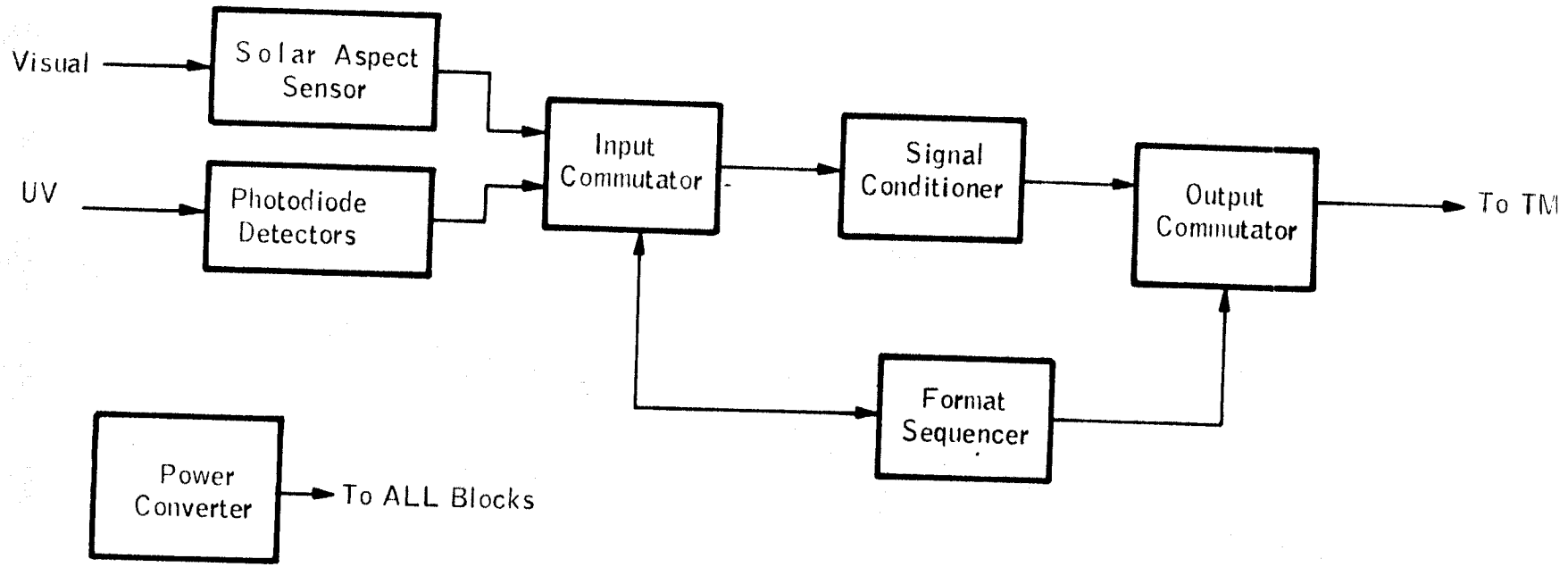

FIG. 2-7 SIMPLIFIED BLOCK DIAGRAM OF SOLAR ULTRAVIOLET INSTRUMENTATION

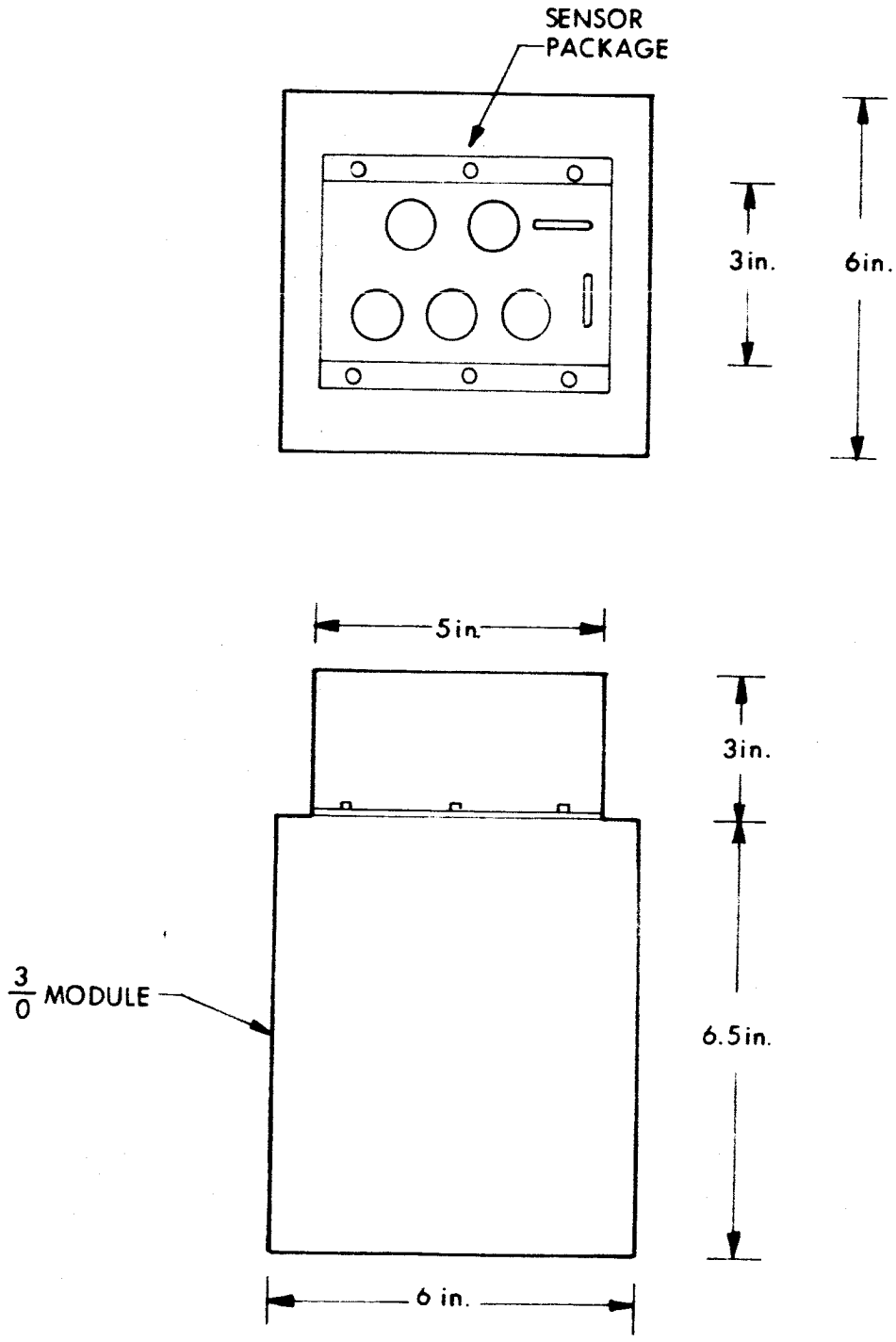

FIG. 2-5 EXTERNAL OUTLINE OF SOLAR UV IN[illegible]

6961-Final(31)

The photocurrent amplifier covers four decades with automatic range switching. Full scale currents are 10^{-10}, 10^{-9}, 10^{-8}, and 10^{-7} ampere. Four current standards of the above values are incorporated into the instrument for calibration purposes and are sequentially connected to the amplifier input by the commutator. The experiment cycle time is 45 seconds, 3 seconds being allotted to each current standard and 5 seconds to each UV sensor. The remaining time (5 seconds) is allocated to housekeeping functions. Temperatures of the photocathodes and of the amplifier feedback resistors are monitored, making it possible to achieve an electrical accuracy of 1 percent of full scale and an overall long-term accuracy of 10 percent for each of the five energy bands.

A block diagram of the circuitry of the sensor package (SP) is shown in Fig. 2-9. S_1 is a thermistor for measuring the temperature of the photocathodes. The commutator is a group of glass-encapsulated high-insulation reed relays controlled by the formatting logic. Four of the photodiodes have sapphire windows and three have additional filters. P_5 has a tungsten cathode which is sensitive to soft x-rays and ultraviolet radiations up to a wavelength of roughly 1400 Å. This tube has no window, being directly exposed to space, since no known window medium is transparent over this energy range. To prevent the detection of positive and negative ions, the anode is screened by two grids, one being charged positively and one negatively. The solar aspect sensor is a standard item, complete with electronics, manufactured by the Adcole Corporation. The two 7-bit digitized outputs give the position of the sun in two coordinates to ± 15 minutes of angle over a field of view in each coordinate of ± 64 degrees.

A somewhat more detailed block diagram of the electronics package (EP) is shown in Fig. 2-10. The operation is briefly as follows: the format consists of a 15-step program actuated by a one-pulse-per-second clock from telemetry or self-generated in an adapter package. The first five steps of the program are used to provide synchronization information and to read out signals from five housekeeping sensors. Two high-level analog telemetry channels are employed according to the following scheme:

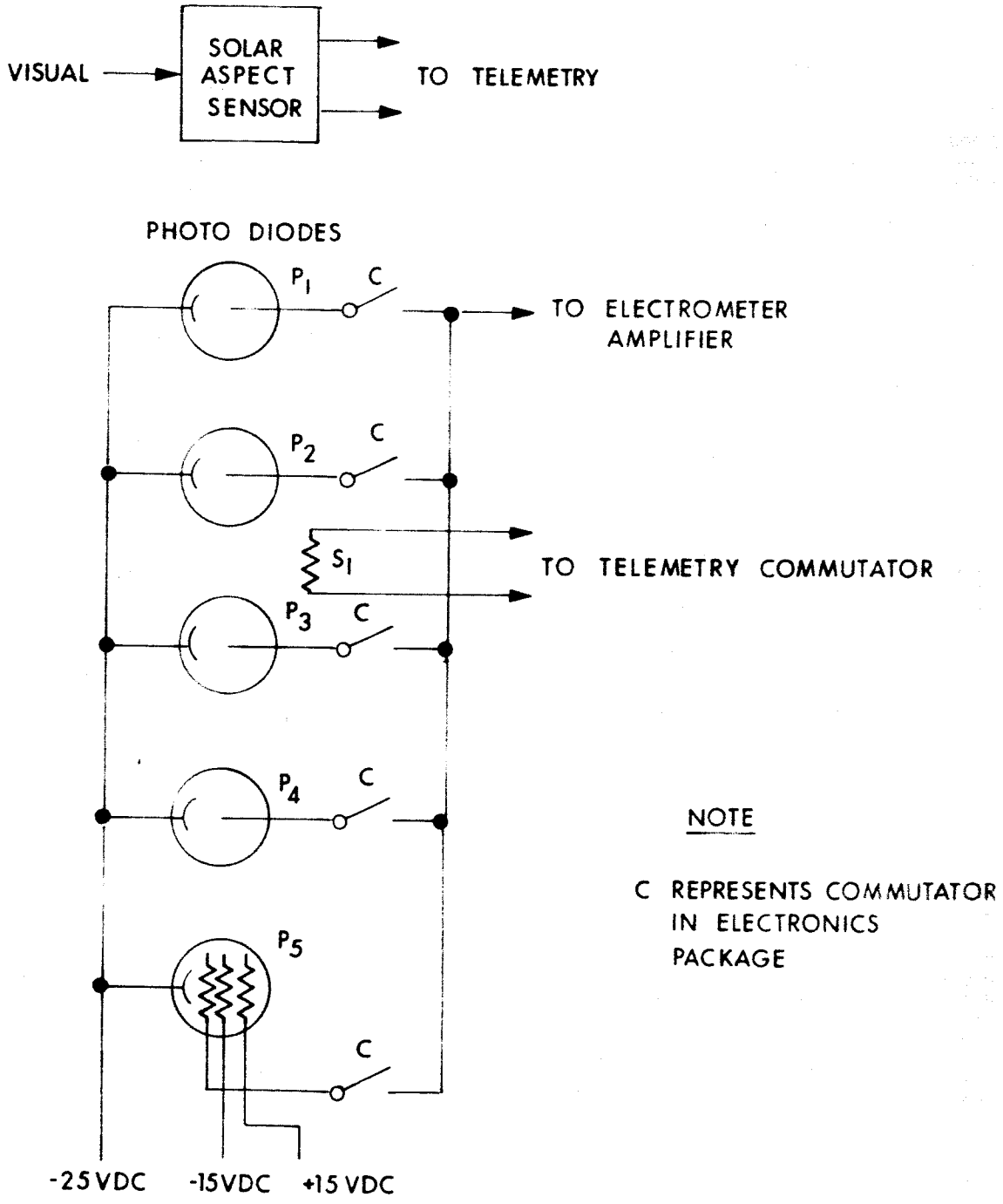

FIG. 2-9 BLOCK DIAGRAM OF SENSOR PACKAGE

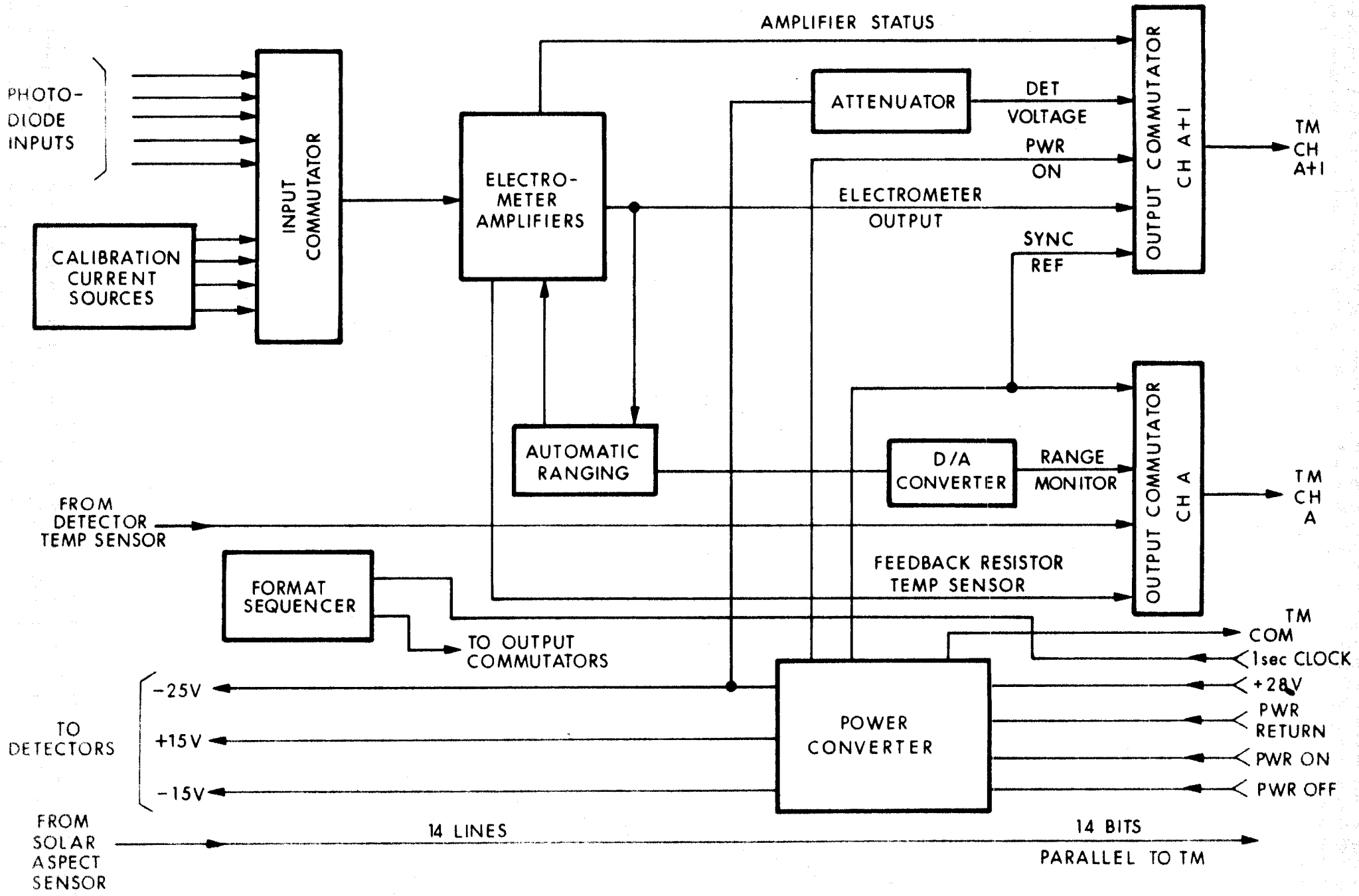
AMPLIFIER STATUS
PHOTO-
DIODE
INPUTS
INPUT
COMMUTATOR
CALIBRATION
CURRENT
SOURCES
ELECTRO-
METER
AMPLIFIERS
ATTENUATOR
DET
VOLTAGE
PWR
ON
ELECTROMETER
OUTPUT
SYNC
REF
OUTPUT COMMUTATOR
CH A+1
TM
CH
A+1
AUTOMATIC
RANGING
D/A
CONVERTER
RANGE
MONITOR
OUTPUT COMMUTATOR
CH A
TM
CH
A
FROM
DETECTOR
TEMP SENSOR
FEEDBACK RESISTOR
TEMP SENSOR
FORMAT
SEQUENCER
TO OUTPUT
COMMUTATORS
TM
COM
1sec CLOCK
+28V
PWR
RETURN
PWR ON
PWR OFF
-25V
+15V
-15V
TO
DETECTORS
POWER
CONVERTER
FROM
SOLAR
ASPECT
SENSOR
14 LINES
14 BITS
PARALLEL TO TM

Program Step	Channel A	Channel A+1
1	Sync voltage	Detector bias
2	Photodiode temperatures	Sync voltage
3	Sync voltage	Power-on voltage
4	Feedback resistor temperature	Sync voltage
5	Sync voltage	Amplifier status

The input to the amplifier is left open for the next three clock impulses and the TM channels are switched to the amplifier output and range monitor. This three-second period is used as a zero check. The next four steps of the program are used for calibration. Four current standards are switched sequentially to the amplifier input, permitting the system to be checked out in each of its four ranges. Three clock pulses are assigned to each of these steps.

The following five steps of the program constitute the prime experiment. Each of the five detectors is sequentially switched to the amplifier input for five clock pulses each. This completes the 45 clock pulses required to step through the complete format and following this the sequence recycles.

The dynamic range of four decades is achieved through the use of four different feedback resistors. These resistors are switched to provide the correct gain as determined by sensing the amplifier output. This function is performed by the automatic ranging section which also provides an analog signal to the range monitor TM channel to indicate which feedback resistor is switched in.

A spare amplifier and a failure detection circuit are also provided. If a failure of the prime amplifier should occur, the spare is automatically switched in and an indication is provided as one of the housekeeping functions.

By employing welded cordwood modules and special potting compounds, highly reliable circuitry will result. Wherever practicable, integrated circuits will be used to improve reliability and to reduce size and weight. Photodiodes P_1 through P_4 are of ruggedized construction with 0.125-inch

sapphire windows and have cathodes especially designed for operation in the ultraviolet and soft x-ray regions. The long-wavelength cutoffs are determined by the photoelectric threshold of the cathode material and the short-wavelength cutoff by the filters. Each filter is mounted with the sapphire plate facing the space environment so that there will always be 0.25 inch of sapphire, or of sapphire and fused silica, between the photodiodes and incoming high-energy charged particles. Calcite and ADP must be protected from the environment; consequently, filters containing these materials will be of sealed construction.

Photodiode P_5 has no window and no filter. Its long-wavelength limit is determined by the threshold of the tungsten cathode, but there is no sharply defined short-wavelength limit. The outermost of the three grids is connected to +15 volts and the middle grid to -15 volts. Thus, the two acting together will collect all low-energy charged particles. While high-energy charged particles will not be stopped by the grids, the flux of such particles is only of the order of $10^5/cm^2 sec$, corresponding to a current of only 1.6×10^{-14} amp. This is an order of magnitude smaller than the amplifier noise current, which is in turn an order of magnitude lower than the postulated minimum current accuracy. The innermost grid is the anode and is 25 volts positive with respect to the cathode. Photoelectrons which are not intercepted by the anode will be repelled by the negative middle grid, increasing the collection efficiency over what it would be if the middle grid were positive.

Since input resistances of the order of 10^{13} ohms must be used if the current-transfer inequality is to be satisfied for such small currents (of the order of a few picoamperes), standard bipolar transistors, even with local bootstrapping, are completely ruled out. Junction field-effect transistors (FET's) have input resistances of about 10^9 ohms and would thus require voltage gains in excess of 1000, placing them in the doubtful category. Insulated gate or MOS FET's, however, have typical input resistances of 10^{15} ohms or more and are thus ideally suited for the present application. Using such a device insures optimum current transfer for any level of gain and thus gain need be considered only

EXPERIMENT II-F

INFRARED EMISSION FROM THE SUN

1. DESCRIPTION OF EXPERIMENT

The goal of this experiment is to determine the energy flux from the sun in the IR region from 2 to 20 microns. This part of the spectrum cannot be investigated from the ground because of the wide bands of atmospheric absorption.

The short-wave limit is chosen because measurements can be made from the earth out to $\sim 2\mu$; the long-wave limit was chosen because only $\sim 10^{-5}$ of the total solar energy lies at longer wavelengths.

Although a measurement of the total power in the 2-20μ band would be useful, it would fail to reveal any departures from black-body emission, therefore, the proposed instrument is designed to have some degree of spectral resolution.

2. DESCRIPTION OF INSTRUMENTATION

The optical system is a slitless spectrograph with a multi-element detector located in the focal plane. The layout is shown in Fig. 2-11.

The first element in the optical train is a germanium prism that disperses the light to form the spectrum. The second element is a gold plated paraboloidal reflector that focuses the light from the prism onto the detector array. At any given wavelength, the parabola will form a small image of the sun, but when the whole spectrum is considered the result will be an infinite series of overlapping images. These images will have an angular diameter, measured at the parabola, of $.5^{o}$, which is much greater than the angular width of the slits in a normal spectrograph. The spectral resolution will therefore be rather low, but the data will nevertheless be far more valuable than if there were no dispersion at all.

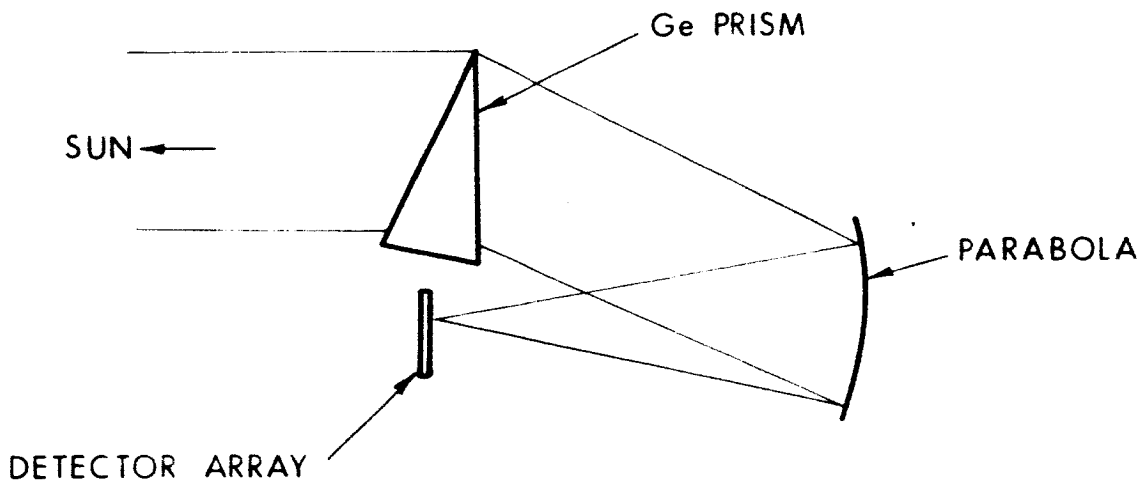

FIG. 2-11 SLITLESS IR SPECTROMETER

Owing to the large bandwidth, no one photoconductive or photovoltaic detector type could be used at all wavelengths. A thermal detector, however, is independent of wavelength, hence the detector array consists of a multiplicity of thin film bolometers, which can easily be formed by vacuum deposition on an insulating substrate. The outputs from the detector elements are sampled sequentially and either stored for later transmission or transmitted directly, depending upon the capability of the telemetry system.

3. INSTRUMENT SPECIFICATIONS

Dimensions:	Optics - 2" x 3" x 6"
	Electronics - 1" x 3" x 6"
Weight:	Optics - 1 lb. Electronics - 1/2 lb.
Power:	1 watt
Mag. Interference:	Not susceptible; shielded to protect other systems.
Electronics:	Commutator, amplifier, programmer, and power supply.
Thermal:	-20^{o} to $+60^{o}$C
Data:	1000 bits sampled twice and orbit
Mounting:	Pointed directly at sun
Preferred Orbit:	None

EXPERIMENT II-C

SEARCH FOR CHARACTERISTIC X-RAY EMISSIONS FROM THE SUN

1. DESCRIPTION OF EXPERIMENT

The purpose of this experiment is to examine the characteristic x-ray emissions of elements in the solar atmosphere, during quiet and active periods. The elements of interest are carbon, nitrogen, oxygen, neon, iron, silicon, and sulphur. The intensity of characteristic emission of these elements is a strong function of temperature, and solar flare emissions should indicate the local temperature of the flare by the spectra observed. This spectral dependence upon temperature may be seen in Fig. 2-12 where the computed x-ray spectra are shown of free-bound emission of these elements over the range of 10^7 to 10^8 degrees kelvin.[1] It is seen that the range of interest is between 0.5 and 10 keV. It should also be noted that the required resolution of an instrument able to sense this spectrum is on the order of an angstrom or less. The x-ray spectra available in this range [2,3] have been obtained from instruments such as proportional counters, scintillation spectrometers, etc., and are very gross in spectral resolution. Figure 2-13 shows several such spectra as derived from krypton-methane proportional counters[3] and illustrates the gross nature of such spectroscopy.

---

[1] Kawabata, K., 1960 Rept. Ion. Space Res. Japan, XIV:405.

[2] Frost, R. J., "Comments On High Energy X-Ray Bursts Observed by OSO I", ASA-NASA Symposium on Physics of Solar Flares, NASA SP-50, 1963.

[3] Friedman, H., "Solar X-Ray Emission - NRL Results" AAS-NASA Symposium on Physics of Solar Flares, NASA SP-50, 1963.

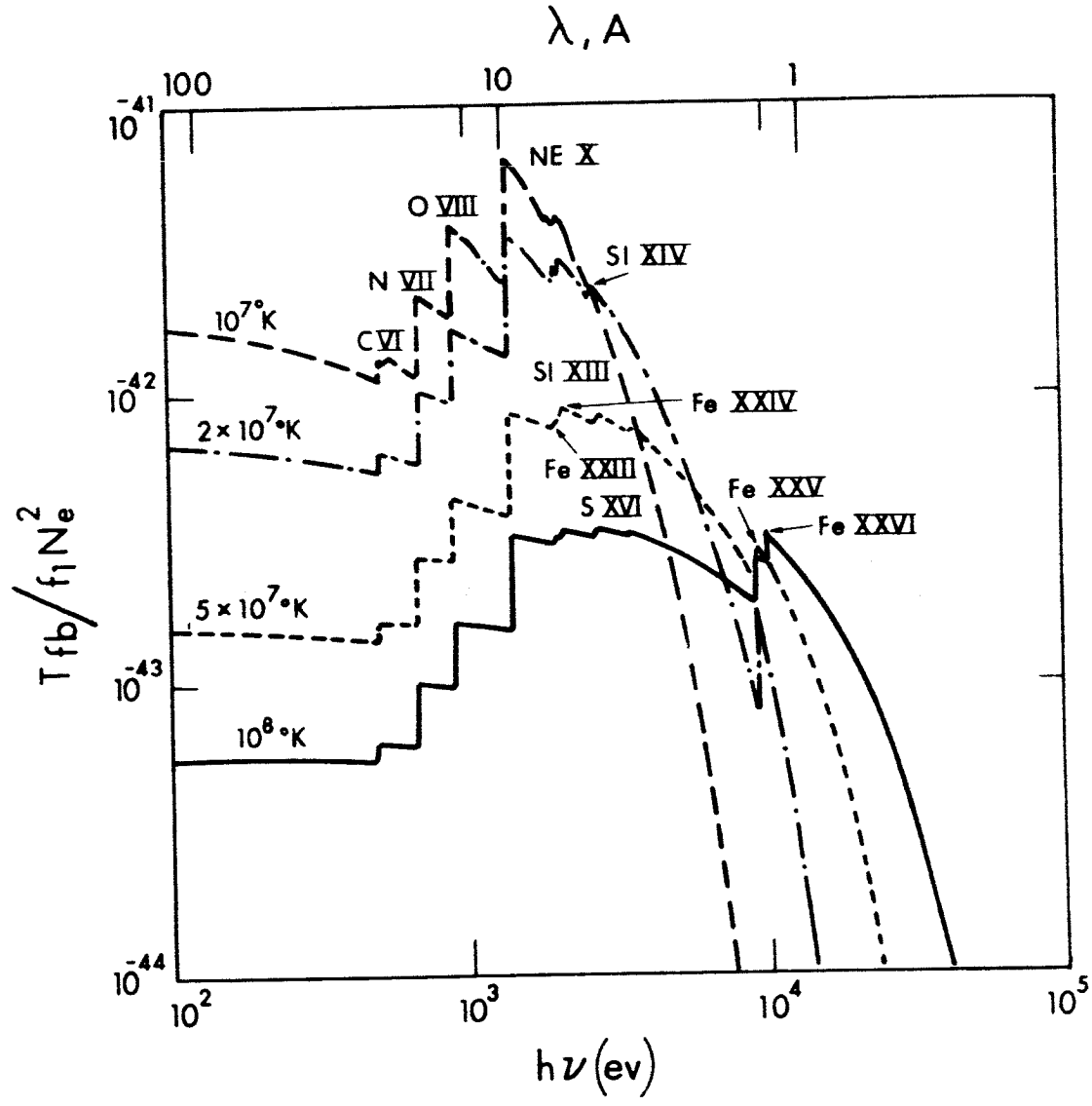

FIG. 2-12 COMPUTED X-RAY SPECTRA OF FREE-BOUND EMISSION. (After Kawabata, 1960)

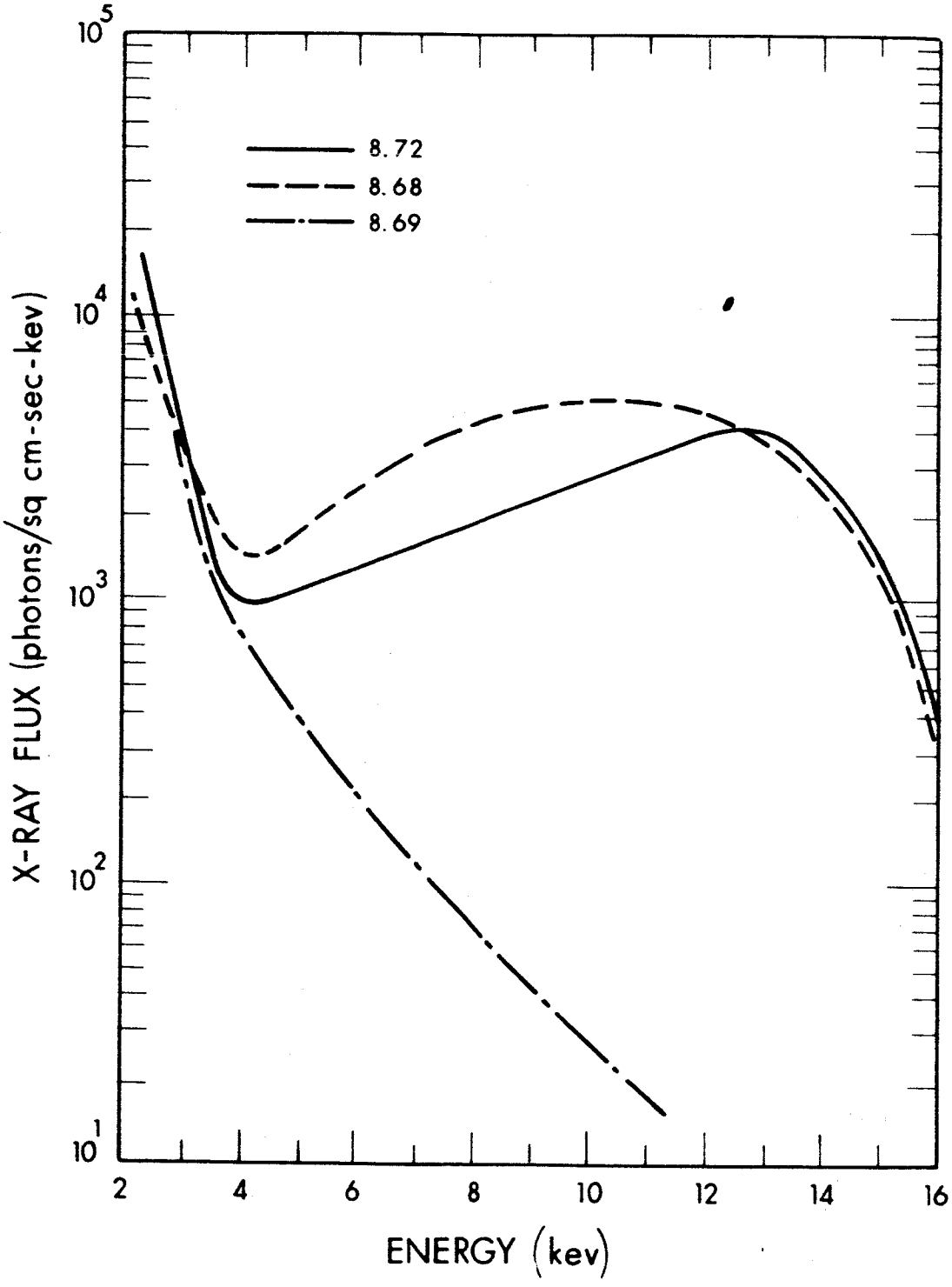

FIG. 2-13 COMPARISON OF SPECTRA OBTAINED FROM PROPORTIONAL COUNTERS ON THREE DIFFERENT FLIGHTS

2. DESCRIPTION OF INSTRUMENTATION

The instrument to be used in this experiment is of much higher resolution and has been used by various experimenters[4] in the far ultraviolet to low-energy x-ray region of solar emission. This instrument is a grazing-incidence bent-crystal spectrometer and is capable of resolving lines less than 0.85 Å apart. This is a much greater resolution capability than that of either proportional counters or scintillation spectrometers and should easily reveal the presence of line emissions (or characteristic edges of spectra such as shown in Figure 2-12 assuming these emissions can be detected above the bremmsstrahlung continuum which is present as background.

The spectrometer schematic (Fig. 2-14) shows an entrance slit, a bent crystal, diffraction analyzer, an exit slit, and an open window photomultiplier. The radiation entering the entrance slit is diffracted and focused at a point along the curved path as indicated in the figure. The exit slit and phototube scan the spectrum by moving along this curved path. The plane of the exit slit is approximately perpendicular to the diffracted ray at all positions along the scanning line maintaining a constant passband of about 1 Å. The exit slit and phototube move on a motor driven carriage traveling on a circular rail. During scanning, the speed of the carriage and exit-slit aperture can be varied as conditions of the experiment may dictate. The phototube is a Bendix M306 photomultiplier with a tungsten photo cathode which is chosen to minimize response to wavelengths above 1500 Å and to reduce sensitivity due to emission properties of the photo cathode.

---

[4] Hinteregger, H. E., "Space Astrophysics", edited by W. Liller, pp. 35-95, McGraw-Hill, 1961

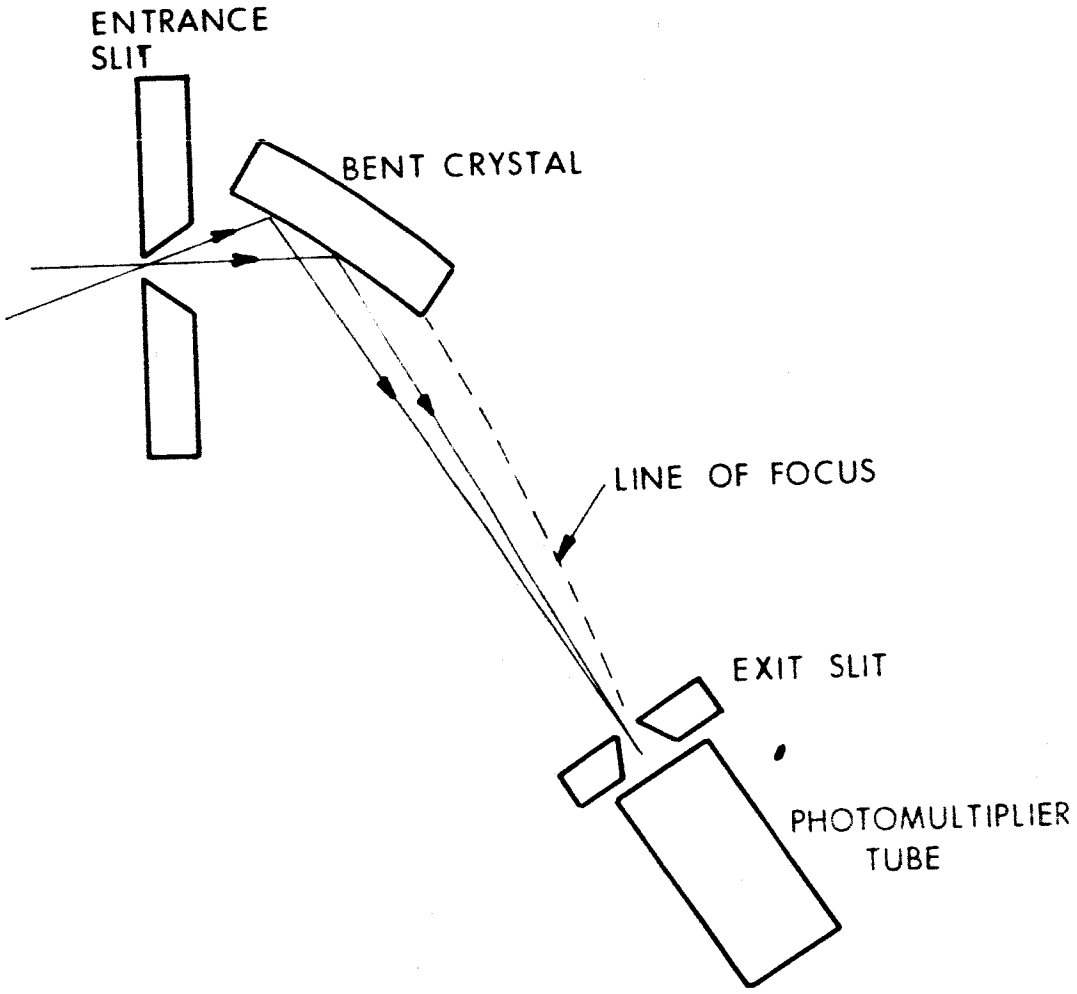

FIG. 2-14 SPECTROMETER SCHEMATIC

During operation of this spectrometer, its pointing direction should be maintained to a sufficient angular accuracy to assure that the entire solar disk is continuously observed. This is an accuracy on the order of 0.5 degree and is not a particularly stringent requirement this solar oriented satellite.

3. INSTRUMENT SPECIFICATION

Dimensions:	25" x 8" x 5"
Weight:	20 pounds
Power:	2 watts at 28 volts
Thermal:	$-25^{\circ}C$ to $+65^{\circ}C$
Data:	500 bits, twice per orbit
Mounting:	Oriented toward sun, 25" length and 25 pounds weight make mounting on secondary panels difficult but not impossible
Preferred Orbit:	None

EXPERIMENT II-H

MONITORING OF SOLAR X-RAY EMISSIONS IN THE REGION OF 0.2 TO 24 Kev

1. DESCRIPTION OF EXPERIMENT

This experiment provides a constant monitoring of the sun's x-ray emission in the region of interest to solar flare investigators. During solar flare activity, the sun's emission in this wavelength region increases greatly and the time fluctuations of intensity are of major importance in understanding flare mechanics. The increase in intensity over that of a quiet sun has been found to be roughly 4 to 1 in the region of 44 to 60 angstroms, 10 to 1 in the region of 8 - 20 angstroms, and 25 to 1 in the region of 8 to 1.5 angstroms[1]. Typical spectra produced by the use of proportional counters and pulse height analysis systems are shown in Figure 2-15. It is seen that there is some variation in spectral distribution over short periods of time. The continual observation of such intense emission in this region is of great importance tor support of optical radio and charged particle studies during solar activity.

Only a few of the many nuclear detection methods are available to the designer of an x-ray spectrometer for the .2 to 20 Kev range. The relatively low fluxes (Fig. 2-15) to be measured and the low photon energies rule out detectors such as ion chambers which provide no multiplication of the ion pairs produced by the absorption of the x-ray. Even the relatively efficient solid state detectors have noise levels of the order of 5 - 14 Kev, precluding high resolution spectrometry.

---

(1) Friedman, H., "Solar X Ray Emission - NRL Results," AAS-NASA Symposium on the Physics of Solar Flares, NASA SP-50, 1961

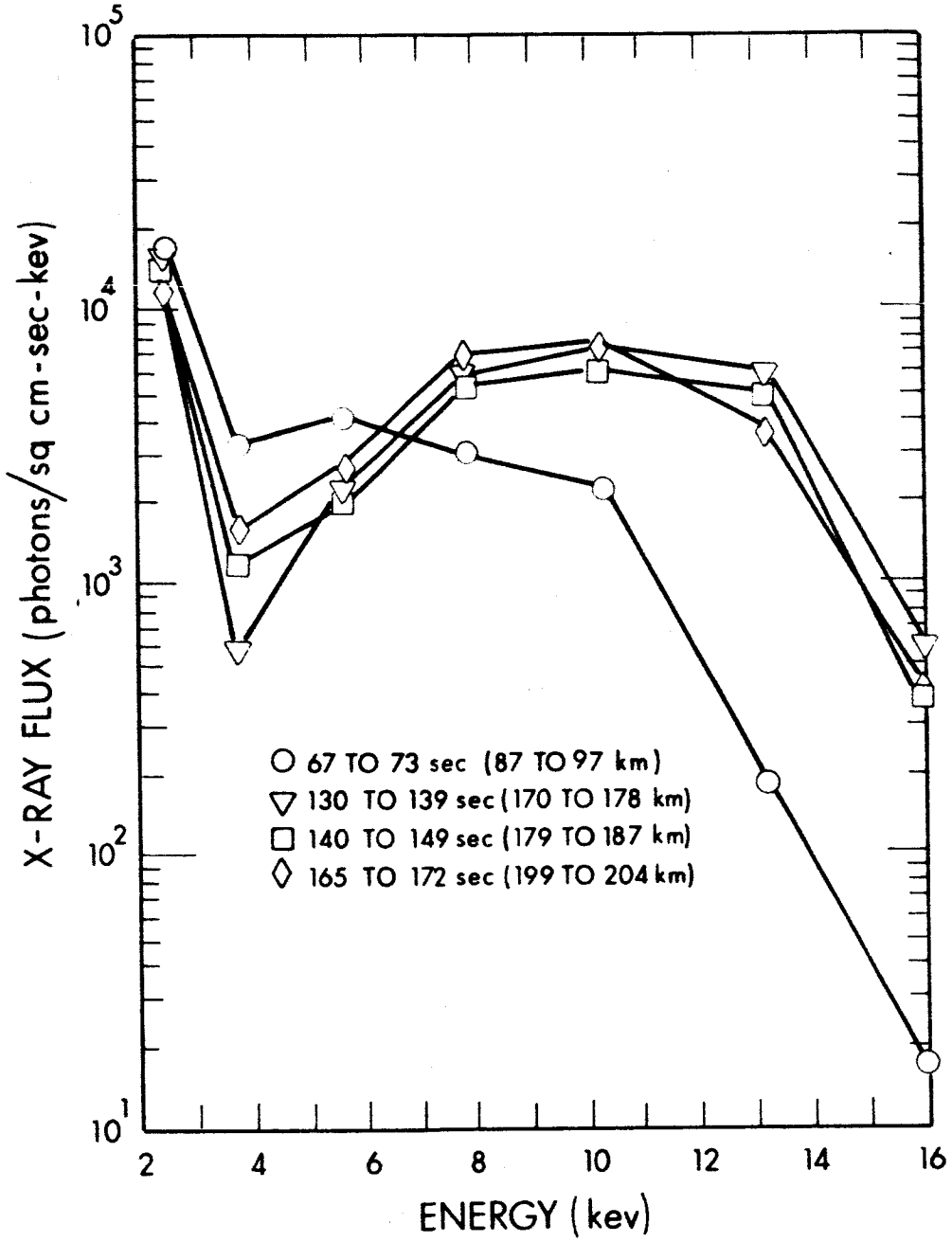

FIG. 2-15 SPECTRAL VARIATION WITH TIME

Scintillators provide high gain through electron multiplication in the photomultiplier tube yet are limited in resolution due to the dependence of their ultimate statistical error on the number of photo electrons produced per photon. (e.g., NaI scintillators produce about 15 photo electrons for a 2 Nev photon). Their resolution characteristically is about 30 percent.

The proportional counter is the best choice for a device which is to provide high sensitivity, and good resolution, for continuous operation. In this device ion pairs, produced in a cylindrical gas filled tube by the photon entering through a thin window, are accelerated toward a thin wire electrode. The fields are strong enough at the thin wire to produce avalanche and ion multiplication in the gas. Multiplication factors from 10^4 to 10^6 are easily achieved and resulting resolution can be less than 20 percent full width at half maximum. Pulse height analysis of the output pulse is an accurate and straightforward method of energy analysis that is well developed and understood.

2. DESCRIPTION OF INSTRUMENTATION

The instrument necessary for this experiment is a side window proportional counter which is 4 inches long and one inch in diameter with a 0.0005 in. beryllium window (with 0.2 in. diameter aperture) in the side of the tube (Fig. 2-16). The fill gas is argon at 2 atmospheres which is sufficient to absorb the greater part of 24 Kev x-rays impinging on the window. The tube will be used with a collimator at the window and sufficient shielding external to the tube to stop all soft and intermediate energy particles. The window and collimator are open to solar flare protons during observation of the solar flare activity; however this radiation is, for the most part, isotropically produced at the earth's distance and only a small solid angle will accept these protons. Magnetic field shielding of the collimator may be used to advantage especially if the satellite orbit is in the trapped radiation belt. The necessity of these precautions for reducing the background is lessened if a low orbit is allowable (i.e., 325 mile circular).

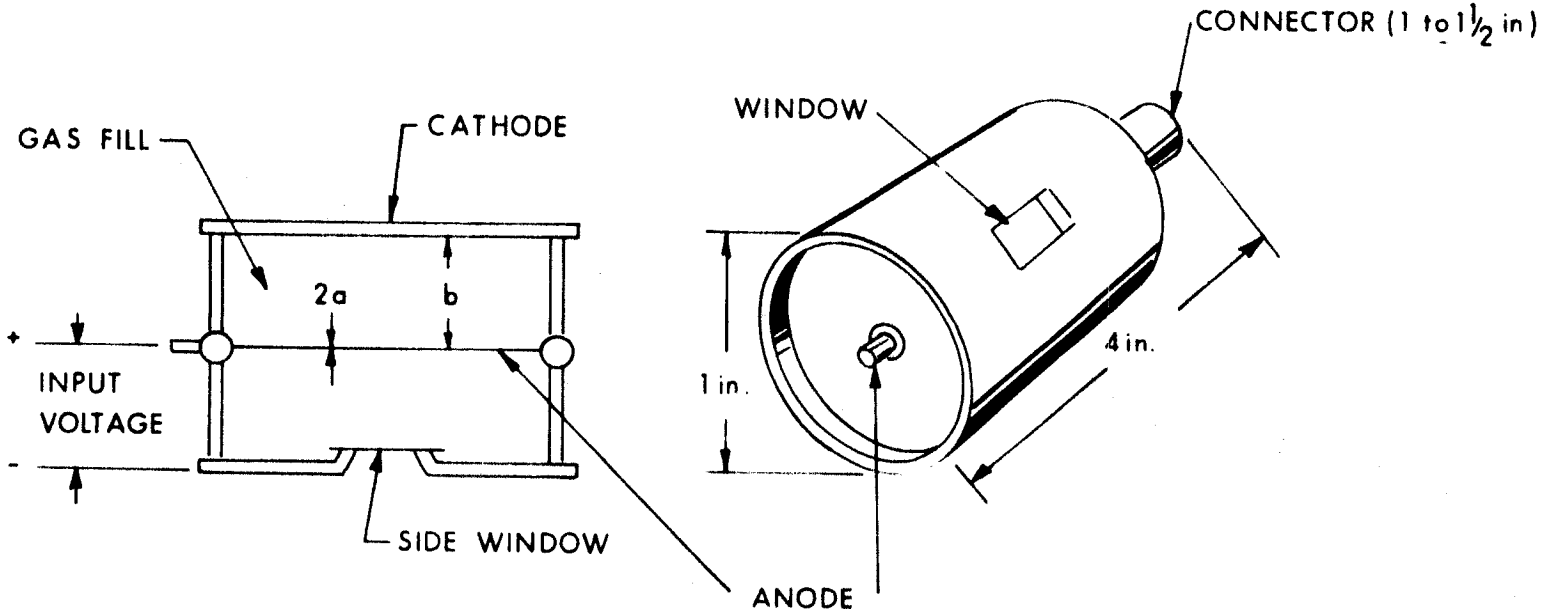

FIG. 2-16 SOFT X-RAY PROPORTIONAL COUNTER

The proportional counter system includes a pulse height analyzer with 12 channels in the following energy allotments:

Channel	Energy Range
1	0.2 - 0.4
2	0.4 - 0.6
3	0.6 - 0.8
4	0.8 - 1.0
5	1.0 - 1.5
6	1.5 - 2
7	2 - 3
8	3 - 6
9	6 - 10
10	10 - 14
11	14 - 18
12	18 - 24

The energy ranges are of course flexible and may be assigned any width reasonable to the abilities of the subsequent data handling circuitry.

The system diagram shown in Fig. 2-17 includes an in-flight calibration source for check against drift in system gain during operation.

3. EXPERIMENT SPECIFICATION

Dimensions:	Length: 7"
	Width: 5"
	Height: 6"
Weight:	5 lb
Power:	1.5 watts at 28 volts
Thermal:	$-30^{\circ}C$ to $+60^{\circ}C$
Data:	100 bits/min continuously
Mounting:	Sun-oriented
Preferred Orbit:	325 nautical mile circular

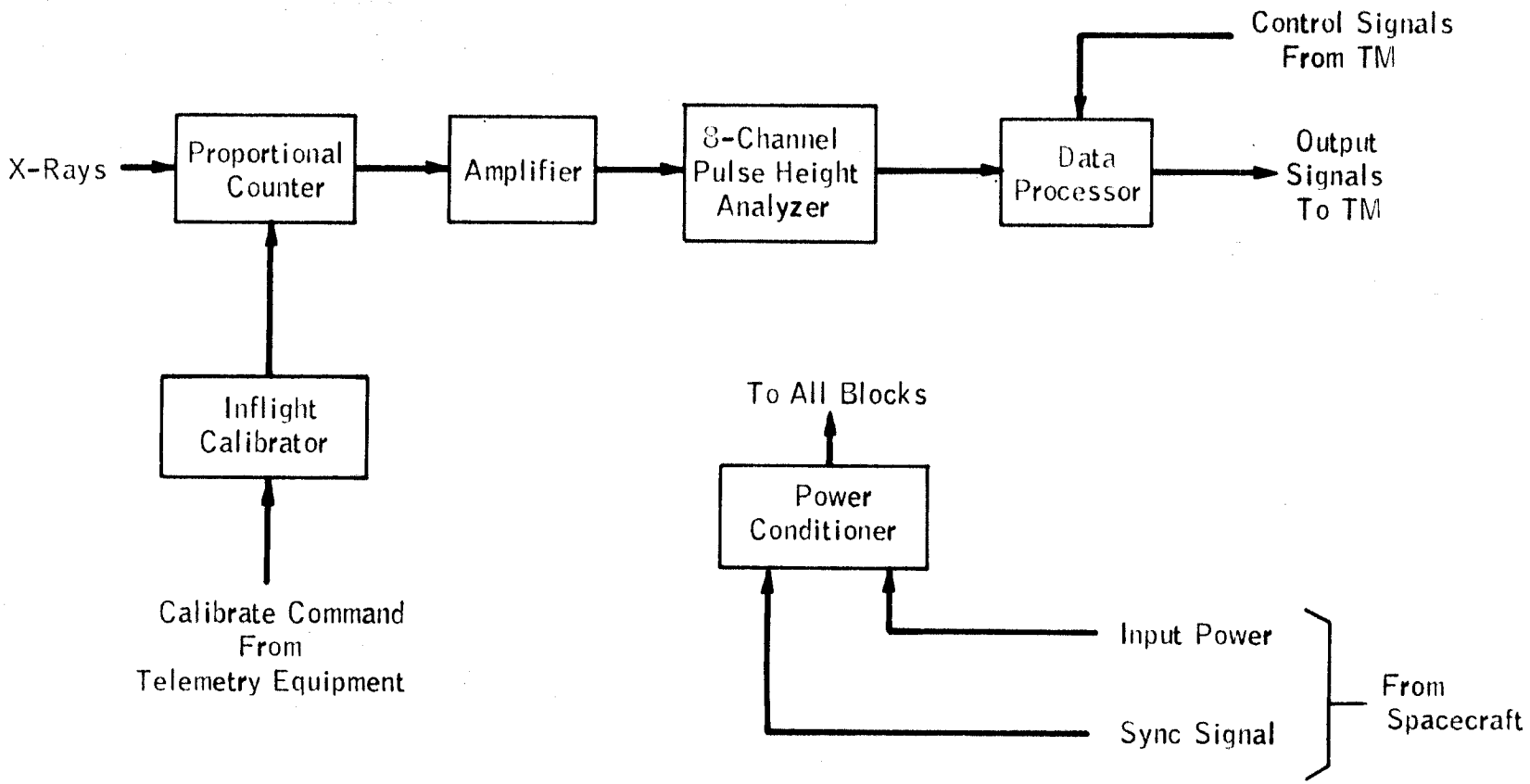

FIG. 2-17 SPECTROMETER FUNCTIONAL BLOCK DIAGRAM

EXPERIMENT II-I

EXTREME ULTRAVIOLET SPECTRUM OF THE SUN

1. DESCRIPTION OF EXPERIMENT

Extreme ultraviolet radiations from the sun are known to be very strongly absorbed in the upper parts of the terrestrial atmosphere. Therefore, their measurement requires experimentation at altitudes high above the earth's surface.

Briefly, the approximate end of the solar spectrum as photographed from the ground is 3000Å. From this point to 2085Å the spectrum is a continuum with Fraunhofer lines similar to the spectrum at longer wavelengths. At 2085Å the continuum level falls abruptly and finally fades into stray light background near 1550Å. Below 1550Å, the solar spectrum is predominately composed of emission lines--with the Lyman continuum conspicuous in the interval 912Å to 800Å.

The solar spectrum has been described by Tousey and others as arising from different levels in the sun's atmosphere, depending on wavelength and atomic species producing the radiation. The emission lines arise from atoms in different stages of excitation, located from low levels at the bottom of the chromosphere, through the region of rapidly increasing temperature, and into the corona itself. As the wavelength decreases the continuum changes from the photospheric continuum with Fraunhofer lines to an emission from the bottom of the reversing layer, with Fraunhofer lines showing only faintly, and finally, into emission from levels low in the chromosphere where the temperature has commenced to rise. The spectrum below 1550Å must arise largely from this last region since its nature is a continuum with lines in emission rather than absorption.

The great remaining unexplored region of the spectrum lies below about 300Å and extends to about 1Å. It has been established from photon-counter and ion-chamber work that radiation is present. Rense has reported photographing lines to 84Å and Hinteregger has already made

photoelectric spectral measurements in this region. The nature of the spectrum is not well established, however, and much more work is needed.

From the point of view of range in wavelength, this part of the spectrum is very extensive. The region from 300Å to 1Å spans roughly the same number of octaves as the entire solar spectrum above 300Å. Although the total energy of the solar emission in this spectral tail is small, the ionizing and energetic nature of the radiation makes it most important. Detection and study of these emissions will contribute greatly to our understanding of the process by which energy travels out through the sun's atmosphere, eventually finding its way to earth.

2. DESCRIPTION OF THE INSTRUMENT

The telemetering monochromator described in the following paragraphs is an adaptation of the GRD rocket monochromator developed by Hinteregger[1].

Photoelectric techniques of solar EUV spectrophotometry not only allow direct telemetry of data, but also can be made so that the instrumental sensitivity to all stray light of longer wavelengths is virtually eliminated. Furthermore, for a photoelectric detector, there is no accumulation of background due to penetrating radiations.

The GRD monochromator is shown in Figure 2-18. It is designed to accept gratings ruled on interchangeable blanks of 2 meter radius of curvature. The ruling with 7500, 15,000, or 30,000 lines per inch provides a convenient choice of instrument scanning range of wavelengths as follows:

RULING (Liner/inch)	RANGE (Å)
7,500	1300-250
15,000	650-125
30,000	325-62

[1] Hinteregger, H. E., "Space Astrophysics," ed. W. Liller, pp 35-95, McGraw-Hill Publishing Co., 1961.

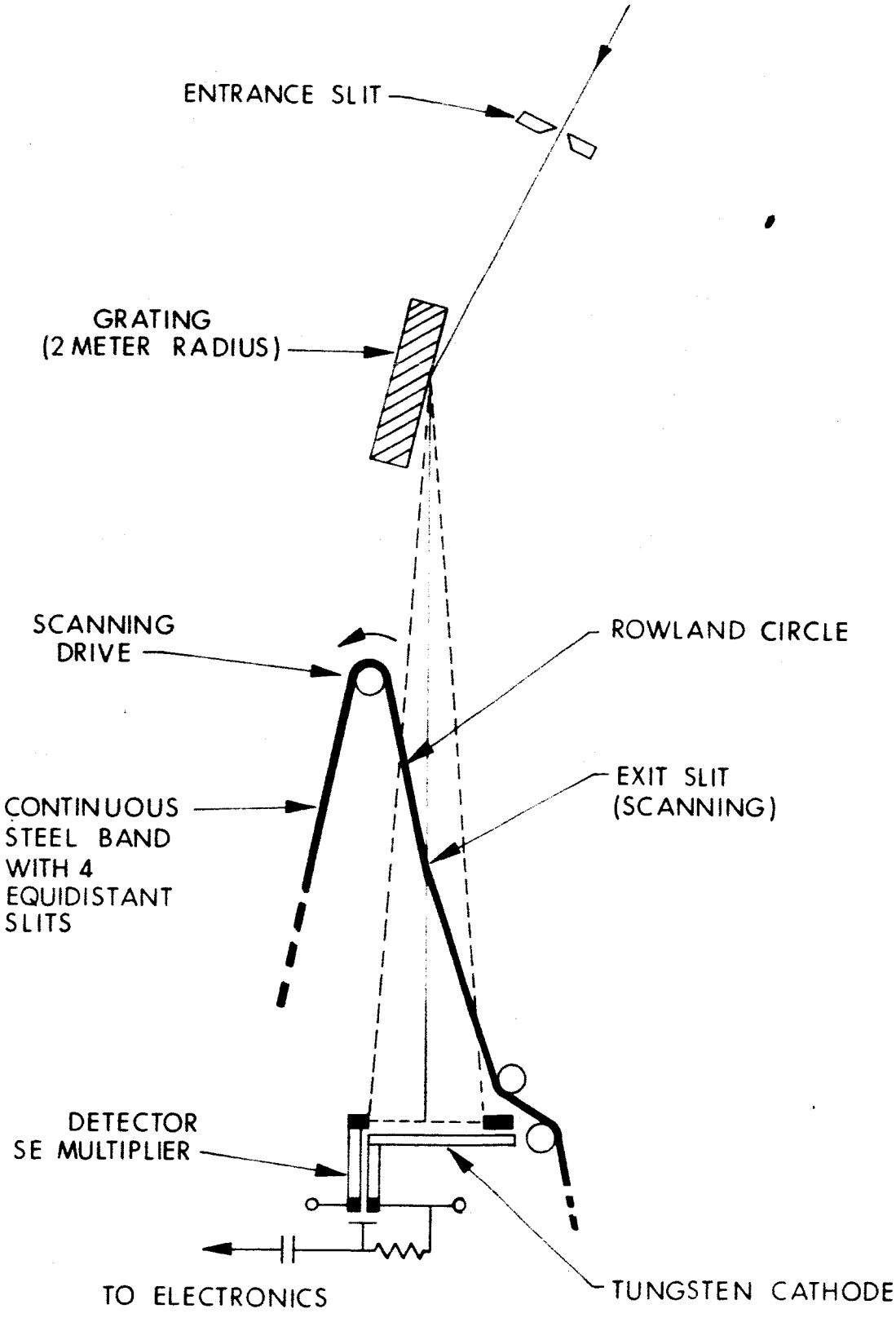

FIG. 2-18 SCHEMATIC ILLUSTRATION OF GRID REPLICA ON MASTER

The wavelength range extending from 325Å to 62Å is especially appropriate to this experiment, and a 30,000 lpi grating will be used.

The grating is held rigidly in a fixed mount for graying incidence at an angle of 86°. The dispersed radiation that passes through the exit slit at any position of the latter during its scan along the Rowland circle is intercepted by the large cathode (1 in x 3.5 in) of a special photomultiplier which is allowed to remain in a fixed position.

The electronic operation of the monochromator is indicated in the block diagram of Figure 2-19. The output pulses of the photoelectron counter are fed into a pulse shaper and amplifier which is connected to two independent banks of binary counters. Each of these scalers is combined with a resistor network which converts the events of subsequent photo-electron counts into a staircase voltage. Referring to Fig. 2-19, Channel III indicates the momentary position of the exit slit along the Rowland circle. This signal has a step voltage superimposed on it whenever a new wavelength scan is started.

The GRD instrument was designed to work with the same type of solar pointing control that was developed by the University of Colorado. The device has been used with good success for many past experiments involving spectrometry solar radiation.

3. INSTRUMENT SPECIFICATIONS

Dimensions:	Length:	36 inches
	Width:	8 inches
	Height:	4 inches
Weight:	23 pounds	
Power:	14 watts at 28 volts	
Thermal:	-20°C to +60°C	
Data:	2500 bits/readout	
Mounting:	Sun-oriented:	length and weight male mounting on secondary panels difficult
Preferred orbit:	None	

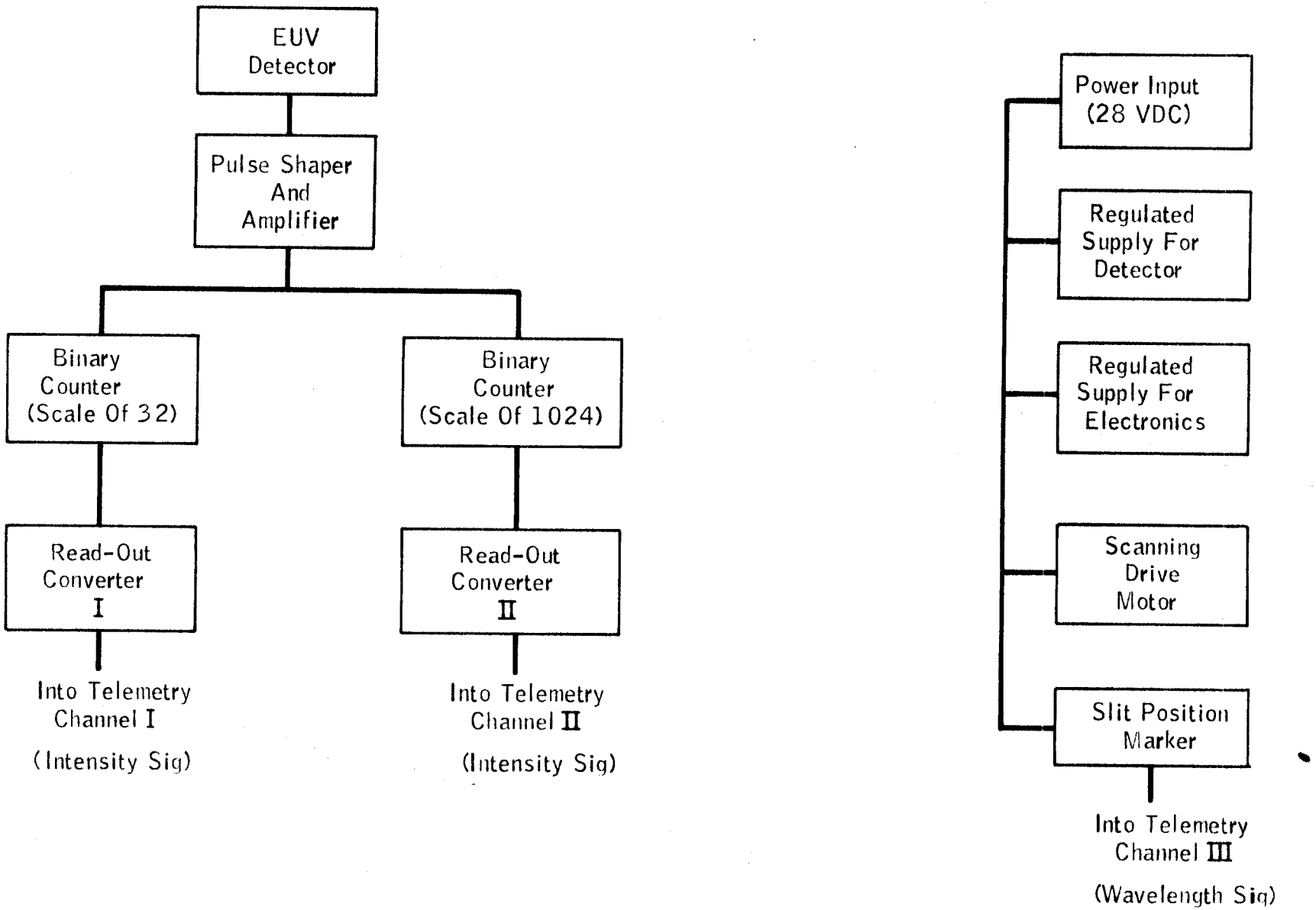

FIG. 2-19 BLOCK DIAGRAM OF ELECTRONIC OPERATION OF TELEMETRY MONOCHROMATOR

EXPERIMENT II-J

PROFILE OF SOLAR LYMAN α

1. DESCRIPTION OF EXPERIMENT

Within the last twenty years, a large amount of data has been gathered on the short-wave radiation from the sun.[1] Of particular interest are the strong Lyman α radiations centered at 1215.67Å. A rocket-borne experiment conducted by Purcell and Tousey[1] with a high resolution spectrograph obtained results which present an excellent profile of the Lyman α band, and show an absorption line from hydrogen in the upper atmosphere.

A high resolution spectrometer flown on a solar oriented satellite would produce additional data of great scientific value. The higher altitude of the satellite would eliminate, or at least minimize the effects of atmospheric hydrogen. An eccentric orbit would be most useful in providing an accurate measurement of the distribution of atmospheric hydrogen. Data from the apogee regions of an eccentric orbit would allow measurements of hydrogen density in interplanetary space to be made.

A satellite-borne instrument has the additional virtue of providing a long measurement lifetime. A one year useful life will provide spectral data over a period of several solar days, and stands an excellent chance of providing data during a number of solar flares. The data obtained from satellite flight would thus provide far more information than could possibly be obtained from many rocket flights.

---

[1] NRL Report 5608 - Papers Presented at the Tenth International Astrophysical Symposium, by Purcell and Tousey

[2] NRL

2. DESCRIPTION OF INSTRUMENT

The most suitable instrument for this study is a grating spectrometer using a high order diffraction to obtain the necessary resolution. The resolution should at least be equal to the 0.03Å obtained by Purcell and Tousey[1] in their rocket flights. A preselection grating must be used ahead of the entrance slit to minimize response to longer wavelengths. An Ebert type spectrometer (Figure 2-20) using a spherical mirror and curved slits is used to image the Lyman α region with high resolution. The exit slit can be replaced by a suitably shaped solid state photodiode as the detector. Such a detector has the advantage of possessing no sensitive area not used to provide data. A photomultiplier tube for example, has a large sensitive area which contributes to the noise, but not to the data.

The data system (Fig. 2-21) consists of a range switching preamplifier providing analog amplitude data within each decade, and a digital decade indicator. The analog data is readily convertible to digital form for telemetry. Wavelength information is derived directly from the logic circuitry used to drive the grating stepper motor.

All of the circuitry can be designed to withstand the launch and space environment without difficulty.

3. INSTRUMENT SPECIFICATIONS

Dimensions: 6" x 8" x 20"

Weight: 12 lb

Power: 2 watts average at 28 volts

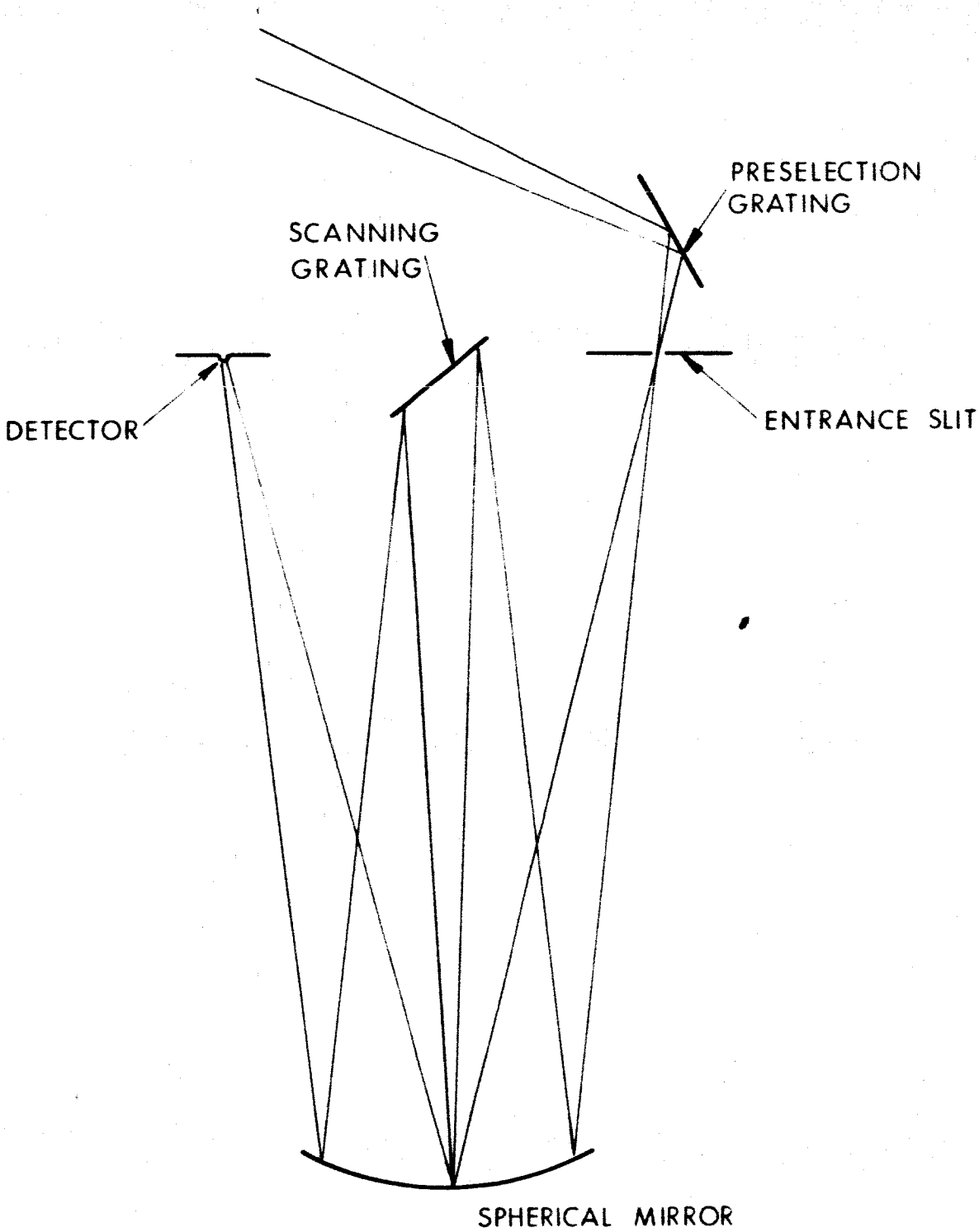

FIG. 2-20 EBERT SPECTROMETER

753

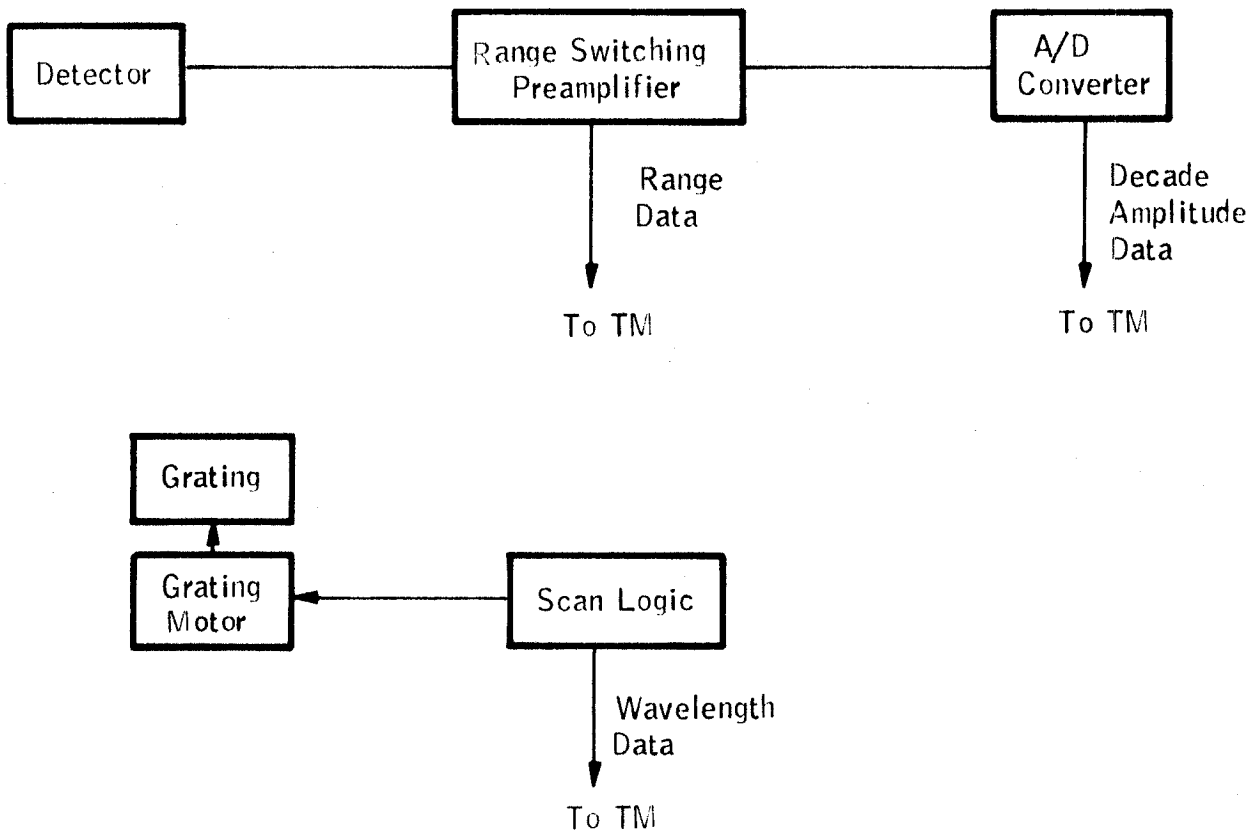

FIG. 2-21 BLOCK DIAGRAM OF LIMAS 4 PROFILE SPECTROMETER

Magnetic

Field produced by drive motor can be shielded as necessary.

The instrument is not susceptible to external fields.

Telemetry

20 bits per second for a 0.02 A/second scan rate.

Thermal

$-10^{o}C$ to $+55^{o}C$

Data

20 bits/second for 0.02 A/second scan rate

Mounting

Sun-oriented

Preferred orbit

Highly elliptical, 200 nautical mile to 25,000 nautical mile

III

PARTICLES AND FIELDS

1. BACKGROUND

1.1 Energetic Particles

The energetic particles discipline is mainly concerned with the study of particles of energy greater than a few electron-volts which are found in the trapped and auroral radiation, solar and galactic cosmic radiation and interplanetary plasmas. The interaction between the charged particles and the magnetic fields is such that they must often be studied simultaneously on the same vehicles in order to understand the phenomena. It is also necessary to make simultaneous measurements at widely separated points, such as on the ground, above the earth in balloons and sounding rockets, in the near magnetosphere using polar nearly-circular satellite orbits, in the far magnetosphere and just beyond using highly eccentric satellite orbits, and in interplanetary space. Some of the phenomena is related to the 11-year solar cycle, and is necessary to monitor them over an 11-year period.

1.2 Galactic cosmic radiation

Galactic cosmic radiation consists of a low flux of electrons, protons, alpha particles and nuclei of heavier atoms. These particles range in energy from a lower limit below 10 MeV to an upper limit in excess of 10^{19} electron volts. The flux varies by a factor of two over the 11-year solar cycle and occasionally decreases sharply for a few days after a solar flare - the so-called Forbush decrease.

The origin of the particles, the mechanism by which they are accelerated to high energies, the nature of the mechanism (or mechanisms) which produces the 11-year solar cycle and the Forbush modulation of the flux - these are some of the questions to be answered.

1.3 Solar Cosmic Rays

After some major solar flares, the intensity of the positively-charged component of cosmic rays has been observed to increase by an amount which varies from barely detectable increases up to increases four orders of magnitude above the cosmic ray background for particles in the energy range from one to several hundred MeV. These particles are given the name solar cosmic rays. The intensity reaches a maximum about one to ten hours after the flare and then begins to decrease, returning to the normal background cosmic ray value about one week after the flare. There is considerable variation in the intensity, duration and energy spectrum from event to event. Solar activity prior to the solar flare and the resulting changes in the interplanetary magnetic fields influence the time required for the particles to reach the earth, the energy spectrum, and the duration and intensity of the event. Therefore, it is important to monitor continuously the intensity of the radiation in interplanetary space, together with measurements of the interplanetary magnetic field. Information is needed on as many of the events as possible to improve statistical interpretations.

1.4 Trapped Radiation

The trapped radiation exists in the region around the earth known as the magnetosphere. Trapped radiation is observed from about 400 miles above the surface of the earth out to the boundary of the geomagnetic field which occurs at about 40,000 miles on the sunlit side of the earth. The geomagnetic field and the trapped radiation appear to terminate at the same place. The characteristics of the

radiation vary with position in the trapping region. There is an inner region which is stable with time and characterized by a high intensity of protons with energies in the range from a few keV to several hundred MeV. The energy spectrum has been observed to vary with position but there is very little variation in intensity with solar activity. Although this region is characterized particularly by high energy protons, there is also a high flux of electrons. Farther out, at about 10,000 miles, there is a region characterized by a high flux of low energy protons. This may be the region associated with the geomagnetic ring current. Also in this region, the trapped radiation is characterized by electrons with energies extending up to several MeV, exhibiting large temporal and spatial fluctuations in their intensity. The lower energy electrons, below about 1 MeV, are found to be precipitated more or less continuously into the upper atmosphere in such numbers that, were there no sources, they would disappear entirely from this outer region in a few hours. This leads to the hypothesis that there must exist one or more mechanisms for the acceleration of such particles in the vicinity of the earth to replenish the supply and populate the outer region.

1.5 The Magnetic Field

The magnetic field investigation encompasses measurement of the magnetic fields of the sun, planets, and natural satellites of the solar system, and of interplanetary and galactic space. Since none of the missions penetrate the magnetosphere, only measurements and correlation about the earth area applicable to this study.

Experiments are to be carried out in conjunction with the scientific investigation of the physical processes causing the fields and their time changes. Simultaneous measurements of particle fluxes and plasma densities are required to understand the interaction between these phenomena and the magnetic field.

EXPERIMENT III-A

SPECTRA OF GALACTIC ELECTRONS

1. DESCRIPTION OF EXPERIMENT

Before 1960, no evidence existed to indicate a flux of galactic electrons at the top of the atmosphere, although a balloon experiment designed to detect them had been undertaken in 1949. The upper limit of any primary cosmic-ray electron flux was estimated to be about $13\ m^{2}sec^{-1}sr^{-1}$ from the data recorded in that flight. However, during 1960 balloon-borne instruments flown by Earl[2] and by Meyer and Vogt[3], independently, there was detected a small component of the electron flux which could not be accounted for by secondary electrons or other means. One of the groups used a cloud chamber similar to that flown in the 1949 experiment. The other used a scintillator range telescope. Their results were in good agreement: Earl estimates the primary flux > 500 MeV at $32 \pm m^{-2}sec^{-1}sr^{-1}$, while Meyer and Vogt give 35 to 190 $m^{-2}sec^{-1}sr^{-1}$ particles greater than 100 MeV.

More recently De Shong and Hildebrand[4] have flown a spark chamber with a permanent magnet to measure the electron-to-positron ratio in the primary flux, hoping to determine which of two possible sources (p-p collisions or supernova explosions) is indicated.

More information is needed before definite answers can be given to questions regarding primary cosmic-ray electrons. It seems clear that a satellite measurement is highly desirable because of the numerous corrections for secondary electrons which must be made even for data gathered at an atmospheric density as low as 4 g/cm^{2}. A second advantage is the better statistical accuracy which can be achieved when the experiment can be operated for long periods of time. The energy range of the proposed experiment is 25 to 1000 MeV.

2. DESCRIPTION OF INSTRUMENTATION

Size and weight limitations make necessary some modification of the balloon instrumentation used for the measurements described above. The scintillator range telescope appears to be most adaptable to light-weight, low-power techniques.

In order to keep the weight of the absorbing material to a minimum, the entrance aperture of the absorber for the proposed instrument is only 1 cm, as shown in Fig. 3-1. A lower limit to the diameter of the absorber is set by the characteristic diameter of the electron showers. According to calculations by Fernbach[5], about 85 percent of the shower particles of energy E are within a zone defined by $X = 2$,

where $X = Er/E_s$

r = distance from the track in radiation lengths

$E_s \cong 21$ MeV

Therefore, even for energies as low as 21 MeV, the shower radius is no larger than two radiation lengths or 1.3 cm. Enough material is added to the skirts of the absorber to make the losses of shower fringes negligible. The total weight of the lead is about 2 lbs.

A total of four scintillators and five silicon detectors make up the detector array. The top two silicon detectors are placed in coincidence and define the telescope aperture. The "range" of the shower produced by an incident electron is measured by determining how many of the six range detectors are penetrated. The first three of these are silicon, but the larger diameter detectors are scintillator-photomultiplier combinations. A plastic scintillator surrounding the telescope acts as an anticoincidence shield.

Discrimination against heavier charged particles is obtained by using the detectors at both ends of the lead stack as dE/dX detectors.

The range telescope requires nine preamplifiers and ten discriminator-coincidence circuits, plus six accumulators.

---

[1] C.L. Critchfield, E.P. Ney and Sophie Oleksa, Phys. Rev. 85, p. 461 (1952)

[2] J.A. Earl, Phys. Rev. Letters, 6, p. 125 (1961)

[3] P. Meyer and E. Vogt, Phys. Rev. Letters, 6, p. 193 (1961)

[4] J.A. Deshong, Jr. and R.H. Hildebrand, Phys. Rev. Letters, 12, p. 3 (1964)

[5] S. Fernbach, Phys. Rev., 82, p. 288 (1951)

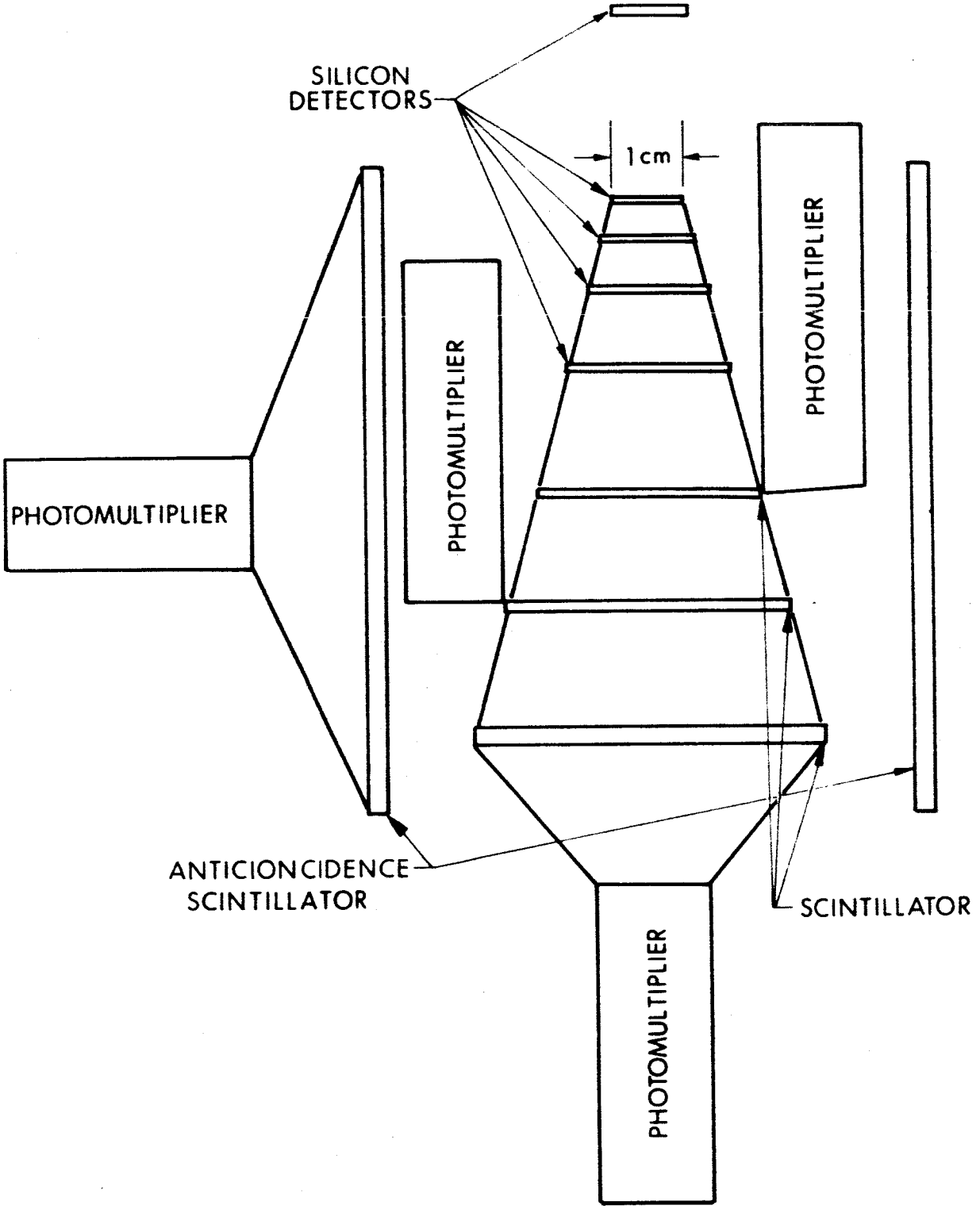

FIG. 3-1 ELECTRON RANGE TELESCOPE

3. INSTRUMENT SPECIFICATIONS (See Fig. 3-2)

Dimensions:

Length:	12 inches
Height:	8 inches
Width:	6 inches

Weight:	6 pounds
Power:	2 watts at 28 volts
Thermal:	$-20^{\circ}C$ to $+60^{\circ}C$
Data:	10 bits/second continuous
Mounting:	30 degree cone angle clear of obstructions away from sun.
Preferred Orbit:	1000 nautical mile modified sun synchronous

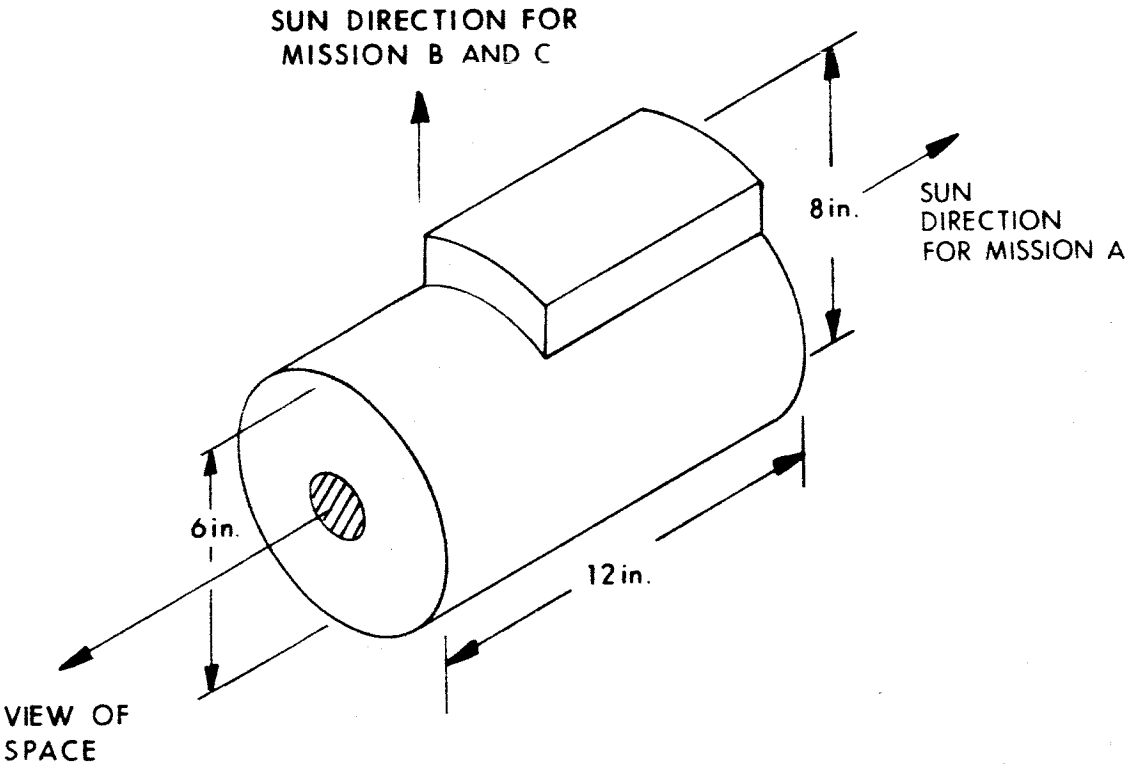

FIG. 3-2 SKETCH OF SPECTRA OF GALACTIC ELECTRONS EXPERIMENT

EXPERIMENT III-B

STUDY OF EARTH'S ALBEDO NEUTRONS

1. DESCRIPTION OF EXPERIMENT

The earth's neutron albedo is produced by cosmic ray primaries interacting with atmospheric nuclei producing nucleonic cascades. The neutrons produced are mostly in the MeV energy region, except for a few which are products of high-energy "knock-on" events. These neutrons are initially above 10 MeV in energy; subsequent collision with atmospheric nuclei moderates them and, for the most part, they are absorbed in the atmosphere in thermal neutron absorption reactions with nitrogen, $N^{14}(n,p)C^{14}$ and $N^{14}(n,T)C^{12}$. The latter reaction produces tritium, and only a few percent of the neutrons enter into this reaction.

Some of the neutrons produced by the cosmic ray events are scattered out of the atmosphere and it is these which are referred to as "albedo neutrons". Their energies are undoubtedly spread over a wide spectral distribution ranging from thermal to high energies of tens of MeV.

The importance of investigation of these neutrons lies in their role as one of the sources of the trapped (Van Allen) radiation found in the earth's magnetosphere. Theory as to the various injection mechanisms for electron and proton radiation belts includes solar protons, albedo neutrons, solar neutrons, etc., the proton-electron decay of the neutrons of course, providing the necessary components. Since neutron half-life is only on the order of 10^3 seconds, the lower energy neutrons cannot travel out of the magnetosphere before decaying and contributing to the radiation belts.

Little is known of the magnitude of the earth's neutron albedo or its spectral characteristics. The uncertainty in the albedo flux approaches an order of magnitude, and the albedo's importance as a major contributor lies with this area of uncertainty.

The neutron albedo theory, i.e., that it is the prime source of trapped radiation, is somewhat popular due to the fact that it surmounts

some of the difficulties associated with trying to understand the means by which charged particles from beyond the magnetosphere are actually trapped. The theory is also compatible with the energies of the protons found in the trapped radiation belt and some of their dynamic properties. The study of these neutrons is certainly important in resolving the theoretical controversy over the origin and perpetuation of earth's trapped radiation. The subject is covered thoroughly in an article by R.C. Haymes[1].

2. DESCRIPTION OF INSTRUMENTATION

Any attempt to cover the range of neutron energies expected from the albedo must conceive of several instruments, each covering a narrower range. Thermal neutrons are generally detected by proportional counters filled with a gas with large thermal neutron absorption cross section such as $B^{10}F_3$ or He^3. The latter gas is an excellent choice, for a proportional counter can be filled with He^3 to pressures on the order of 10 atmospheres and operated at moderate voltages with efficiencies around 70 percent, since the absorption cross section is 5500 barns for thermal neutrons. The measurement of thermal and slow neutrons could be accomplished by the use of three proportional counters:[2,3]

1. He^3-filled for measurement of the thermal neutrons
2. He^3-filled with sufficient cadmium shielding to exclude neutrons below cadmium resonance
3. He^4-filled to allow subtraction of charged-particle-induced counts

The proportional counters would be identical in geometry and gas pressure and presumably matched for charged-particle response. The thermal neutron counter can be made directional, as can the epicadmium counter with proper choice of shielding. The He^4 counter should be used in anticoincidence with the two neutron detectors to eliminate background, since any heavily ionizing radiation will produce charge pulses on the order of the reaction energies of the $He^3(n,p)T$ process.

Fast neutrons (0.5 Mev to 15 Mev) are difficult to measure directly. The popular method for fast neutron detection in this range is to use a moderator material with a $B^{10}F_3$-filled proportional counter relying on the slowing of the neutrons to the energies that allow good absorption efficiency. This type of counter does not have good absolute efficiency (< 0.1 percent) and some theoretical spectrum must be assumed, since no spectral information is available.

Techniques of more acceptable character have been used recently, employing no moderator and enabling pulse-height analysis of recoil protons directly created by neutron-proton recoil in an organic scintillator. The assembly is an organic scintillator with a 10 to 20 percent collection efficiency surrounded by an inorganic scintillator. The inorganic scintillator interacts very little with fast neutrons and provides a charged particle pulse-shape discrimination mechanism, since the pulse is much longer from the inorganic field. The organic scintillator has very short pulse-relaxation times, and counting of neutrons is done by sensing the pulse-decay time from the proton knock-on. The energy of the proton is roughly proportional to the incident neutron energy, though energy resolution may be poor due to the wide-angle scattering of protons from lower energy neutrons. Shielding for directionality could be accomplished; however, an anticoincidence technique using a thick, second organic scintillator as an outer cover would be more fruitful due to the large bulk of hydrogenous material nec necessary for total slowing of the higher energy neutrons.

Fast neutrons from the earth's albedo are perhaps the most interesting and least explored energy region. The energies of neutrons from high-energy cosmic ray interactions are undoubtedly less abundant, and count rates would be correspondingly low. These neutrons have energies up to 100 MeV and may be sensed by use of a proton knock-on radiator plate with a proton range spectrometer to collect the knock-on proton. Fig. 3-3 shows a conceptual drawing of such an arrangement. Directionality of this detector rests on the predominantly forward scattering of the proton knock-on and geometry of the neutron-proton converter plate

or radiator. An anticoincidence shield of inorganic scintillator is used to provide anticoincidence rejection of charged-particle background.

The basic problems are several. The n-p collision is not, in general, a total conversion process; thus only a lower limit to the neutron energy can be obtained. Also, the directionality is limited to the fact that the recoil proton cannot go backward. However, at higher energies the relativistic kinematics tend to favor the forward angles for the collision process (essentially a charge-exchange collision with small momentum transfer), and the directionality is improved. The other problem is that the hydrogenous radiator usually has carbon also, and the n-carbon reactions are more complicated and less directional.

Another problem concerns efficiency. The n-p cross section at higher energy gets relatively small (~0.1 barn) so that the conversion efficiency becomes poor. A converter that would allow the passage of a 50 MeV proton would have a conversion efficiency of only about 2 percent.

Such problems notwithstanding, the following instrument is a beginning toward such a detector.

3. DESCRIPTION OF NEUTRON DETECTOR

Figure 3-3 shows:

(1) a plastic scintillator, totally enclosing detector used for anticoincidence isolation from charged particle background

(2) a solid-state dE/dX counter

(3) a second solid-state dE/dX counter

(4) a copper-absorber solid-state detector sandwich which is a proton telescope with maximum range of about 300 MeV protons

(C) a CH_2 converter

Detector Operation

(1) vetoes all entering charged particles. Neutron enters (C) knocking out a proton, which triggers (2), (3), and (4). The logic and discriminator levels are set on (2), (3), and (4) to distinguish protons

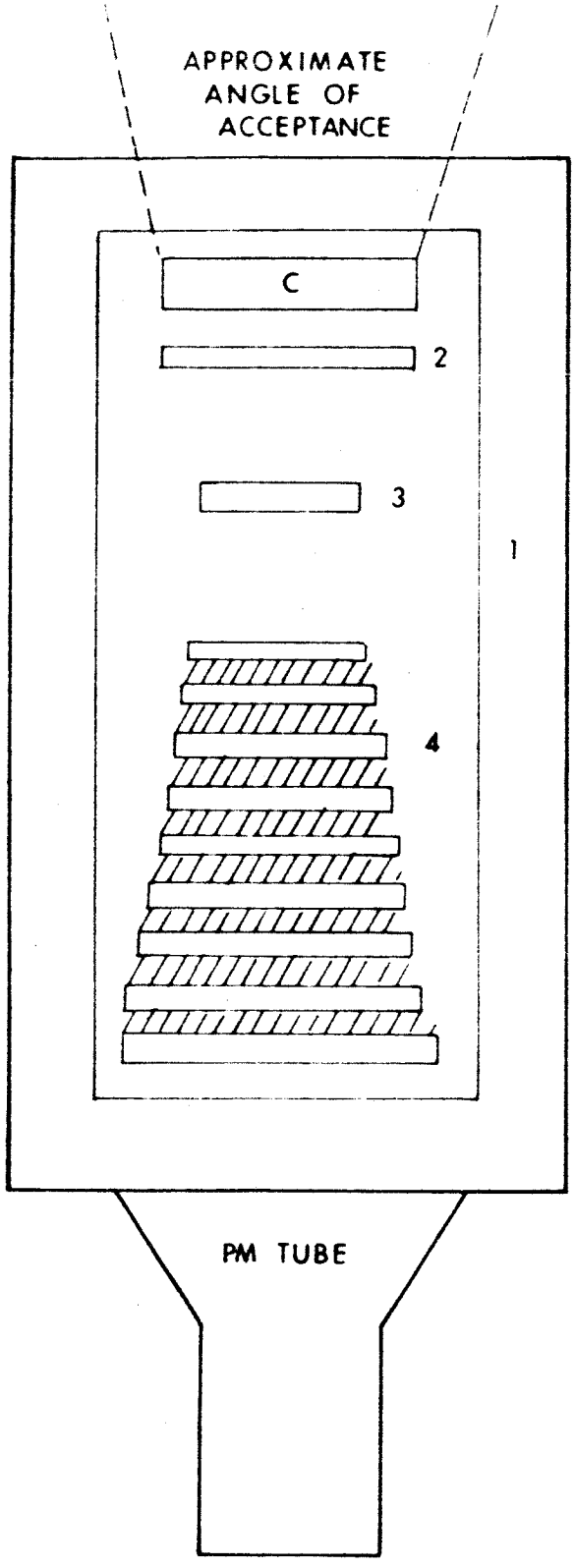

FIG. 3-3 [illegible]

from electrons, thus eliminating counts due to gamma conversion. The proton telescope, in conjunction with (2) and (3), tells energy of proton (range and identification).

The entire assembly could be covered with a layer of lead to convert gammas, thus vetoing them. (This probably would add too much weight, however, and is rejected for this instrument.)

The above device would measure neutrons, put a lower limit on their energy, and measure directions crudely, i.e., about $\pm 45^{\circ}$-- enough to identify the earth as the source, rather than the sun.

4. INSTRUMENT SPECIFICATION

Dimensions:

Length:	12 inches
Height:	6 inches
Width:	6 inches

Weight:	~ 10 pounds
Power:	3 watts at 28 volts continuous
Thermal:	-20°C to $+60^{\circ}$C
Data:	8 bits/second continuous
Mounting:	Mission B or C 180° from sun line; Mission A 90° from sun line
Preferred Orbit:	None

---

[1] R.C. Haymes, Rev. of Geophys., 3, p. 545 (1965)

[2] D.J. Williams and C.O. Bostron, J. Geophysical Res., 69, p. 377 (1964)

[3] W.R. Mills, R.L. Caldwell and J.L. Morgan, Rev. Sci. Instr., 33, p. 866 (1962)

EXPERIMENT III-C

INTENSITY AND ABUNDANCE OF THE

LIGHT AND MEDIUM NUCLEI IN GALACTIC COSMIC RADIATION

1. DESCRIPTION OF EXPERIMENT

Within the past few years, a considerable amount of data has become available on the spectra of the components of galactic cosmic radiation with charges from Z = 1 (hydrogen) to Z = 8 (oxygen) in the rigidity range 0.5-10 BeV.[1,2] The present experiment would add to this body of data and provide information on the short term (from a few hours to a few months) variations in intensity and composition.

As the name implies, galactic cosmic radiation is believed on theoretical grounds to originate within our galaxy, although a few measurements of particles of energy so high as to suggest extra-galactic origin have been made.[4] The problem of the origin and acceleration of cosmic rays is still a matter of some speculation; it is just for this reason that additional data is needed. It is known, of course, that the sun is a source of energetic particles (called solar cosmic rays to distinguish them from the subject of this experiment) and the stars in our galaxy presumably are similarly important sources of cosmic radiation.

A question which immediately arises is whether the composition of galactic cosmic radiation is similar to that of the sun. It already has been established that significant differences exist.[1] It remains to be determined whether these differences reflect differing source abundances, acceleration efficiencies, or loss processes. Accurate measurements of relative abundances can shed some light on this problem. For example, McDonald and Webber[2] found that the ratio of alpha particles to medium nuclei ($6 \leq Z \leq 9$) does not appear to show an increase toward

---

[1] C.J. Waddington in Progress in Nuclear Physics, Vol. 8, pp. 1-45 (Pergamon Press, New York, 1960)

[2] F.B. McDonald and W.R. Webber, J. Geophys. Res. 67, p. 2119 (1962)

[3] V.K. Balasubrahmanyan and F.B. McDonald, J. Geophys. Res. 69, p. 3289 (1964)

[4] J. Linsley, L. Scarsi, and B. Rossi, J. Phys. Soc. Japan 17, Suppl. A-III, p 91 (1962)

low energies that would be predicted after passage through $4 g/cm^2$ of interstellar hydrogen if the original rigidity (momentum) spectra were similar.

It is well known that galactic cosmic ray intensity and solar activity show an inverse relationship over the 11-year solar cycle. Because so much of the detailed information in the rigidity range below a few BeV/nucleon has been obtained with balloon instrumentation, short-term correlations of light nuclei spectra with solar activity and solar flares would be interesting in itself and helpful in the interpretation of balloon measurements. An experiment aboard a relatively long-lived satellite offers the opportunity for such correlations.

2. DESCRIPTION OF INSTRUMENTATION

The most suitable detector for light and medium nuclei spectral measurements from an unmanned satellite is a scintillator-Cerenkov telescope of the type developed at the State University of Iowa.[2,3,5] It consists of a pair of scintillators and a Cerenkov detector; the passage of a particle of interest is indicated by a coincident output from the three detectors. The pulse height from a Cerenkov detector is proportional to $Z^2(1-1/\beta^2 n^2)$ where n is the index of refraction; and the scintillator output is proportional to Z^2/β^2. Pulse height analysis of each of these outputs permits both Z and β to be determined. Detailed discussion of some of the necessary corrections is given by McDonald and Webber.[6]

For a satellite-borne experiment with severely limited weight, power, and telemetry capacity, the balloon instrument technique using two or three 512-channel pulse-height analyzers does not appear feasible. However, it appears that the particle identification problem can be readily handled by on-board data processing equipment.

---

[5] F.B. McDonald, Phys. Rev. 104, p. 1723 (1956)

[6] F.B. McDonald and W.R. Webber, Phys. Rev. 115, p. 194 (1959)

Figure 3-4 shows the approximate boundaries separating the various nuclei in the scintillator output vs Cerenkov output plane. These boundaries imply that the identification of a given nucleus can be accomplished by a pulse-height analysis of the quantity S-kC, where S is the scintillator output and C is the Cerenkov detector output. Thus only an 8-channel pulse-height analyzer would be required for the particle identification function. A second 12-channel pulse-height analysis of C alone would yield energy information. Thus a total of 96 accumulators is required. A block diagram of the system is given in Figure 3-5.

For a telescope with a 5 cm^2-ster geometrical factor, count rates of the order of 10 counts/sec are expected. Thus low-speed circuitry can be used throughout the instrument. No particular susceptibility to damage from the launch or space environment is anticipated.

3. EXPERIMENT SPECIFICATIONS (See Fig. 3-6)

Dimensions

Optics: 6" diameter x 12" long

Electronics: 6" x 6" x 9"

Weight

Optics: 7 pounds

Electronics: 5 pounds

Power: 5 watts at 28 volts

Thermal: $-5^{\circ}C$ to $+60^{\circ}C$

Data: 1400 bits/orbit

Mounting: Mission B and C 90 degrees to earth-sun axis;
Mission A 180 degrees to the sun; 30 degree field of view

Preferred Orbit: Any of three missions

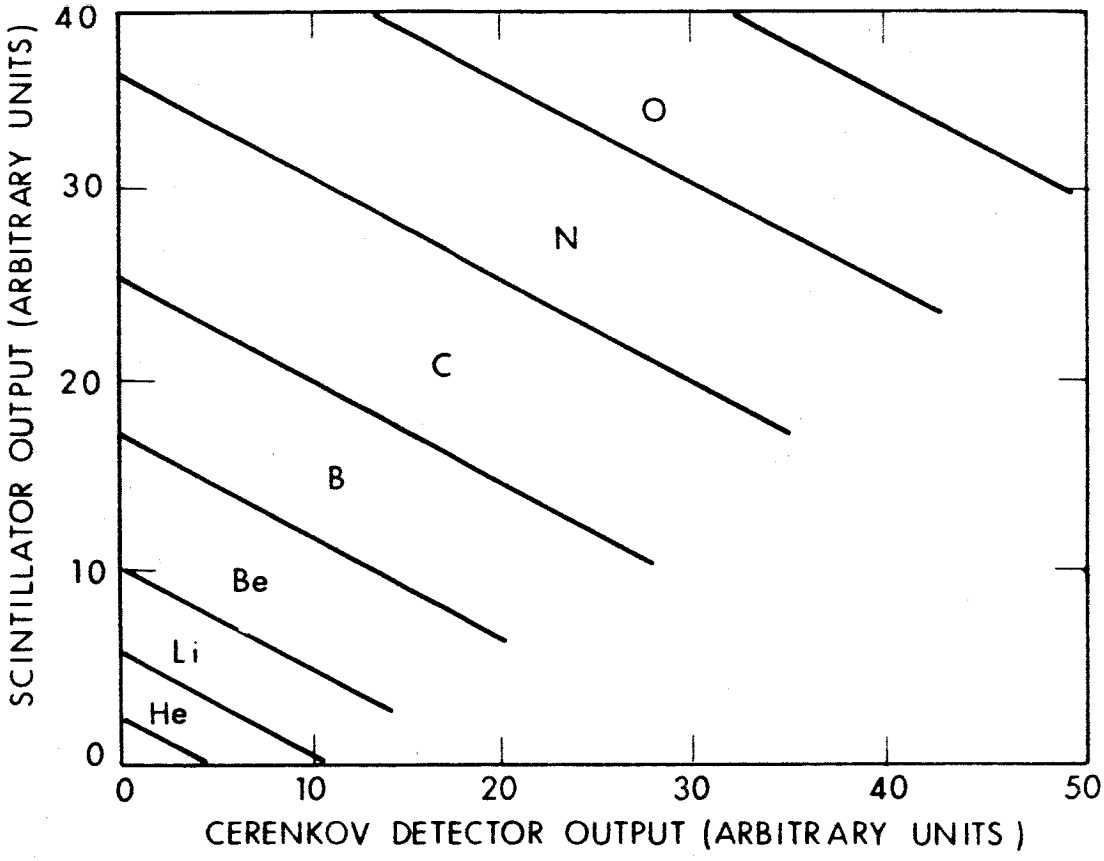

FIG. 3-4 PARTICLE IDENTIFICATION BOUNDARIES

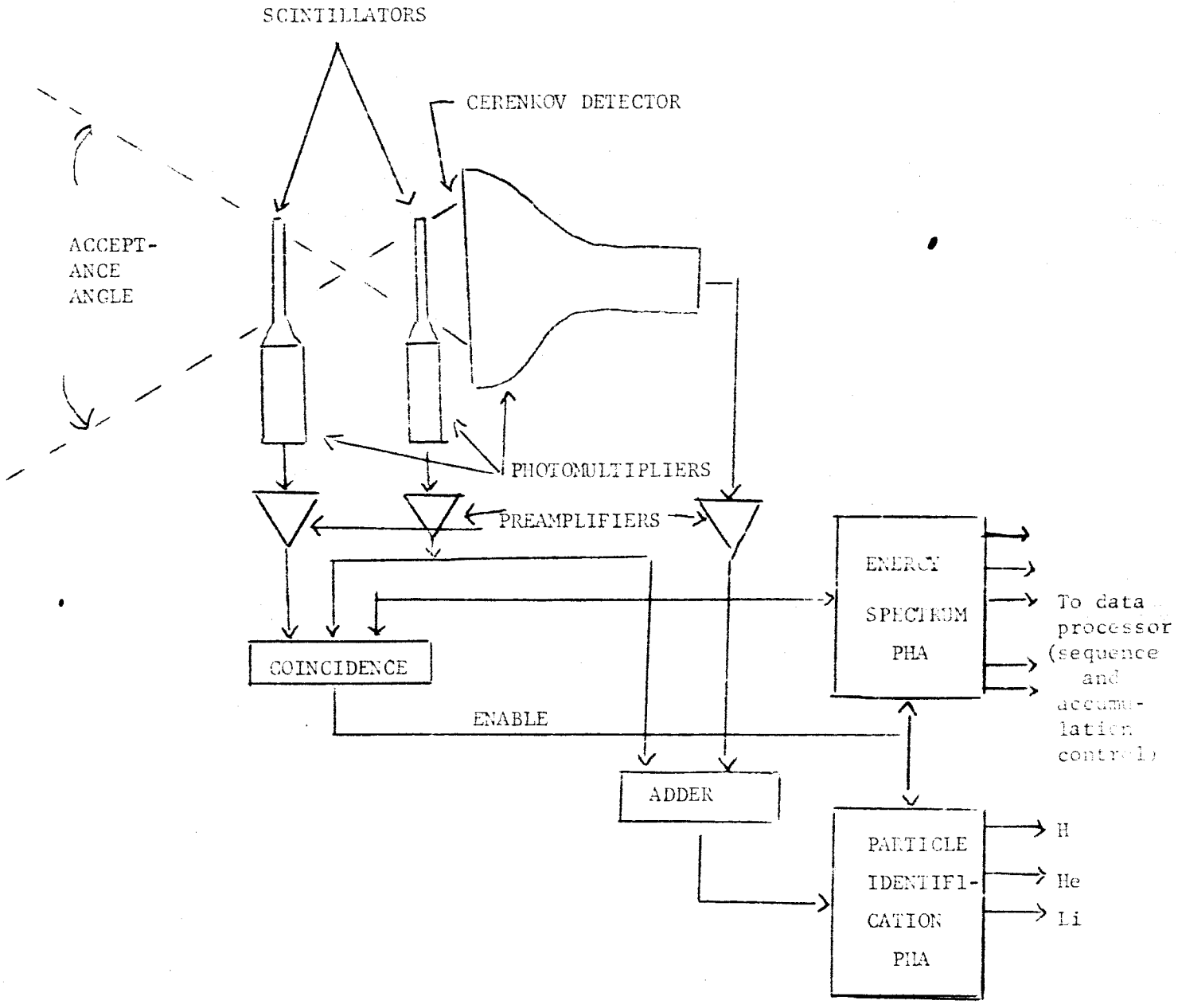

FIG. 3-5 BLOCK DIAGRAM OF CERENKOV-SCINTILLATOR DETECTOR

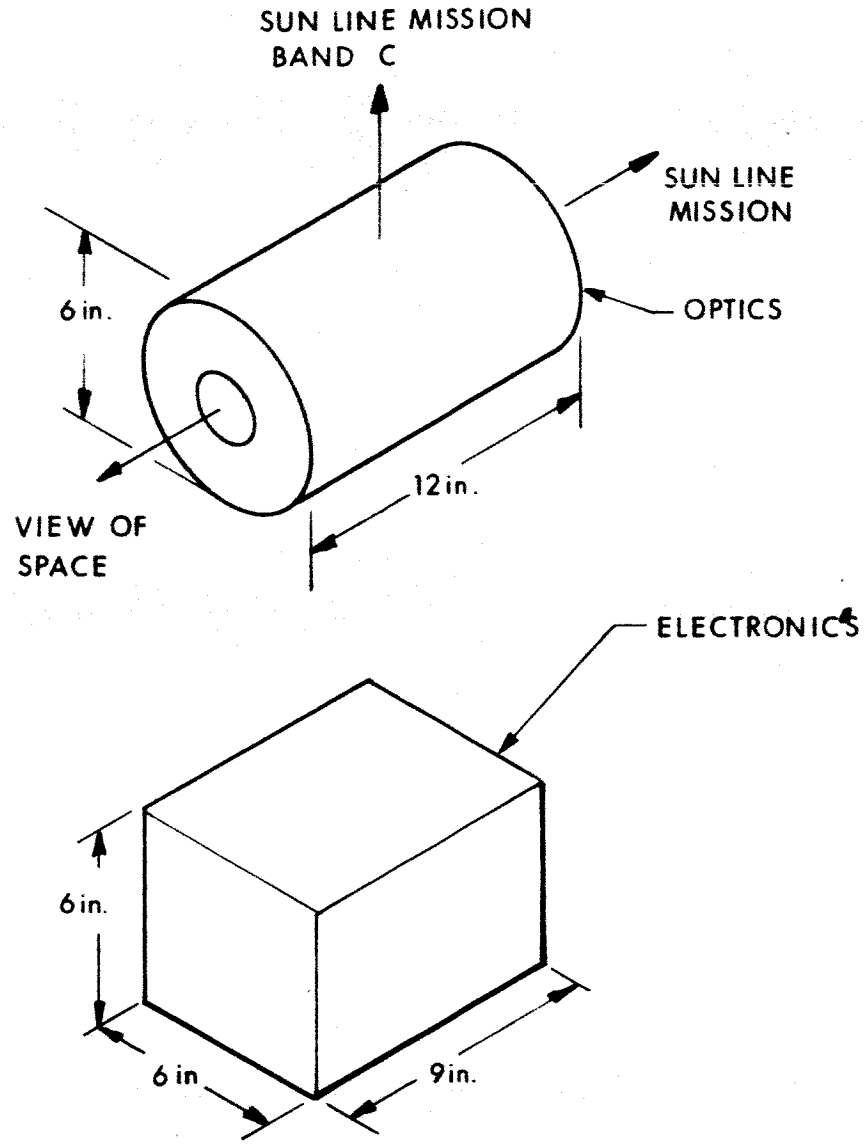

FIG. 3-6 SKETCH OF EXTENSION EXPERIMENT

EXPERIMENT III-D

TRAPPED PARTICLE EXPERIMENT

1. DESCRIPTION OF EXPERIMENT

The purpose of this experiment is to obtain experimental data about the energetic charged particles which are trapped in the geomagnetic field.

The two types of particles which are of interest are electrons and protons with energies sufficiently great so that the effects of gravitational fields can be ignored, and whose motions in the geomagnetic field will accordingly be dictated solely by Lorentz forces.

The characteristics of geomagnetically trapped particles can be completely described if the function

$$ji(r,\psi,\theta,l,m,n,E,t)$$

can be determined, where

where ji = the unidirectional intensity expressed as particles-cm^{-2}-sec^{-1}-$steradian^{-1}$, of particles of type i having energies between E and E + dE

r,ψ,θ = the geographic polar coordinates of an arbitrary point in the vicinity of the earth

l,m,n = the direction cosines or pitch angle with respect to the magnetic field vector at r,ψ,θ

E = particle kinetic energy

t = time.

The motion of a geomagnetically trapped particle is helical, being composed of a circular motion in a plane normal to the magnetic field about a point known as the "guiding center", and a motion of the guiding center along the field lines. As the guiding center moves toward the north or south magnetic pole, the field lines converge and more and more of the energy must go into the cyclotron motion. The radius of gyration decreases (being inversely proportional to the magnetic field strength) and, if

the particle is not scattered or absorbed in the atmosphere, a point is ultimately reached where all of the energy has gone into the circular motion. The guiding center comes to a momentary stop at a "mirror point" and reverses its direction of motion, heading back along the field lines toward a conjugate mirror point in the opposite hemisphere. In addition to the helical motion just described, there is a general drift to the east for electrons and to the west for protons, caused by the radial component of the field gradient.

Although trapped radiations have been the subject of many experiments and a fairly consistent picture is emerging, a great many questions remain to be answered and much additional data is required. More sophisticated instrumentation must be developed to enable data to be collected from which relations between particle energy and particle lifetime can be derived and details of the injection and loss mechanisms inferred. Data regarding pitch angles, energy, and flux for ptotons and for electrons are needed over extended periods of time so that correlations between particle injection and such factors as solar flare occurrence, terrestrial and solar magnetic field variations can be determined. Longitudinal drift rates need to be measured. Parameters governing the altitudes of mirror points must be investigated. To date, no instruments with good energy resolution and good directional resolution have been built and flown.

2. DESCRIPTION OF INSTRUMENTATION

Instrumentation for this experiment consists of a curved plate electrostatic analyzer to analyze electrons and protons in the 1 to 150 keV range, and a solid-state telescope to analyze electrons between 150 keV and 10 MeV and protons between 150 keV and 200 MeV.

The solid-state telescope consists of a dE/dX detector, total E detector, and a series of absorbers and detectors for range analysis. The outputs of these detectors are fed into an electron-proton identification logic pulse-height analyzer and a proton-range analyzer.

The two instruments are shown in Figs. 3-7 and 3-8, and a general block diagram in Fig. 3-9.

3. INSTRUMENT SPECIFICATIONS

Size:	8 x 14 x 14 inches
Weight:	20 lbs
Power:	10 watts
Particle Type:	Electron and proton
Energy Range:	Electrons, 1 keV to 10 MeV
	Protons, 1 keV to 200 MeV
Dynamic Range:	10^1 to 10^9 particle/cm^2-sec-ster
Thermal:	$-20^{\circ}C$ to $+60^{\circ}C$
Data:	100 bits/min
Mounting:	Clear view of environment (180 degrees)
Preferred Orbit:	Highly elliptical or modified sun synchronous

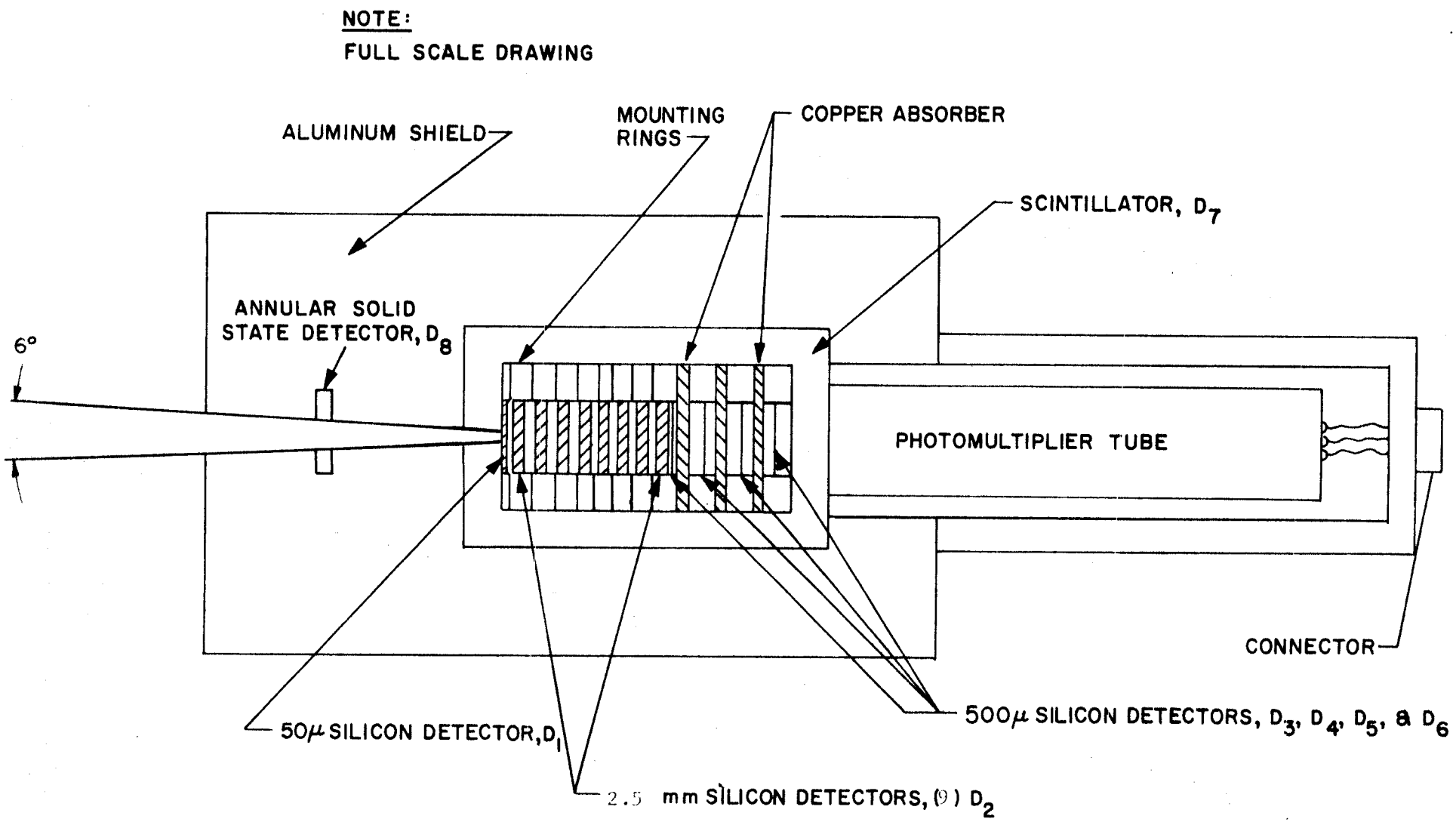

FIG. 3-7 HIGH ENERGY TELESCOPE CONFIGURATION

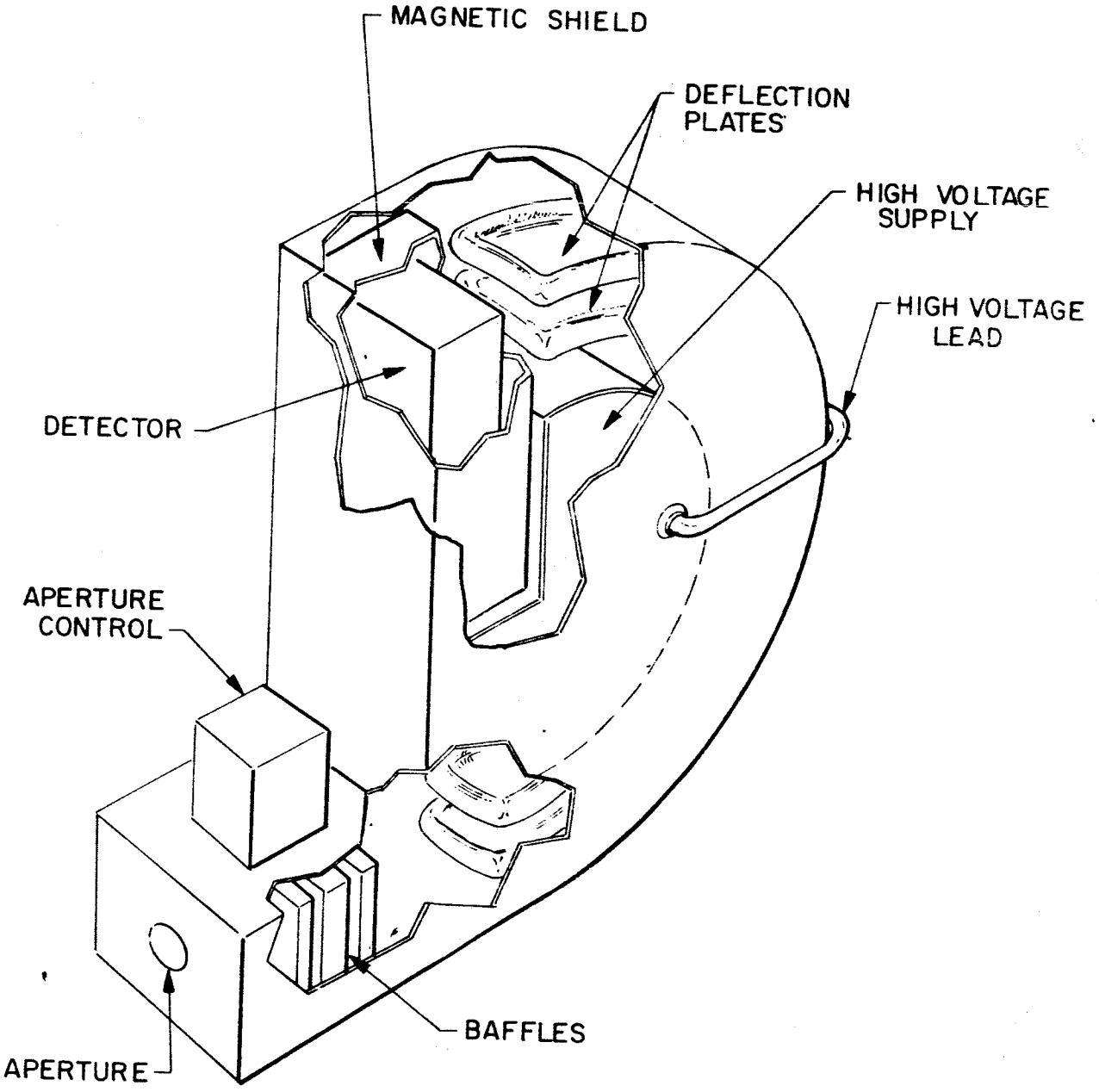

FIG. 3-8 CONFIGURATION OF THE ELECTROSTATIC ANALYZER

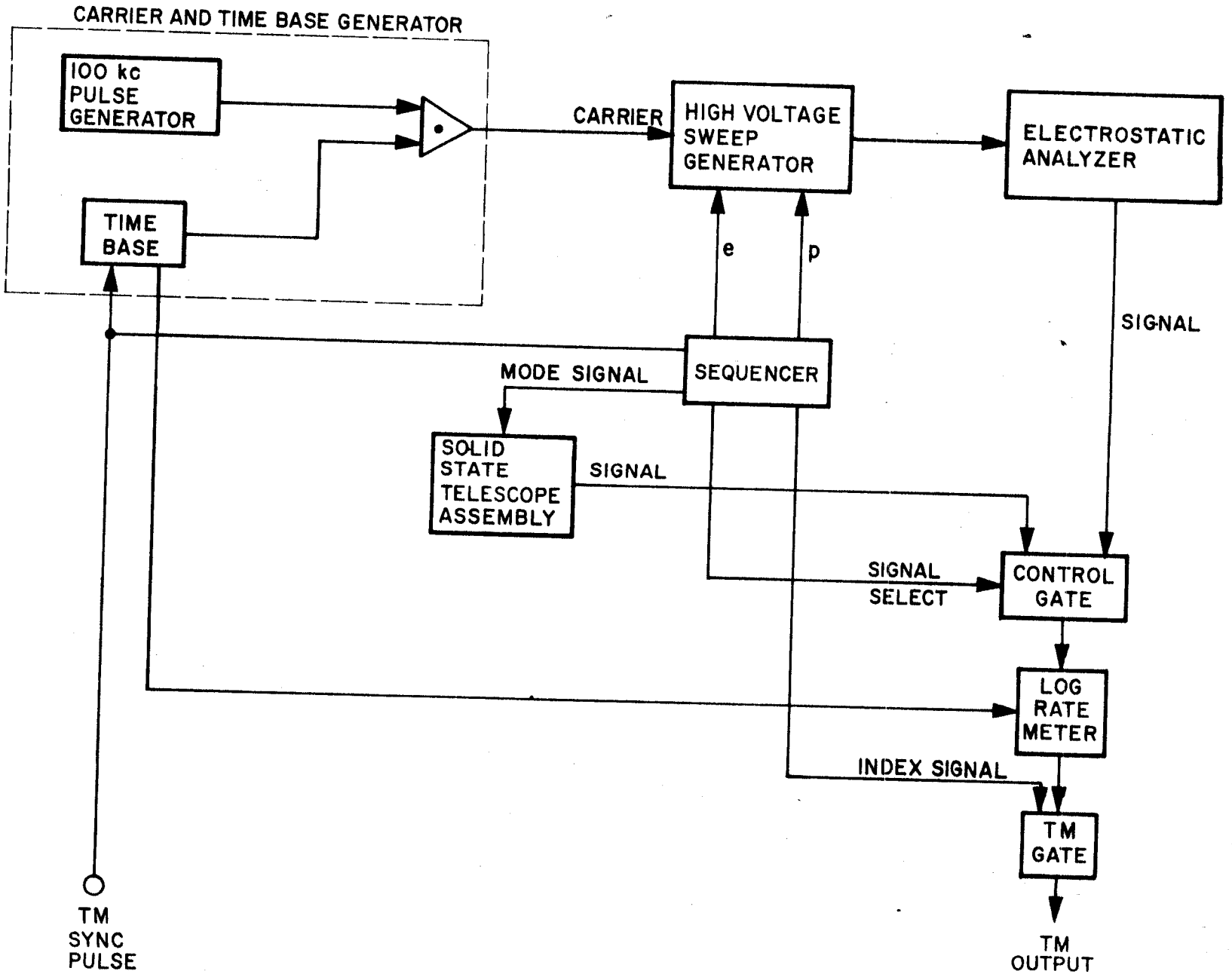

FIG. 3.9 BLOCK DIAGRAM OF [illegible] SPECTROMETER

EXPERIMENT III-E

DETECTION OF HIGH ENERGY GALACTIC GAMMA RADIATION

1. DESCRIPTION OF EXPERIMENT

Gamma radiation is the only cosmic radiation, with the exception of the infrequent, extremely energetic charged particles, which reaches us directly from the galactic source, unaffected by magnetic fields. The three sources of very high energy gamma (100 to 1000 MeV) are the cosmic ray nuclear collision reactions, proton-antiproton annihilation and high energy electron bremsstrahlung. In all but the last case, the gamma is produced through decay of a π^0 meson which results from the primary interaction. The first is considered predominant and most significant. Since there is no known means of producing these interactions without very high energy charged particles, any gamma rays detected would provide indication of such charged particles in galactic space. If a sufficiently directional detector could be used, indications as to the position could also be available.

Some study of such gamma rays already has been pursued. The artificial satellite Explorer XI carried a high-energy gamma telescope[1] into orbit on April 27, 1961 and recorded about 100 gamma rays in this energy range over approximately 9 hours of scanning. Several other instruments capable of detection of this type of gamma ray have been built[2,3]. One particularly suited for this use and apparently with some ability to resolve gamma ray energy was built for flight in the Orbiting Solar Observatory, Satellite S-17, with the University of New Mexico as experimenter[3].

Due to the very low flux of high-energy gamma rays, slow scanning (low roll rate) is necessary if an instrument is to accomplish any angular resolution. A long period of observation is also necessary for collection of significant counts. A detector placed on a solar oriented satellite rotating at less than one degree per second would sweep most of the sky during one-year transit through earth orbit path. Directional aperture should be at least 30 to 45 degrees solid angle for good collection efficiency and coverage.

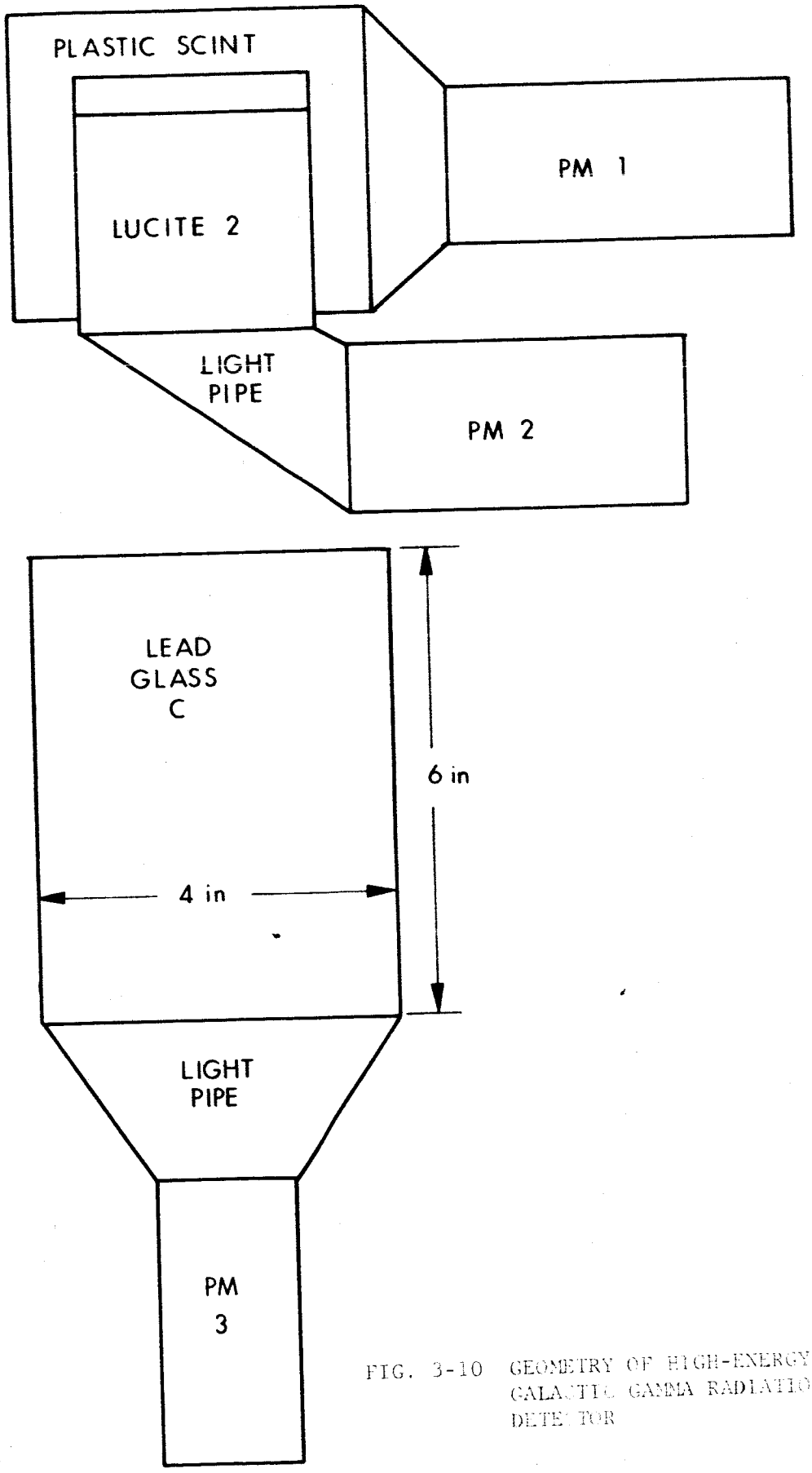

FIG. 3-10 GEOMETRY OF HIGH-ENERGY GALACTIC GAMMA RADIATION DETECTOR

2. DESCRIPTION OF INSTRUMENTATION

The instruments which have been designed for this type of detection are all variations on a single technique. That is to convert the gamma ray to a charged pair (e^-, e^+) by use of a high Z converter plate, usually lead, and detect the pair in a fluorescent scintillator. The scintillator must be sufficiently thin to pass the charged pair without too much energy degradation if spectrometry is employed. A second scintillator or Cerenkov detector is used either to establish directionality or to totally absorb the electrons and note their energy. This energy would be proportional to the gamma energy and pulse height analysis can be used to fair advantage. If the electrons are totally absorbed, a thick, wide Cerenkov detector must be used to accommodate the total absorption of all branching reactions and resulting bremsstrahlung. Lead glass is generally used to achieve such stopping power.

The geometry of such a detector is shown conceptually in Figure 3-10. The incident gamma must pass through the anticoincidence counter (1), which has low absorption cross section, and be converted in the lead plate. High conversion efficiencies, on the order of 50-75 percent, may be used depending on the subsequent geometry. The electron position pair produced from the absorption is projected forward into the first Cerenkov detector (2). The pair dissipate their remaining energy in the lead glass Cerenkov detector (3). Pulse height analysis of the energy deposited in such a detector will yield energy resolution on the order of 20 to 30 percent.

Anticoincidence is provided by requiring that only (2) and (3) coincidences are counted. (2) is protected from charged particles by the shielding of (3) and the anticoincidence scintillator (1). A charged particle penetrating all three detectors is vetoed as is any particle

creating a count in only one detector or in (1) and (2). The interface between (1) and (2) is painted non-reflective black, reducing the response of (2) to rear-entering charged particles due to the directionality of the charged particle Cerenkov radiation.

The associated electronics consist of conventional coincidence circuitry and pulse-height analyzers, data accumulators, power supplies, etc. Photomultiplier tubes will be chosen for convenience to geometry, but consistent with the requirement that they be of ruggedized construction. A sketch of the system appears in Fig. 3-11.

3. INSTRUMENT SPECIFICATIONS

Dimensions:	Length 18"
	Width 6"
	Height 8"
Weight:	17 pounds
Power:	2 watts at 28 volts
Thermal:	$-30^{\circ}C$ to $+65^{\circ}C$
Data:	10 bits/min continuous
Mounting:	30 degree clear field; 90 degrees away from sun mission B or C and 180 degrees away from sun mission A
Preferred Orbit:	Any

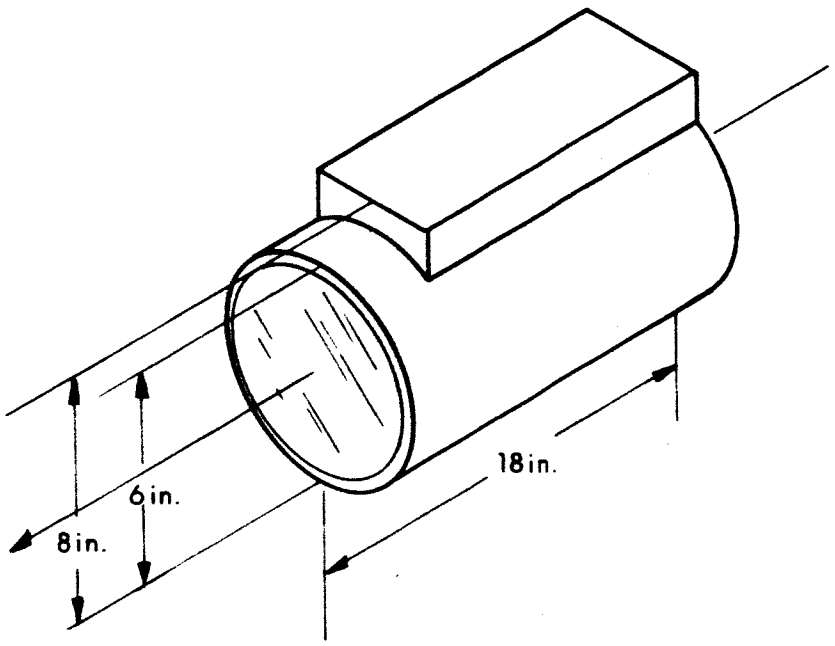

FIG. 3-11 SKETCH OF HIGH ENERGY GALACTIC GAMMA RADIATION INSTRUMENT

REFERENCES

1. Kraushaar, W. L., Clark, C. W., "Gamma Ray Astronomy" Scientific American, May 1962, Vol. 206 No. 5.

2. Leavitt, C. P., "High Energy Gamma Ray Satellite Experiment" IRE Trans. on Nuclear Science, NS-9 1962.

3. Fazio, G. G., Cook, C. J., and Hafner, E. M., "High Energy Gamma Ray Astronomy", IEEE Trans. on Nuclear Science, Vol. NS-10, 1963.

EXPERIMENT III-F
PROTON DOSIMETER

1. DESCRIPTION OF EXPERIMENT

Based on measurements and calculations of various types of radiation in space, it has been determined that the most serious radiation threat to humans in space is presented by solar flare and trapped protons. The proton dosimeter experiment is designed to monitor the proton fiological dose rate in an accurate way, taking into account the rather complex relationship between energy loss and biological dose rate. Data from this experiment will be useful for the estimation and prediction of radiation damage to humans in future manned space missions.

Most experiments for the detection of protons are designed to measure the energy spectrum of the radiation over a given range. In principle, the resulting data can be used to evaluate the radiation health hazard by making use of known relationships between the proton flux at a given energy and the resultant tissue damage. However, this approach is impractical since measurement of the entire spectrum requires a much more elaborate instrument than one designed to measure the relative biological effectiveness (RBE) of the radiation as a function of energy-loss rate.

Thus, as described below, this experiment will use a specially designed multi-shell omnidirectional ionization chamber. Its response will be proportional to the biological dose rate (obtained by multiplying the RBE by the absorbed dose). Depending on the specific organ for which the dose is to be evaluated, different RBE's may be defined. One recommended set of values is given in the Table III-1.[1]

---

[1] International Commission on Radiological Protection. Brit. J. Radiol. Suppl. 6 (1955).

Table III-1. Relative Dose Rate as a Function of Energy Loss Rate

Energy Loss Rate $\frac{-dE}{dx}$ (keV/μ of H_2O)	RBE	Biological Dose Rate $\frac{dD}{dx}$
3.5	1	3.5
7.0	2	14
23	5	115
53	10	530
175	20	3500

In general, the giological dose rate has the form $dD/dx = f\ (dE/dx)$ so that the total relative dose rate absorbed by a human is given by

$$D = \int_0^{X_{max}} f\left(\frac{dE}{dx}\right)\ dx$$

where X_{max} is a tissue thickness typical of a human. The quantity D is a function of energy since dE/dx is a known function of proton energy. We can thus calculate the total biological dose per incident proton as a function of the incident proton energy E_o, $D\ (E_o)$. Fig. 3-12 shows a sketch of such a curve.

It should be remarked that if the function $D(E_o)$ is multiplied by the proton flux $j(E_o)$ measured in protons/cm^2-sec-keV, and integrated with respect to energy, the resulting quantity is the average or whole-body biologically effective dose rate in rem (if the proper units are used). This quantity may be compared without further computation with similarly derived measures of the absorbed dose for other types of radiation when biological effects are being studied.

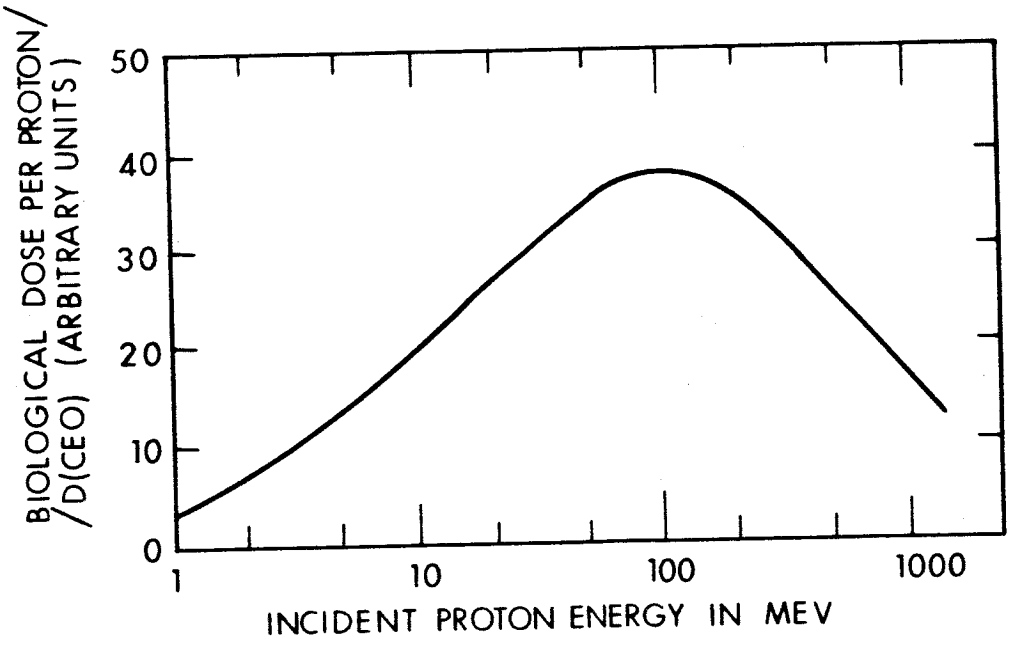

FIG. 3-12 SKETCH OF THE RELATIVE BIOLOGICAL DOSE PER PROTON

2. DESCRIPTION OF INSTRUMENT

In section 1, a method for assigning a measure of the biological damage caused by a single proton has been described. The biological dose D was found to depend on the proton energy E_o. It remains to be shown that an instrument can be devised to measure the total biological dose which would be absorbed by a human in the same proton flux. A spherically symmetric instrument is described which has the property that its output is very nearly proportional to $\int_o^\infty D(E_o)\, j(E_o)\, dE_o$, where $j(E_o)$ is the flux of a beam of protons which is monodirectional and uniform over an area large compared to the instrument. The instrument is also linear so that a superposition of beams in various directions is correctly measured.

The instrument consists of a series of concentric conducting spherical shells, the space between the shells being filled with argon. Alternate shells are connected together electrically, and a typical ionization chamber voltage is applied, so that ions generated in any portion of the gas are collected at a common detector. In order that the detector produce the proper output as a function of particle energy, we must arrange varying spacing of the concentric shells, or varying thickness, or both. As an example, we assume that the spacing varies. In practice, there would be a few ($\sim$ 10) such spacings, but we assume a continuous function of an illustrative solution. Then let the gap width (the "gas shell" thickness) be described by W(r), where r is the radial coordinate from the center of the sphere. Here we assume for simplicity that all absorber shells are the same thickness and of the same material. Then the response of the instrument to a proton at a radius, r, in the chamber is proportional to $-W(r) \frac{dE}{dx}$.

Now we illustrate the form of the equation which must be solved to define the function W(r). We refer to the sketch below. Let r be the

radial coordinate from the center of the sphere to a point on the trajectory of a proton. The polar coordinate axis, $\theta = 0$, is oriented parallel to the direction of the incoming proton. For an incoming proton of energy, E_o, the energy loss $-\frac{dE}{dx}$ is determined in a calculable way by the amount of material it has traversed. Thus

$$-\frac{dE}{dx} = f(E_o, S, \rho)$$

where ρ is the average density of the stopping material in the sphere, and S is the distance the proton has penetrated into the sphere. If the gas shells are negligibly small compared to the absorber shells, ρ can be taken as constant. If not, we must write

$$\rho = \rho_o [\, 1 - k\, W(r) \,]$$

where k is a constant. Now we can write the response of the instrument to a proton injected at r_o, θ_o, of energy E_o, as

$$dR(E_o) = K \int_0^{S_o} W(r)\ f(S, \rho, E_o)\, dS$$

where S_o is the length of travel in the sphere. Then note $dS = \frac{r}{\sin\theta}$, and obtain

$$dR = K \int_{\theta}^{\pi-\theta_o} W(r)\, f\,(S, \rho, E_o)\, \frac{r}{\sin\theta}\, d\theta$$

$$= K \int_{\theta_o}^{\pi-\theta_o} W(r)\, f\,(S, \rho, E_o)\, \frac{r_o \sin\theta_o}{\sin^2\theta}\, d\theta$$

since $r = \frac{r_o \sin\theta_o}{\sin\theta}$. Here K is a constant. If the particle stops before traversing the whole sphere, f is considered zero after the end of the range. To extend the response to all r_o, θ_o, we put in the area factor $2\pi \sin\theta_o$, and have, finally,

$$R(E_o) = \int_0^{\pi/2} \int_{\theta_o}^{\pi-\theta_o} \frac{2\pi \sin^2\theta_o}{\sin^2\theta} W(r)\, f\,(S, \rho, E_o)\, r_o\, d\theta\, d\theta_o$$

To employ this more explicitly, we recognize that

$$S = r_o \sin\theta_o\, (\mathrm{ctn}\,\theta - \mathrm{ctn}\,\theta)$$

$$r = \frac{r_o \sin\theta_o}{\sin\theta}$$

The function $R(E_o)$ must now be equated to the desired proton dose as a function of energy $D(E_o)$, and the equation solved for W(r). This is quite straightforward to the accuracy we are seeking. One simple method is to make a "guess" at W(r), solve numerically to get $R(E_o)$, and vary W(r) to get the best fit. The function f (S, ρ, E_o) is actually a function only of $\int_r^{r_o} \rho\, ds$, and is a known function which can be found from the range-energy-energy loss relation.

Note that the stopping power of the sphere should be comparable to an average slab of the human body. This would be about 30-40 gms/cm^2.

If the sphere were made of a relatively heavy material, like copper (the most favorable case), then it would be of the order of 5 cm in diameter, weighing somewhat less than a pound and a half. Better results might be obtained with a somewhat larger sphere, but the above would be adequate.

The rest of the instrument package consists of a low-current, high-voltage power supply and an electrometer circuit. The simplest system would result if an analog telemetry channel of a few cycles bandwidth were available, but suitable modifications to adapt the experiment for periodic digital readout are straightforward. A block diagram of the proposed instrument is shown in Figure 3-13. A sketch of a proton dosimeter instrument is shown in Figure 3-14.

3. DESIGN SPECIFICATIONS

Dimensions:	Length 5"
	Width 3"
	Height 6"
Weight:	3 pounds
Power	1 watt at 28 volts
Thermal:	$-30^{\circ}C$ to $+60^{\circ}C$
Magnetic:	No magnetic fields stronger than 10 gauss allowed around instrument
Data:	20 bits/second continuous
Mounting:	Spacecraft should block as little of solid angle as possible
Preferred Orbit:	Highly elliptical or modified sun synchronous

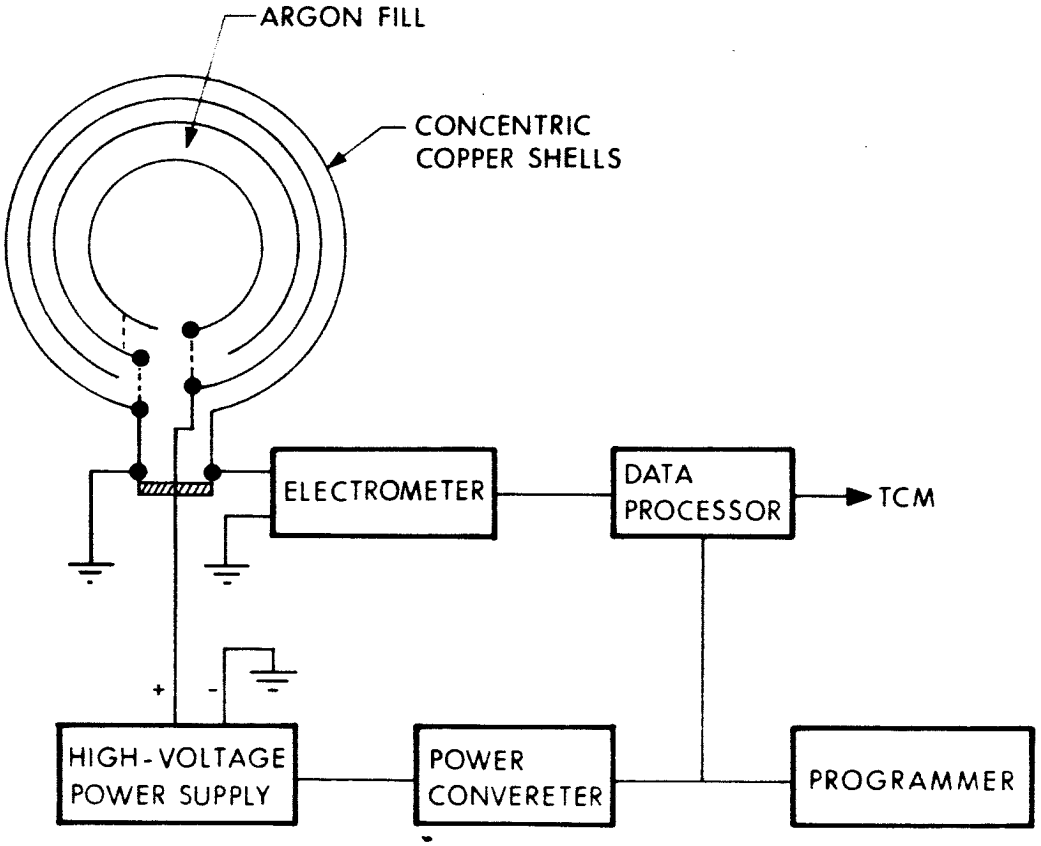

FIG. 3-13 BLOCK DIAGRAM OF THE PROTON DOSIMETER

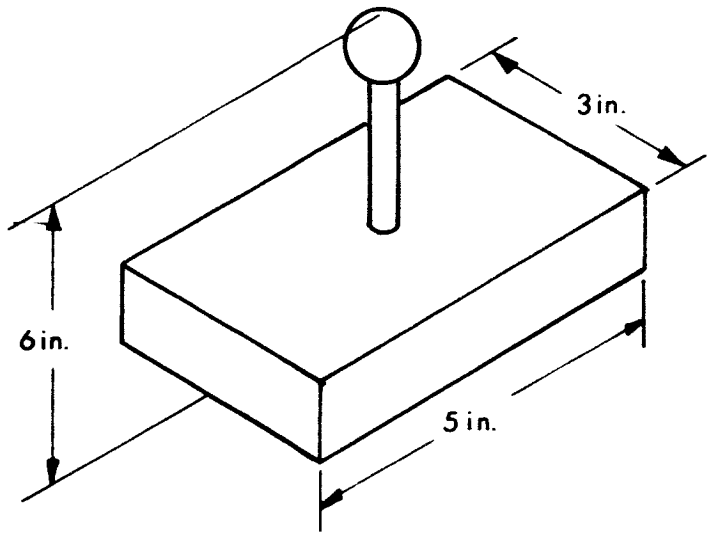

FIG. 3-14 SKETCH OF PROTON DOSIMETER INSTRUMENT

EXPERIMENT III-G

SEARCH FOR KEY GALACTIC GAMMA RADIATIONS

1. DESCRIPTION OF EXPERIMENT

The objective of this experiment is the detection of galactic gamma radiations characteristic of certain nuclear reactions and processes of importance to astrophysicists. Gamma radiations provide the most convenient probe of galactic nuclear reactions because of their lack of charge and low probability of interaction with galactic hydrogen. Thus, a search for gamma photons of galactic origin with energies characteristic of known reactions provides astrophysicists with a means for assessing the abundance of such reactions in stellar atmospheres and galactic clouds. Efforts toward determining the intensity of such photons have been scant and the data are lacking in spectral information. The more moderately energetic reactions which produce gamma radiation are the prime concern of this experiment. Those reactions which produce gamma radiation in the 0.1 meV to 10 meV region are:

(a) Deuterium production through neutron proton capture reactions, H (n,γ) D, resulting in 2.23 meV gammas.

(b) Positron-electron annihilation radiation at 0.511 meV.

(c) Electron-proton bremmstrahlung radiation caused by relativistic electrons in stellar atmospheres (no characteristic energies).

(d) Carbon, nitrogen and oxygen emission from de-excitation of excited states produced by proton inelastic scattering.

Little is known concerning the relative abundance of photons in the galaxy from each of these processes.

The first process, deuterium production, is essentially a slow neutron interaction and must occur where neutrons can be produced by higher energy charged particle collisions, in material-rich regions where the neutrons can be moderated sufficiently for the low energy

absorption by hydrogen, and where the neutrons mean free absorption path is at least on the order of the neutrons decay range. The conditions described correspond to stellar and planetary atmosphere with sufficient density to assure moderation and capture before escape or decay of the neutron. The abundance of such reactions may be low since the primary source of this characteristic radiation is the cosmic ray production of neutrons.

Annihilation gammas find their origin in the annihilation of positrons created by pair production from very high energy gamma rays. These high energy gammas are the result of the decay of π mesons produced by very high energy proton-proton collisions. The source of annihilation gammas should be strong compared to the deuterium production gammas because of the greater abundance of very high energy protons and hydrogen in the galaxy.

Electron-proton bremmstrahlung are produced predominately in stellar atmospheres and are believed to be the most prominent contributor in the region of 0.01 to 1 meV. Solar emissions of this radiation vary from 2×10^{-3} photons/cm^2-sec to 10^{-2} photon/cm^2-sec during solar flare activity.[1] The intensities expected from galactic sources would probably be several orders of magnitude lower than the emission from the sun.

Characteristic emission from oxygen, nitrogen, and carbon in the region of 1-10 meV results from proton inelastic collisions and should be present in any high-level stellar activity such as flares or novae. Little information is available as to the expected abundance of this type of radiation.

The reactions discussed above are for the most part, dependent upon the energetic proton activity in the galaxy or the density of hydrogen in galactic space. Information as to the intensity, energy distribution and general directionality of such radiation would aid greatly in the understanding of the high energy processes at work in

---

[1] Fazio, Giovanni G. "Comments on Gamma Rays," AAS-NASA Symposium on the Physics of Solar Flares 1963 NASA SP-50.

the galaxy. Little data is presently available since this region of the galactic gamma spectrum has for the most part been unexplored.

This experiment is designed to detect 0.51 and 2.23 meV galactic radiation and must be oriented in such a manner as to view this area of the celestial sphere for as great a portion of the operating period as possible due to the very low expected flux. Stable orientation is desirable; however, if the direction of the aperture of the detector is known as a function of time, the background sources (i.e., the earth and sun) can be easily recognized since their source strength is so much greater. Orbital characteristics of the satellite should be such that as much time as possible is spent out of the earth's trapped radiation field. A low roll rate is desirable to allow time for recognition of background sources.

2. DESCRIPTION OF INSTRUMENTATION

In order to reduce the background from solar flare protons, and terrestrial trapped radiation, the instrument must have good directional properties. Generally, shielding and anticoincidence techniques are used to this end. Moderate angular resolution is necessary in this application due to the solid angles subtended by galactic sources and the low flux.

The detector to be used in this experiment is a $C_sI(Tl)$ crystal 1 inch in diameter by two inches long, inserted into a well, bored into a larger $C_sI(Tl)$ crystal. The smaller crystal is viewed by a one-inch diameter photomultiplier tube such as an RCA C715D. The smaller crystal is blanked off optically from the larger and serves as the gamma detector. The large crystal is viewed by four similar tubes, the outputs of which are added and operated in anticoincidence with the output of the central tube.

The choice of cesium iodide for this application is dictated by its high gamma collection efficiency, great physical ruggedness, and its availability in large crystals. The gamma

detector aperture is in the direction of the central tube. Gammas arriving at other angles are absorbed in the Cesium Iodide anticoincidence shield. Similarly, charged particles are either absorbed and not registered or penetrate both crystals and are rejected with anticoincidence. Very high energy gammas have about the same absorption cross section and produce charged pairs which are also rejected by anticoincidence. The effective aperture of this device as described is on the order of one steradian and has front to back background reduction of about 10 to 1. The reduction of background from the wide is by a factor of three. This background reduction could be increased by increasing the size of the anticoincidence shield. The weight of the detector as described is about 3 pounds.

The detector is used with a pulse height analyzer using 10 channels, 5 channels centered on the 0.51 meV energy and 5 channels centered on 2.23 meV. Data in each channel are accumulated during the observation of the galactic source and transmitted before the detector accumulates data from backgound sources which may be subsequently viewed during the scanning period. The electronic circuitry in general is comprised of the following:

Preamplifiers
Pulse shaping amplifiers
Discriminators
Coincidence circuits
Accumulators
Commutators
High-voltage power converters
Low-voltage power converters
Voltage dividers

3. INSTRUMENT SPECIFICATIONS

Dimensions:	Length 12"
	Width 6"
	Height 6"
Weight:	15 pounds
Power:	6 watts at 28 volts
Magnetic:	Magnetic shield on PM tubes
Thermal:	$-30^{\circ}C$ to $+60^{\circ}C$
Data:	~500 bits/orbit sampled once per orbit
Mounting:	90 degrees from sun line on mission B; 180 degrees from sun on mission A; 45 degrees field of view
Preferred Orbit:	Highly elliptical; modified sun synchronous

EXPERIMENT III-H

SPECTRUM AND FLUX OF HIGH-ENERGY GALACTIC PROTONS

1. DESCRIPTION OF EXPERIMENT

The following experiment is designed to measure the flux of galactic protons as a function of energy. As a result of numerous spacecraft measurements in outer space, before the energetic particles have had opportunities to interact with atmospheric nuclei, considerable data are being gathered by scientists regarding cosmic ray phenomena. For example, a recent experiment on the IMP-1 satellite[1] permitted a determination of the intensity and energy spectra of primary cosmic ray protons in the 15- to 75-Mev range. However, additional measurements, particularly at higher energies, are essential before astrophysicists will be able to determine the nature and origin of these particles, their relations to the origin of the universe and to atmospheric interactions.

High-energy galactic protons are energetic particles that originate from outside the earth's atmosphere. These protons have the following properties:

(a) Flux rates of 10^{-14} protons/M^2-sec-ster for 10^{19} ev particles and 1500 protons/M^2-sec-ster for 10^9 ev particles[2]

(b) Single-particle trajectories

(c) Accompanied by alphas, gamma rays, electrons, neutrons, and stripped atomic nuclei

(d) Traverse large regions in space

(e) A considerable percentage of the radiation flux contains particles having energies in excess of 500 Mev

---

[1] McDonald & Ludwig, "Measurement of Low-Energy Primary Cosmic-Ray Protons on IMP-1 Satellite," Physical Review Letters, 13, 28 Dec. 1964.

[2] D. P. LeGalley and A. Rosen, Space Physics, Wiley, 1964.

High-energy galactic protons originate in the galaxy and may travel great distances through interstellar space before reaching the solar system. These particles therefore provide a probe for determining the properties of galactic and interplanetary magnetic fields, and the density and composition of matter in the universe. Particles originating in stellar bodies make possible a determination of the life-cycle mechanisms of stars.

The use of satellites and space probes for the study of galactic cosmic rays is still in its infancy, and a great many experiments remain for future missions to confirm the reliability of existing data and to obtain new data on previously unmeasured phenomena. The proposed experiment will collect data on protons with energies from 6 to 500 Mev. Thus, in addition to high-energy proton measurements, back-up data will be obtained to verify low-energy proton measurements.

2. DESCRIPTION OF INSTRUMENTATION

The proposed proton detector (Figure 3-15) will consist of a solid-state-scintillator combination range telescope. The detector assembly will be cylindrical, 3 inches long, and 1.5 inches in diameter. Seven solid-state detectors and five tungsten absorbers will be surrounded by a plastic scintillator anticoincidence sheild (Figure 3-15). The proton spectrum will be measured with an average energy resolution of 20 percent up to 200 Mev. Above 200 Mev, the resolution and counting efficiency of the detector may decrease to 30 percent. The energy spectrum will be divided into seven "bins" as follows:

6 to 12 Mev
12 to 25 Mev
25 to 50 Mev
50 to 100 Mev
100 to 200 Mev
200 to 350 Mev
350 to 500 Mev
> 500 Mev

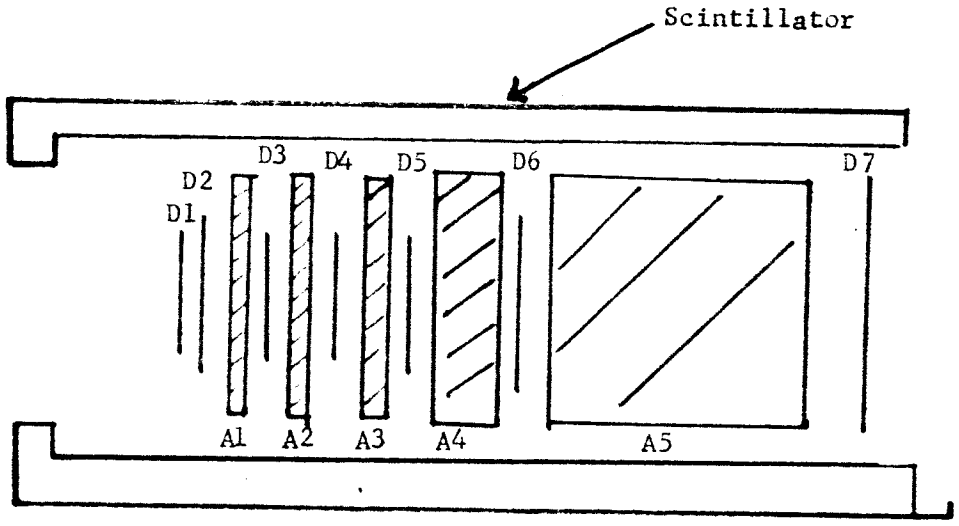

NOTE: D_i = Solid-State Detector

A_n = Tungsten Absorber

FIG. 3-15 PROTON DETECTOR ASSEMBLY CROSS SECTION

Instrument resistance to damage from radiation and environmental extremes is high and a very reliable instrument for spaceflight applications is feasible. (A reliability of 0.90 for 1 year of continuous operation is a practical figure for the proposed instrument.)

A block diagram of the instrument is shown in Figure 3-16. The instrument consists of a proton detector, pulse conditioner, proton selection logic, pulse height analyzer, accumulator, data processor, program control, and power conditioner. Particles other than protons (alphas, betas, etc.) will be rejected on the basis of their different rates of energy losses in the detectors when compared to protons. Solid-state circuits available for the electronics assembly have proven ability to sustain high radiation levels without serious degradation in performance.

3. INSTRUMENT SPECIFICATIONS (See Fig. 3-17)

Dimensions:	Length 9"
	Width 8"
	Height 8"
Weight:	7 pounds
Power:	2 watts at 28 volts
Thermal:	$-10^{\circ}C$ to $+60^{\circ}C$
Data:	9 bits/minute, continuous
Mounting:	Aperture toward space, 45 degree field of view, center of field 90 degrees away from sun mission A
Preferred Orbit:	Any mission

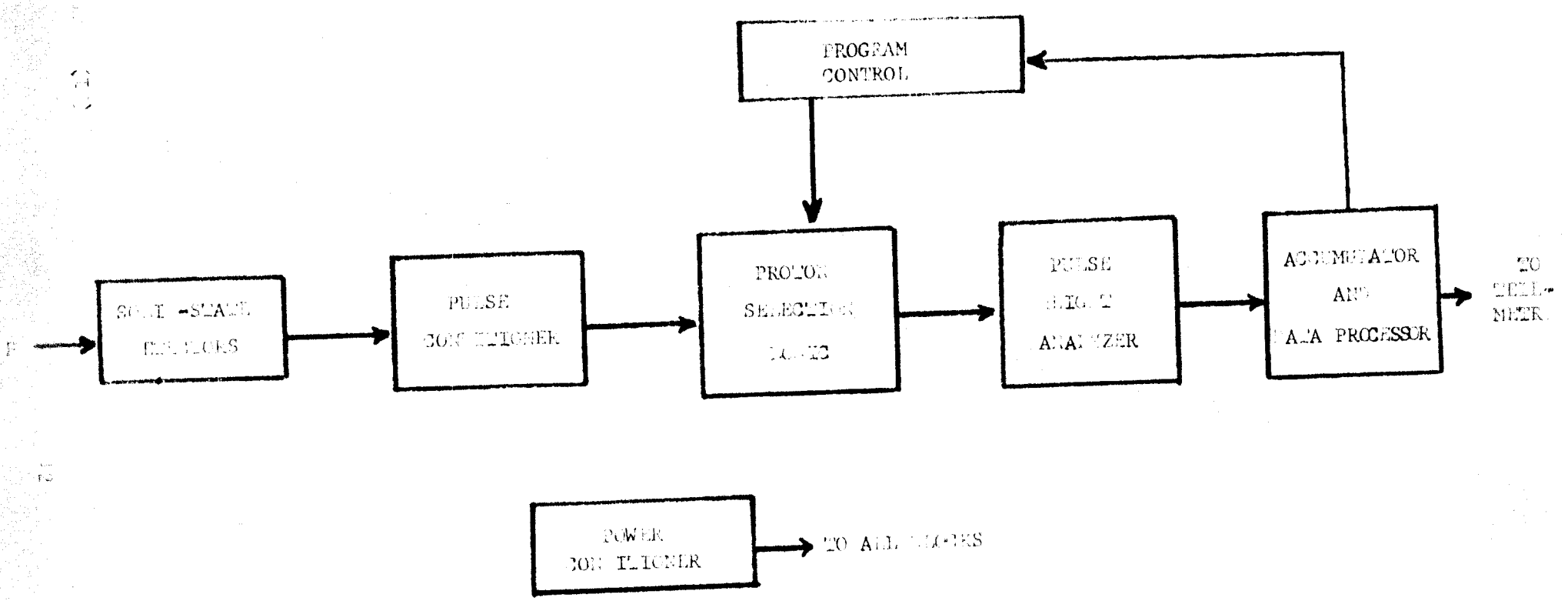

FIG. 3-16 HIGH-ENERGY GALACTIC PROTON SPECTROMETER

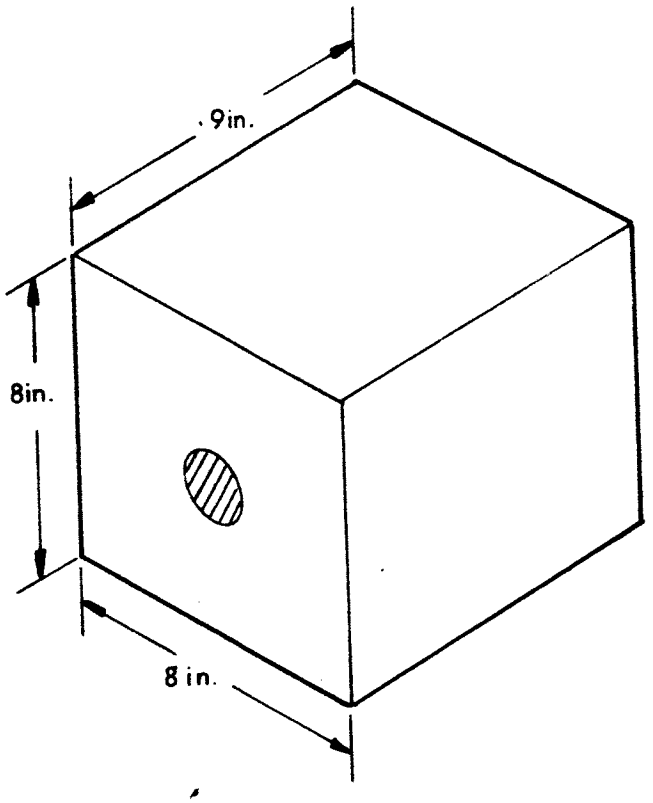

FIG. 3-17 SKETCH OF SPECTRUM & FLUX OF HIGH ENERGY

EXPERIMENT III-I

LOW ENERGY PROTON SPECTROMETRY

WITH DIFFERENTIALLY SHIELDED SOLAR CELLS

1. DESCRIPTION OF EXPERIMENT

A considerable amount of data has been accumulated on proton and electron fluxes in earth space. Such data organized in B-L coordinates have yielded the information necessary to allow construction of a model for the radiation belts.

While the instantaneous nature of counter type nuclear detectors has provided much scientific information it has sometimes led to ambiguity. When particle flux intensities rise to higher than anticipated levels, counters may block. Likewise, the use of instantaneous detectors in radiation environments where rates fluctuate as a function of time, makes the normal averages difficult to obtain.

A crystal dosimeter radiation detector may be used to advantage in certain applications. It has a large dynamic range, extending over four to five integrated flux decades. It provides a measure of the time average of radiation incident upon it (accumulated dose). A convenient embodiment of such a semiconductor crystal dosimeter is the solar cell. Solar cells have become better known in terms of radiation damage history than any other semiconductor device. The use of such devices for dosimetry has certain important advantages.

1. The devices are self powered and do not require an associated power supply.
2. Since the usual rates of damage accumulation are low, the readout requirement is modest, being of the order of a few bits per week.
3. Depending upon the intended mode of operation, the electrical characteristic may be utilized to elicit information about the damaging particle.
4. In certain impedance configurations, the signal is quite insensitive to device temperature.

5. The devices are quite reproducible and can be fabricated sufficiently alike to allow control tests in a laboratory in order to simulate expected space conditions.

Inherent in the advantage of the integrating nature and low bit rate of such solid state dosimeters is the disadvantage that instantaneous flux information cannot be obtained and recorded information will represent a time and space average of the encountered instantaneous particle irradiation.

Frequently the time and space rate of change of fluxes is so rapid that a considerable amount of uncertainty exists about average rates based upon a rapid instantaneous survey. It is therefore submitted that a simple inexpensive dosimeter experiment placed in circular orbits at various altitudes will provide statistically useful information.

Recent experimentation has resulted in the ability to apply inorganic window materials to solar cell surfaces. These window materials are bonded intimately to the surface of the silicon solar cell without any intervening adhesive. The range of thickness achievable varies from less than one micron up to hundreds of microns.

Data from experiments on Explorer XII and Relays I and II have indicated that extremely large fluxes of low energy protons appear to exist in the environment of near earth space. Energy-discriminating particle detectors are the conventional tools for electron or proton spectrometry. They are a part of reasonably sophisticated systems requiring controlled power, exacting environmental conditions (temperature, etc.), and large information storage and transmission capability. In view of these requirements, such detectors are not put on every available vehicle simply because of a cost, weight, and power requirement, although the gathering of additional reliable data would be useful. This experiment seeks to eliminate the sophistication element from the proton dosimeter and thereby make the experiment amenable to every space vehicle in circular orbit. The use of such detectors on a highly elliptical orbit is meaningful from an engineering standpoint

only. The intended energy discrimination comes about through the use of solar cells with differing amounts of shielding on their surface. In this way, it is expected that one may go from 100 KeV protons by the use of a grown SiO_2 layer of 0.9 micron thickness to a proton energy of 2 MeV for a 50 micron thick shield (Figs. 3-18 and 3-19). Higher energy protons will provide a residual background for these devices which is independent of shield absorber thickness. The same holds true for electrons. In the case of electrons, an energy of only 100 KeV is sufficient to penetrate the thickest shield. Since the electron threshold energy for observable damage in silicon is 145 KeV in N type material and 200 KeV in P type, those electrons incapable of penetrating the thickest shield are also incapable of causing damage. The amount of damage resulting from the higher energy electron fluxes should be approximately equal for all specimens and independent of shield thickness.

The radiation damage, due to high energy particles, in silicon solar cells, manifests itself mainly as a loss in short circuit current. The open circuit voltage degradation follows the short circuit current loss reasonably well, especially when the increase in saturation current is accounted for.

In the case of low energy particles, which produce most of their damage very close to the surface, a departure from the above occurs.

The low energy proton damage manifests itself as a relatively rapid drop in cell operating voltage with only a slowly falling short circuit current.

In view of these differing effects, cells for dosimetry would be operated in equal absorber pairs, so that both high impedance and low impedance configurations can be monitored. In a typical experiment, one would fly cells with glass coatings to give the following energy intervals:

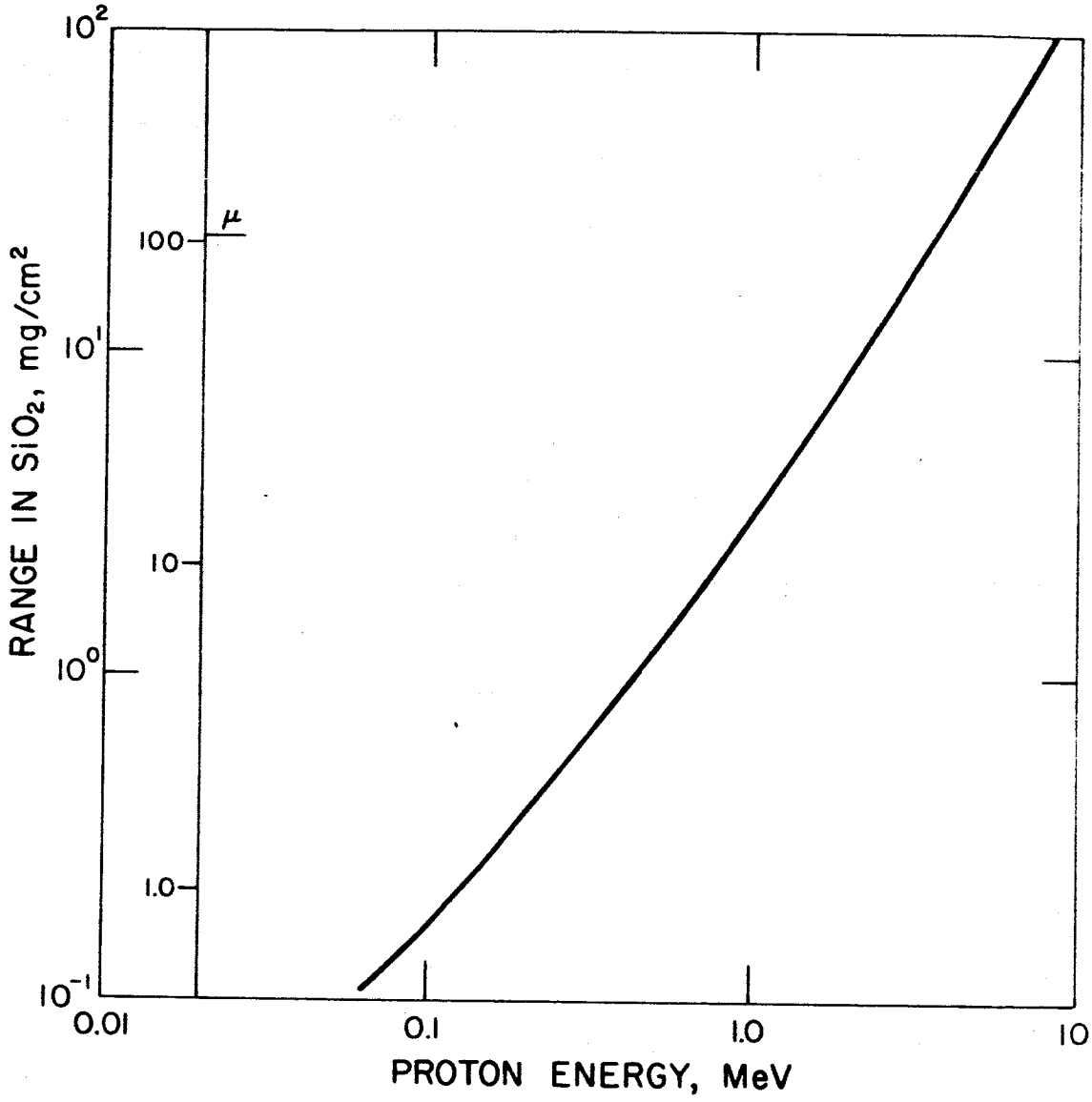

FIG. 3-18 RANGE OF PROTONS IN QUARTZ

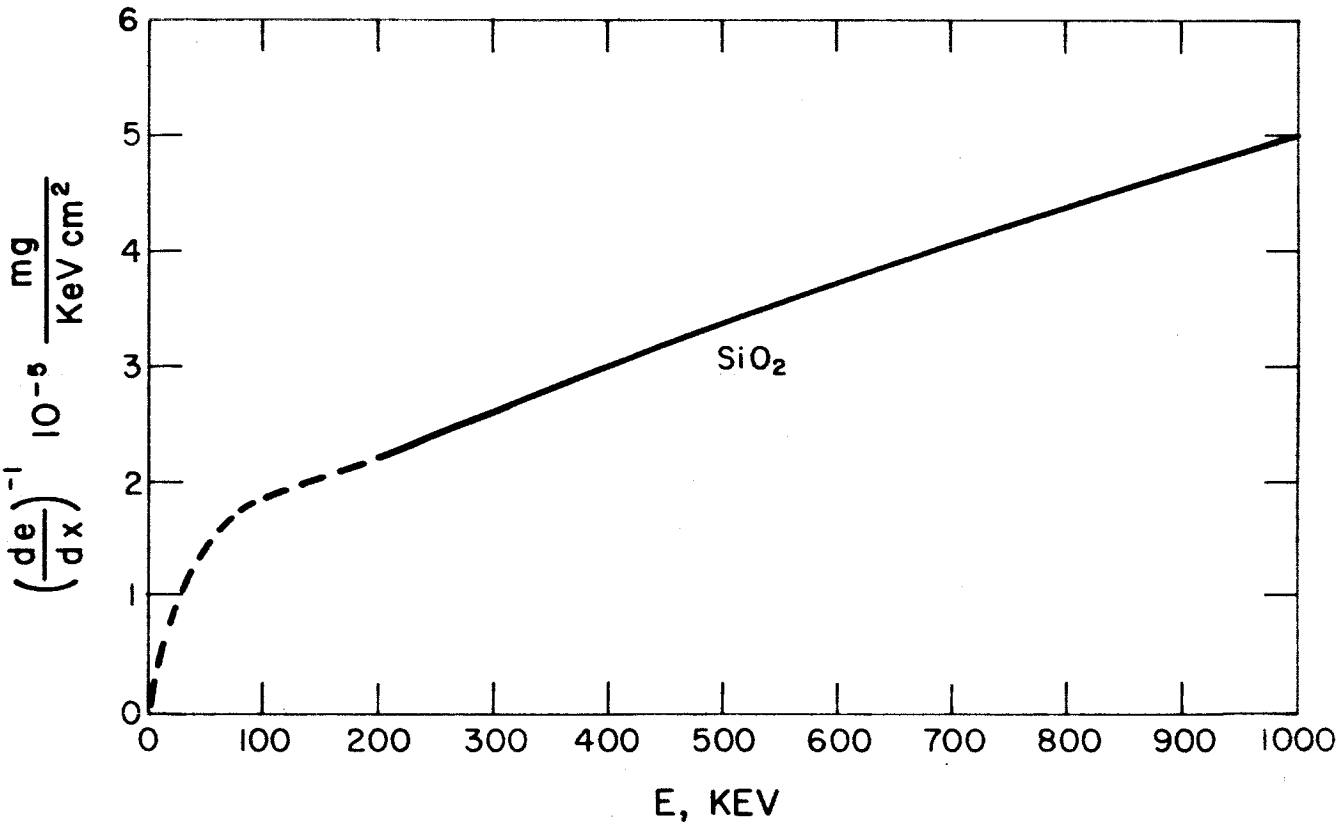

FIG. 3-19 RECIPROCAL STOPPING POWER OF SiO_2 FOR LOW ENERGY PROTONS (after V. J. Linnenbom)

Energy Interval	Glass Shield Thickness
Less than 100 kV	base solar cells
100 to 250 kV	1.0 micron
250 to 500 kV	2.2 microns
500 kV to 1 MeV	5.5 microns
1 MeV to 2 MeV	45 microns

If ample telemetry is available, one would commutate all pairs once per day for a total of 10 telemetry bits per day.

2. DESCRIPTION OF INSTRUMENTATION

In order to finalize experimental parameters, it is necessary to undertake a detailed experimental study assessing the effect of low energy protons with different energy spectra upon solar cells with glass coatings. This experiment will comprise the following steps:

1. The fabrication of 40 cells with dimensions 1 x 1 cm^2 with integral glass coatings of various thicknesses such as

   10 cells with glass shield 1μ thick
   10 cells with glass shield 2μ thick
   10 cells with glass shield 6μ thick
   10 cells with glass shield 25μ thick

2. The design of a proton irradiation experiment to be carried out at a suitable facility. A minimum of 5 cells of a desirable size will be selected from each category and will be subjected to irradiations to proton doses sufficient to cause damage ($\Phi = 10^{11}$ protons). The irradiation will be done with protons of different energies, from 100 KeV to 1-2 MeV; current-voltage plots of cells will be made after each irradiation.

3. The data development in (2) will be analyzed, and the incident proton spectrum will be unfolded from the electrical characteristics. Complete set of cells for flight experiment will be furnished.

3. INSTRUMENT SPECIFICATIONS

Dimensions:	Length 6"
	Width 6"
	Height 0.5"
Weight:	1 pound
Power:	0.2 watt for thermistors for 10 minutes
Thermal:	$-30^{\circ}C$ to $+70^{\circ}C$
Data:	10 bits/orbit
Mounting:	Sun-oriented
Preferred Orbit:	Any

EXPERIMENT III-J

SATELLITE CHARGING AND DISCHARGING CHARACTERISTICS

1. DESCRIPTION OF EXPERIMENT

This experiment is designed to measure the characteristic times required for charging and discharging a satellite to potentials much larger than those associated with ionospheric thermal energies. Pulsed electron and ion guns would supply the charging current, and satellite charge would be measured by a vibrating-piston electrometer or rotating field mill.

By means of Langmuir probes and more complex electrostatic plasma analyzers a considerable amount of data has been amassed[1-4] considering density and temperature of ions and electrons as a function of altitude, local time, solar activity, and other parameters. In many cases the measurements also result in the determination of the potential of the vehicle with respect to the plasma. Potentials of the order of a volt, almost always negative, are obtained. This result is consistent with the measured plasma properties and in qualitative agreement with rough calculations based on kinetic theory. Basically, the satellite charges to a potential such that the net current to the satellite is zero. For most satellite altitudes the most important contributions to this current are made by the ion ram current, the electron and ion thermal currents, and photoelectric current.

---

[1] R.E. Bourdeau, Space Research II, Proc. of International Space Science Symposium (p. 554 (Florence, 1961)

[2] H. Friedman, Proc. of International Conf. on the Ionosphere (London, 1962)

[3] R.C. Sagalyn and M. Smiddy, Space Research IV, Proc. of International Space Science Symposium, p. 371 (Warsaw, 1963)

[4] N.W. Spencer, L.H. Brace, C.R. Carignan, D.R. Taeusch, and H. Niemann, J. Geophysics Research 70, p. 2665 (1965)

When the satellite carries an additional source of current, for example an ion engine or station-keeping rocket with an incompletely neutralized exhaust, potentials corresponding to energies much greater than thermal (about 0.1 eV for the ionosphere) may be produced. There is an upper limit to the satellite potentials which can be produced in this way, for eventually electrostatic forces will reduce the exhausted current to zero. In many instances the equilibrium potential will be much smaller, for the normal current sources will tend to compensate for the "artificial" current.

If a satellite or rocket is charged to a high potential and the source of charge suddenly removed, the vehicle will return to thermal potentials in a time determined by the rate at which electron or ion neutralizing currents discharge it.

Although rough estimates for the magnitude of ram, plasma, and photoemission currents can be made, a detailed calculation of the net available current as a function of vehicle potential is not possible. There are two reasons for this: 1) detailed information on the charge density and velocity distribution, secondary emission coefficients, work function, etc., are often not available; and 2) mathematical complexity, introduced by the complex geometry, vehicle motion, ambient magnetic fields and other factors, precludes a detailed analysis.

The knowledge of satellite potential as a function of current and of satellite discharge times is of some importance on vehicles with potential current sources aboard. High satellite potentials may significantly reduce the efficiency of ion engines, and sustained potentials produced by pulsed sources could affect the operation of instruments and equipment on the vehicle.

Very few measurements of the type envisioned here have been reported. The satellite Explorer 8 carried an electric field mill[5], as well as several plasma probes but had no source of charging current. Rocket measurements by both U.S. and Russian experimenters[6,7] have indicated

[5] R.E. Bourdeau, J.L. Donley, and E.C. Whipple, Jr., NASA TN D-414 (Apr 1962)

[6] R.E. Bourdeau, J.E. Jackson, J.A. Kane, and G.P. Serbu, Space Research, Proc. of International Space Science Symposium, p. 328 (Nice, 1960)

[7] I.M. Imyanitov, G.L. Gdalevich, Ya. M. Shvarts, NASA TT F-8529 (Oct 1963)

field strengths of no more than a few volt/cm, but in several cases it is suspected that plasma currents may have interfered with the measurements. In any case, no correlation with engine charging current is available.

2. DESCRIPTION OF INSTRUMENTATION

The proposed experiment uses an electron gun, ion gun, and electric field meter. The guns are pulsed on for about a second, with fast rise and fall times. The total charge expelled is such as to raise the potential of the vehicle by no more than 1,000 volts (a lower limit for the capacity of the satellite is the free space value), and an acceleration voltage of 5 eV is used. Thus the vehicle potential will have little effect on the gun operation. Electron and ion guns are operated alternately at intervals of about 20 seconds (all estimates of discharge times seem to give results below 1 second). The rise and fall times of the surface electric field strengths, as well as the maximum field strength, are obtained from the output of an electric field meter of the rotating vane or vibrating piston type. If sufficient telemetry bandwidth is not available, some means of sampling the output may have to be provided.

The electronics required include a high-voltage power supply (5 kV at a few microamps), a low-voltage pulser, filament supplies, and amplification and data conditioning circuitry for the field meter. A small gas source with a solenoid-operated valve is required for the gas source. Intermittent operation of the experiment for about 3 minutes at a time is anticipated.

3. INSTRUMENT SPECIFICATIONS

Dimensions:	See Fig. 3-20
Weight:	4 pounds
Power:	10 watts (operating) 0 watts (standing)
Thermal:	$-20^{\circ}C$ to $+60^{\circ}C$
Magnetic:	Fields above 50 gauss must be excluded
Data:	Analog 0 to +5 volts, 100 cps for three minutes
Mounting:	180 degree clear view of space for electron/ ion source; electric field meter flush with spacecraft surface
Preferred Orbit:	Any; moderate additional data available from highly elliptical orbit

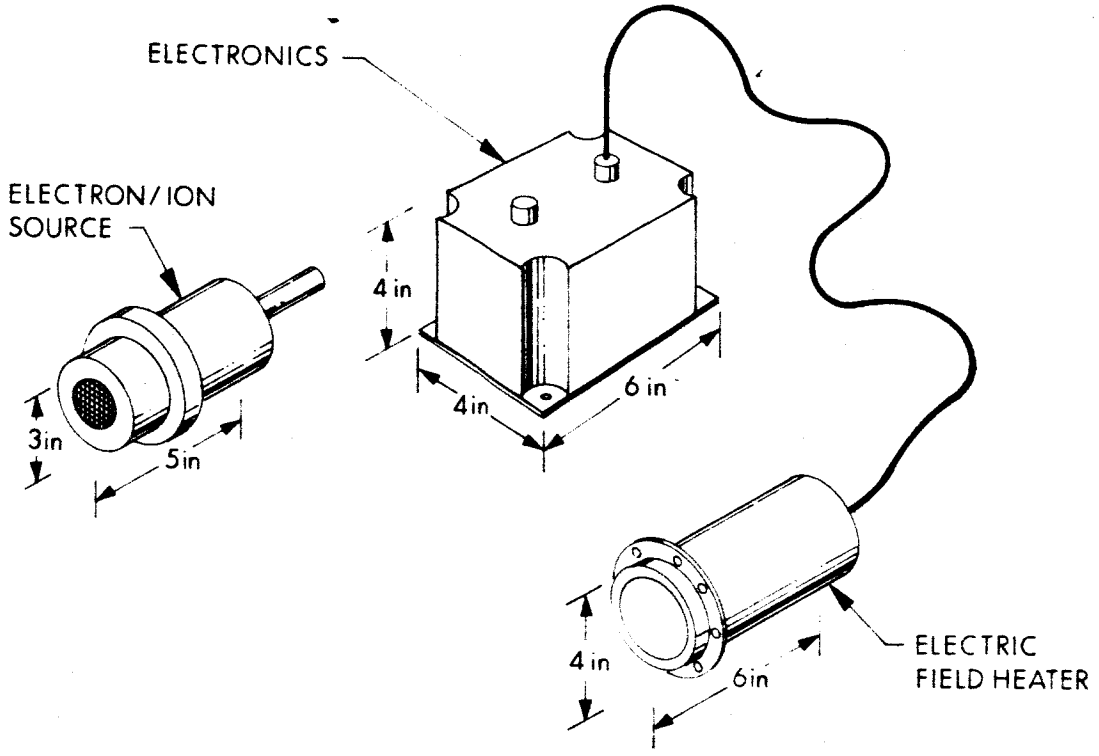

FIG. 3-20 SKETCH OF SATELLITE CHARGE AND DISCHARGE INSTRUMENT

EXPERIMENT III-K

IONIZATION CHAMBER EXPERIMENT

1. DESCRIPTION OF EXPERIMENT

During the past 5 years, many ionization chamber experiments have been flown on space vehicles[1] to measure integrated radiation flux in near and outer space. These experiments have provided valuable scientific data on the radiation environments in space.

The proposed experiment will provide backup data for correlation with other radiation or engineering experiments. Radiations measured will include Van Allen belts, solar flare protons, cosmic rays, and secondary emissions from the ATS spacecraft. The following experiments will profit from ionization chamber data:

(a) Radiation damage investigations

(b) Proton dosimetry

(c) Detection of high-energy galactic gamma radiations

(d) Spectra of galactic electrons

(e) Trapped particle measurements

(f) Spectrum and flux of high-energy galactic protons

(g) Solar flare proton spectrum measurements

A key objective of this experiment will be to measure a broad range of radiation fluxes with an accurate knowledge of threshold energies for protons and beta particles. The ionizing effectiveness of proton and beta particles is a function of shell wall thickness and the internal pressure of the sphere. Thus, for a constant radiation flux density and particle energy, greater ionization will be produced when the walls of the chamber are made thinner and the chamber filler

---

[1] Ranger, Mariner, Pioneer, Explorer, and OGO.

gas density is increased. The ionizing effectiveness of gamma rays is primarily a function of gas density and is relatively independent of wall thickness. Thus all gamma rays will be detected. The minimum energies required for protons and betas to penetrate a shell wall can be easily determined by a simple computation. The thickness constant for the shell material can be obtained for standard materials such as iron[2]. To achieve the desired broad measurement threshold range (e.g., 0.5 to 1000 Mev), five ionization chambers will be required. Because of low ionization current (3×10^{-8} to 1×10^{-14} amperes/second), chamber pressures will vary from 4 to 8 atmospheres of argon.

2. DESCRIPTION OF INSTRUMENT

A quartz-fiber electrometer ionization chamber is the best type of instrument for measuring integrated radiation flux and has been used by many experimenters throughout the world to perform radiation surveys and to monitor cosmic radiation.

The typical chamber consists of a thin stainless steel or aluminum sphere 5 inches in diameter and filled with argon. When the chamber is exposed to ionizing radiations, ion pairs formed within the chamber gas are collected by an aquadag-or platinum-coated quartz collecting rod. This rod is initially charged to a high voltage. As charge is neutralized, the rod potential drops to a preset voltage, the fiber again makes contact with the rod and recharges it. (See Figs. 3-21 and 3-22).

The dynamic range of the instrument is 2 mr/hr to 100 R/hr. Typical threshold energies for one chamber are listed below:

Protons $\geq$ 10 Mev

Betas $\geq$ 0.5 Mev

Gamma rays - all

---

[2] Bethe, "The Ranger-Energy Relations for Slow Alpha Particles and Protons in Air," Review of Modern Physics, Vol. 22, 1950.

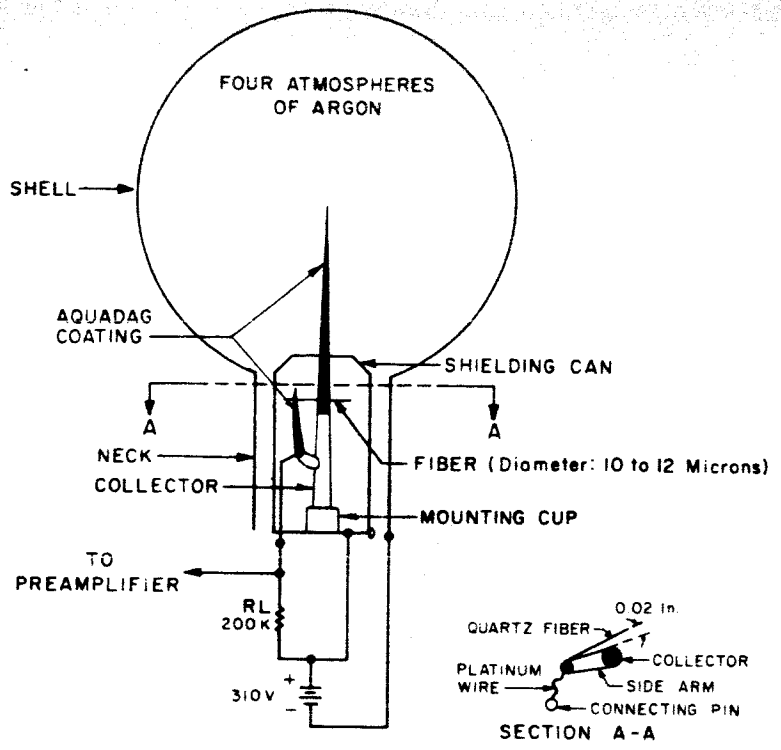

FIG. 3-21

SIMPLIFIED ILLUSTRATION
OF ION CHAMBER

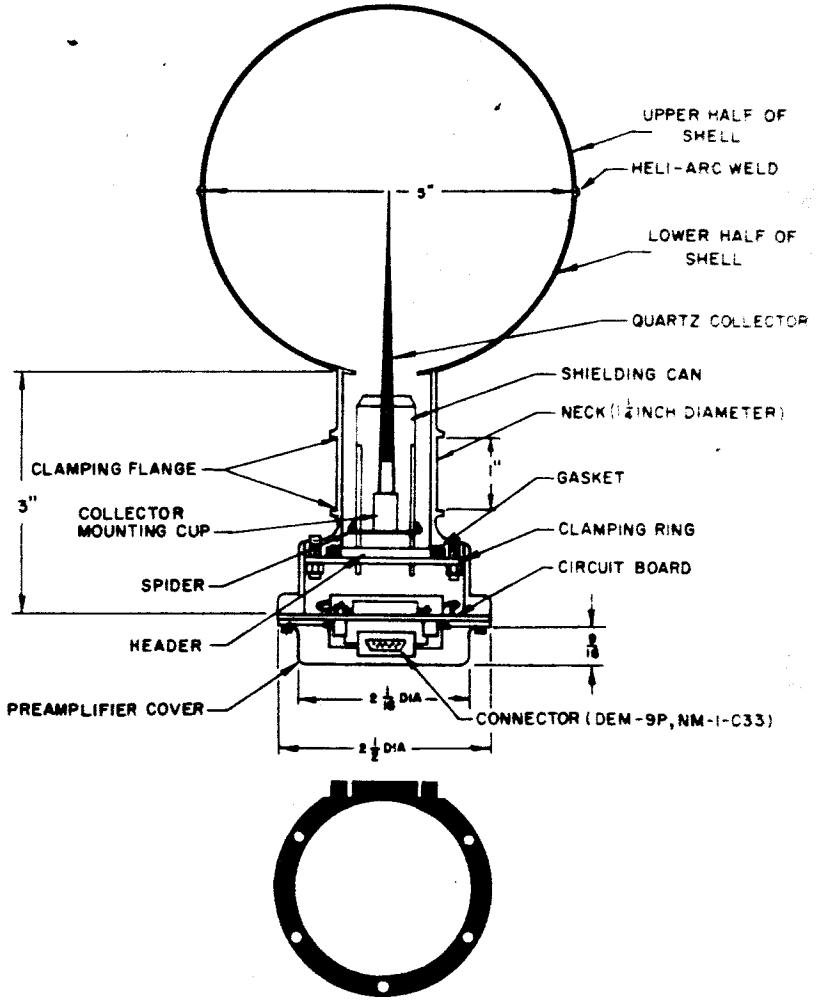

FIG. 3-22

CROSS SECTION OF
ION CHAMBER

The ionization chamber is not susceptible to radiation damage and can withstand launch and space environments. The instrument's light weight (< 1 lb) and low power consumption (< Mw) make it ideal for spacecraft applications.

A possible instrument block diagram is shown in Fig. 3-23. Five chambers with different shell thicknesses for different threshold energies could be used.

The electronics for the experiment is very simple. Signal conditioners, a data control, and power conditioner are the only circuits required. Small-current (10^{-14} μa) preamplifier designs for the signal conditioner are currently available for this application and no new advancements are necessary.

The operating voltages will be 300 Vdc, 12 Vdc, and -112 Vdc generated internally from +28 volts. The unregulated electronics stability will be better than ± 2 percent from -50°C to 150°C, susceptibility to radiation damage is negligible.

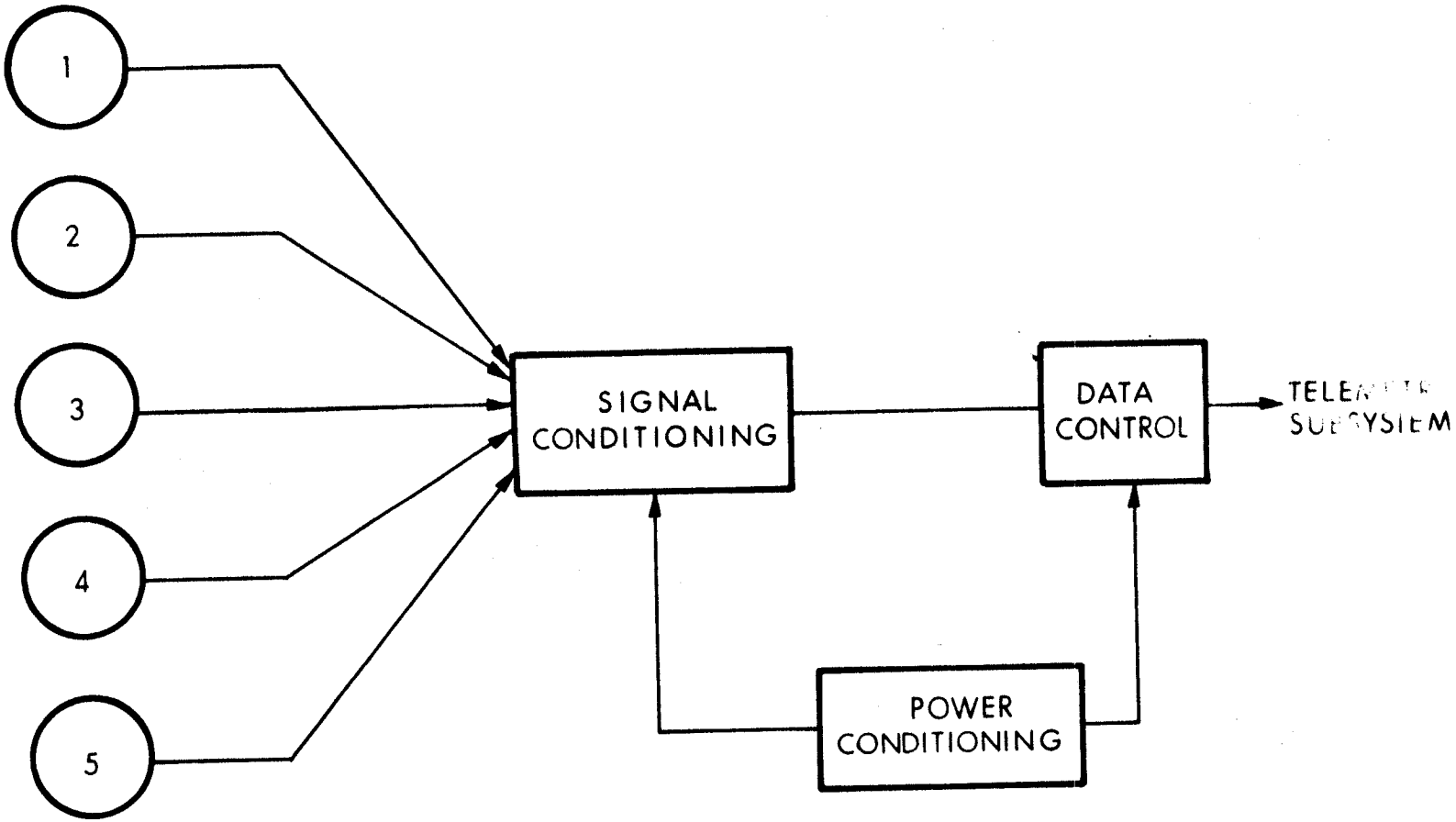

FIG. 3-23 BLOCK DIAGRAM OF ION CHAMBER INSTRUMENT

3. INSTRUMENT SPECIFICATIONS

Dimensions:	
5" diameter x 10" long (each)	
Weight:	6 pounds
Power:	1.5 watt at 28 volts (each)
Thermal:	$-50^{o}C$ to $+150^{o}C$
Magnetic:	< 5 gamma
Data:	100 bits/second continuous
Mounting:	Boom mounted away from spacecraft
Preferred Orbit:	any

IV

PLANETARY ATMOSPHERES

BACKGROUND

The planetary atmospheres discipline covers the research on the atmospheres of the earth, the other planets, and the moon. This section is concerned with the earth's atmosphere.

The study of the earth's atmosphere is primary concerned with the region of the atmosphere above approximately 30 km. Aside from the variations in moisture content, temperature and pressure as altitude increases, a significant departure from the sea level characteristics occurs at about 30 km where ozone becomes important in determining the behavior of this region of the atmosphere. Here, the behavior and characteristics of the atmosphere are determined by a trace constituent not significant at lower levels. The experiment contained herein relates to the characteristics of the earth's ozonosphere.

EXPERIMENT IV-A

MEASUREMENTS OF EARTH ULTRAVIOLET RADIATION FLUX

1. DESCRIPTION OF EXPERIMENT

Ultraviolet radiation, which is reflected or emitted from the earth, will be an information-packed portion of the spectrum and is scientifically interesting.

Because of the nature of the ozonosphere, it is considered most desirable to concentrate the measurements for this particular experiment in the ultraviolet region between 2000 and 3000Å. There are four reasons for this choice. First, the total energy at wavelengths from 0 to 2000Å is less than 0.0002 of the total solar energy, while that between 2000 and 3000Å is some sixty times greater than this. Second, most of the radiation at wavelengths below 2000Å is confined to numerous emission lines, so the spectrum is a line spectrum and requires reasonably high resolution spectrometers for proper measurements. Such sophisticated instrumentation, and the attendant high communication requirement, is outside the scope of that anticipated for this satellite. The spectrum in the 2000 to 3000Å region, on the other hand, is largely continuous, thereby being amiable to meaningful measurements with simple instrumentation. The third reason for investigating the 2000 to 3000Å region is a purely scientific one. Radiation at $3000Å > \lambda \geq 2000Å$ penetrates down in the atmosphere to the ozone layer at altitudes of 30 to 60 kilometers, whereas radiation at the shorter wavelengths is effectively absorbed at the 100 to 150 kilometer altitude. Thus the characteristics of the ozonosphere are observable in the first, but not the second, spectral region.

The objective of the experiment is to measure the intensity of the ultraviolet radiation at selected wavelengths in the 2800 to 3000Å region in order to determine the large scale distribution of atmospheric ozone.

2. EXPERIMENT DEFINITION

The experiment would make measurements of the intensity of radiation in the 2800 to 3000Å region, for a scientific investigation of atmospheric ozone. This type of study has been performed only from a theoretical standpoint, so a successful completion of these measurements would be of basic significance. The instrument, the design of which is outlined below, should provide the necessary data.

3. EXPERIMENT DESIGN

The ultraviolet experiment would consist of:

1. A broadband instrument for measuring the earth-reflected ultraviolet flux. The spectral extent would be through the entire 2000 to 3000Å range as defined by the broadband optical filter. The optical system would consist of a simple objective lens made of quartz, a filter, a Fabre lens, and a photomultiplier tube. The filter could be made of nickel sulfate hexahydride crystal as reported by Childs. The extra transmission window at $\lambda > 3500$Å would be of no consequence if an appropriate detector were selected. The detector could be any one of several photomultipler tubes, such as the ITT FW 157-1 with a fused silica window. A field of view of a 2-1/2 degree, half-angle cone would be reasonable. In order to compute the total flux on the spacecraft components one would have to make a series of measurements as the field of view of the instrument was swept across the earth disc (accomplished mechanically). A burst of twenty measurements

during one 180 degree sweep would furnish the required data, the burst to be repeated once per minute while the satellite is over the sunlit hemisphere of the earth.

3. A narrowband ultraviolet photometer would measure the intensity of the earth-reflected radiation for the purpose of determining the ozone distribution in the atmosphere. This would be a three-channel instrument for measurements of earth-reflected sunlight in thee2800 to 3000Å region. The spectral bandwidth should be of the order of 10Å for each channel, but a definition of the best wavelengths still requires some computations. This instrument also would take a burst of twenty measurements on each channel as the field of view was swept across the disc of the earth (also accomplished mechanically). A one-minute repetition rate would be adequate. Any of the commercially available photomultiplier tubes of high sensitivity in the 3000Å region would be suitable for this type of measurement and many different materials are available for the optical components. Commercial interference filters of 10Å bandwidth in this range are readily available.

On-board calibration of the photometers would be necessary in order to assure interpretable results throughout bhe long lifetime of the experiment. A convenient standard for the broadband channels is a mercury source which emits a strong mercury line at 2537Å. For the three narrowband channels a low-intensity continuum source would be indicated.

4. EXPERIMENT/SPACECRAFT INTERFACE REQUIREMENTS

The interface requirements for the ultraviolet experiment are:

Special Instruments:	1 broadband radiometer, earth-oriented
	1 narrowband multi-channel photometer

Size:	4 in. x 4 in. x 3 in. per instrument
Weight:	Broadband radiometer (earth-oriented)
	1.5 pounds
	Narrowband multi-channel photometer
	2.5 pounds
Power:	3 watts
Data:	250 bits/minute during sunlight earth
Thermal:	$-20^{\circ}C$ to $+60^{\circ}C$
Mounting:	View sunlight portion of earth

The instruments should view the earth, the fields of view being swept across the disc of the earth from horizon to horizon by mechanical means. For purposes of data correlation, the fields of view of both earth-oriented instruments should coincide.

The earth sensing portion of this experiment would be eliminated in the case of a highly elliptical orbit because the large variations in altitude would make it difficult to design an experiment that would yield meaningful data.

EXPERIMENT V

IONOSPHERES AND RADIO PHYSICS

1. INTRODUCTION

The earth's ionosphere is that part of the upper atmosphere which is sufficiently ionized to affect radio waves. For this study, the ionospheres and radio physics is concerned primarily with investigating the nature, origin and behavior of these ionized regions, as well as their influence on radio waves.

The earth's ionosphere is produced by the interaction of solar radiations and energetic particles with the neutral atmosphere. Much progress has been made in establishing the density, temperature, and neutral composition of the atmosphere. Progress has also been made in measuring the flux of the ionizing radiations. For easier reference, the ionosphere has been divided into three regions. In the D-region, 50-85 km, the ion density is low and the collision frequency is high. The E-region, 85-140 km, defines a transition zone in which the ionization rises rapidly with altitude and the collision frequency is still high enough to cause radio-absorption. The highest electron densities occur in the F-region at an altitude of about 300 km. The collision frequencies are too low to cause much absorption and the major effects on radio-propagation are caused by the high refractive index.

The most advances in ionospheric physics have been made in the exploration of the region above the peak of electron density at about 300 km. This was made possible by means of a satellite mounted ionosonde (Topside Sounder), the development of the high powered incoherent backscatter radar, and the direct measurement of electron concentration and ion masses with probes carried in rockets and artificial satellites.

An important result derived from this investigation is the discovery of ionized helium in the upper atmosphere. It was generally supposed that the atmosphere at heights greater than about 300 km consisted of oxygen at the lower altitudes and hydrogen at the higher altitudes. Air density studies from satellites indicated that helium probably was an important constituent. This was later verified by mass spectrometer measurements from satellites.

Many unknowns still exist in the knowledge of the topside of the ionosphere. More knowledge is required on the temperature of the electrons, ions, and neutral constituents. Gaps exist in the knowledge of the densities and composition of the neutral constituents above the F2 maximum.

EXPERIMENT V-A

TOPSIDE SOUNDER

(1000 km or Higher Orbits)

1. DESCRIPTION OF THE EXPERIMENT

The topside sounder experiment is designed to measure the electron density profile of the ionosphere above the point of maximum density at about 300 km. The principle of the measurement is based on the fact that a radio wave incident on a plasma will be reflected if the local plasma frequency $f_p = 9\sqrt{n_e}$, where n_e is the density in m^{-3}, is equal to or greater than the frequency f of the radio wave. Consequently, the distance from a transmitter to a plasma layer of a given density can be determined by measuring the time required to receive an echo when the layer is illuminated with a radio wave with $f \geq f_p$. If the frequency of the radio wave is swept, a plot of echo time vs frequency can be interpreted as a density profile. The density and echo frequency are related by the expression given above, while the altitude is obtained from the echo time by a computer analysis based on the known propagation characteristics of radio waves in a plasma.

When an ionospheric sounder is carried aboard a satellite at high altitudes, the technique described above yields a profile of the ionosphere below the satellite. Since the ionospheric electron density is characterized by a maximum at about 300 km, only the region above that altitude can be studied; any wave of a frequency high enough to penetrate the F_2 peak will also penetrate the plasma below it.

The first topside sounder was designed for the joint U.S.-Canadian Satellite Alouette[1]. Developmental models were first tested on rockets launched from Wallops Island and produced interesting data[2] which could be interpreted as echoes from field-aligned ionization irregularities. The wealth of data obtained from Alouette[3] has already established the topside sounder technique as one of the most valuable for obtaining detailed information on the electron density profile and structure of the upper ionosphere. Of particular interest is the possibility of obtaining cross-sections or "contour maps" of the ionosphere[4] which give a broader picture of its structure than can be obtained by other techniques.

2. DESCRIPTION OF INSTRUMENTATION

A block diagram of the topside sounder is shown in Figure 5-1. A sweep frequency from 2 to 10 Mc is generated by beating a fixed 10 Mc oscillator against a swept 12-20 Mc oscillator. This technique is used to reduce the bandwidth required of the swept oscillator. The 2-10 Mc signal (corresponding to plasma densities from (4.7×10^4 cm^{-3} to 1.18×10^6 cm^{-3}) is fed to a pulsed transmitter. Transmitter pulses of 100 μsec. length are separated by 900 μsec. receiving periods during which the echoes are detected. A complete sweep from 2-10 Mc is completed in 5 sec.

---

1 J. H. Chapman and E. S. Warren in Electron Density Distribution in the Ionosphere and Exosphere (North-Holland, Amsterdam, 1964), p. 307.

2 W. Calvert, T. E. VanZandt, R. W. Knecht, and G. B. Goe, Proc. International Conf. on the Ionosphere (London, 1962), p. 324.

3 J. E. Jackson in Electron Density Distribution in the Ionosphere and Exosphere (North-Holland, Amsterdam, 1964), p. 325.

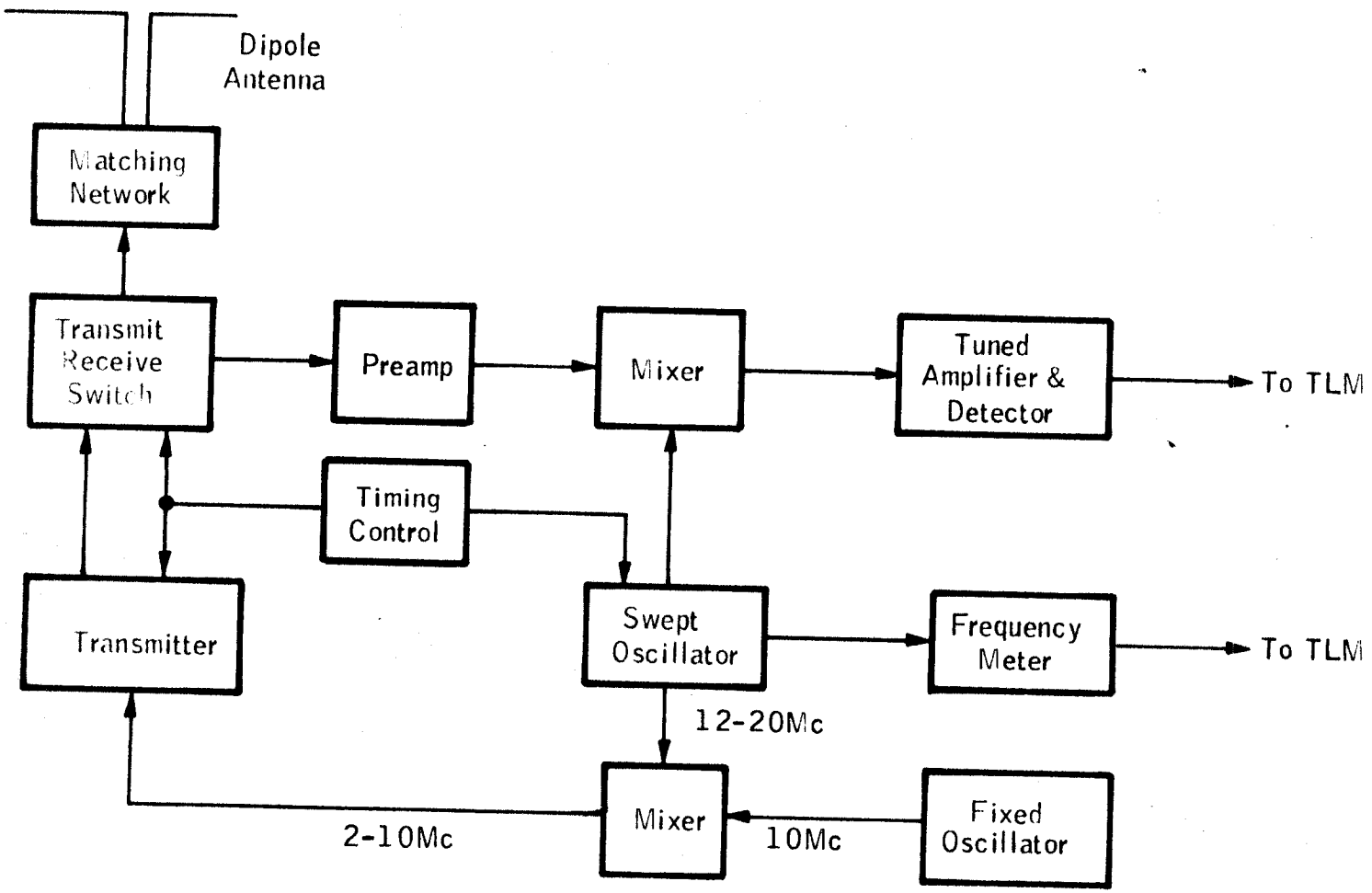
Dipole
Antenna
Matching
Network
Transmit
Receive
Switch
Preamp
Mixer
Tuned
Amplifier &
Detector
To TLM
Timing
Control
Transmitter
Swept
Oscillator
Frequency
Meter
To TLM
12-20Mc
Mixer
Fixed
Oscillator
2-10Mc
10Mc

The transmitting and receiving antenna presents a special design problem in a topside sounder; a reasonable efficiency can be achieved only with a very large antenna. In this case, a dipole antenna 100 feet tip-to-tip will be used. Two retractable steel tubes 50 feet in length extended from the satellite after injection will form the antenna. An even longer antenna was successfully deployed on Alovette, so this does not represent an advance in the state-of-the-art [illegible].

3. INSTRUMENT SPECIFICATIONS

Dimensions: 15" x 6" x 8" electronics
2 deployable 50-foot antennas

Weight: 25 pounds

Power: 15 watts at 28 volts (on 2 minutes)

Thermal: -10°C to +60

Data: 600 bits/second

Mounting: 2 apertures 180° apart for antenna required

Preferred Orbit: 1000 nautical miles modified sun synchronous

EXPERIMENT V-B

INVESTIGATION OF THE COMPOSITION OF THE UPPER IONOSPHERE

1. DESCRIPTION OF EXPERIMENT

Although a vast amount of data on the density, composition, and dynamics of the ionosphere have been collected, relatively little information is available for the regions above 500 to 1000 km. It is proposed to measure the densities of the ionized constituents above 800 km (500 miles) by means of a gridded spherical electrostatic probe used as a mass spectrometer. The measurements will be continued to apogee (40,000 km), thus yielding information over a large part of the magnetosphere.

Measurements of the kind proposed in this experiment have been infrequent because most rockets and satellites are confined to lower altitudes, and the ionosphere above the F region maximum at about 300 km is inaccessible to radio probing from the ground, except for the limited information obtained from the study of whistlers.

It has been suspected for some time that helium must be an important constituent of the upper ionosphere[1]. Using a rocket measurement of the total ion density, Hanson[2] has computed the densities of the various constituents, shown in Fig. 5-2. It will be noted that Hanson's model predicts that He^+ will be the most abundant ion species from about 1000 km to 3500 km, and that H^+ will dominate above 3500 km. Roughly similar behavior is predicted for the neutral composition. The layer of helium is known as the "heliosphere" and the hydrogen-dominated outer region as the "protonosphere". The latter refers to the thermal plasma, not to the trapped proton belts.

A few direct measurements have been made which verify the existence of a layer of He^+ ions. The methods used by Bourdeau, et al.[3] and by Willmore, Boyd and Bowen[4] are essentially the same and involve the identification of the ion mass by measuring the effective kinetic energy they acquire as the result of the satellite velocity. An r.f. mass spectrometer also has been employed[5].

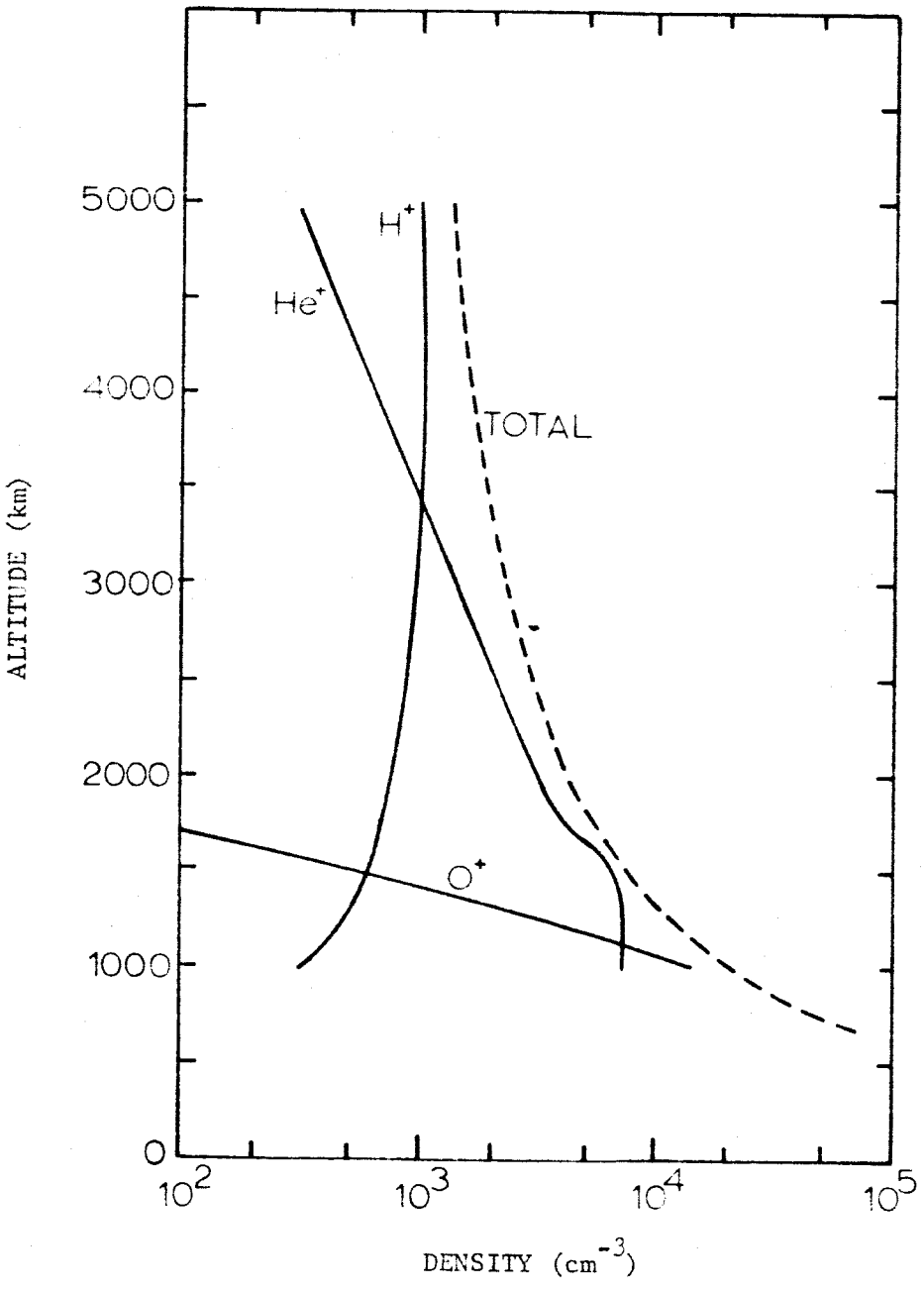

FIG. 5-2 THEORETICAL IONOSPHERIC COMPOSITION (after Hanson)

Relatively little is known about the variations of the densities and boundaries in the helium and hydrogen layers. The data of Williams, Boyd and Bowen shows that the lower boundary of the heliosphere may contract from 950 km to below 650 km at night. Strong variations associated with ionospheric storms have been deduced from whistler observations.[6] Measurements over a long period of time are needed to provide basic data for ion production and recombination calculations.

2. DESCRIPTION OF INSTRUMENTATION

A block diagram of the spherical analyzer proposed for mass spectrometric analysis of the upper ionosphere is shown in Fig. 5-3. The sensor is a spherical grid 4 inches in diameter surrounding a 3.5-inch diameter collector. A constant negative potential is applied to the outer grid so that only the ion currents are measured at the collector. In order to measure the energy spectrum of the ions, a swept positive potential plus a small ac voltage (1 kc) are applied to the collector; the second harmonic of the ac collector current (2 kc) is measured and telemetered to the ground. It can be shown that the 2 kc component of the probe current is proportional to the second derivative of the probe characteristic d^2i_+/dV^2 and that the ion energy distribution f(E) is given by[7]

$$f(E) = \frac{\beta}{2Ae}\left(\frac{m}{e}\right)^{1/2} V^{1/2} \frac{d^2 i_+}{dV^2}$$

where E = eV

e = electronic charge

m = ion mass

A = collector area

β = grid transparency

Now, the ion energy distribution for each species in a frame at rest with respect to the ionosphere presumably consists of a Maxwellian with zero mean velocity. However, in a frame moving with the satellite velocity V_S, the energy distribution for a given species will have a peak at $E_o = 1/2mV_S^2$. The second derivative d^2i_+/dV^2 will, therefore, exhibit

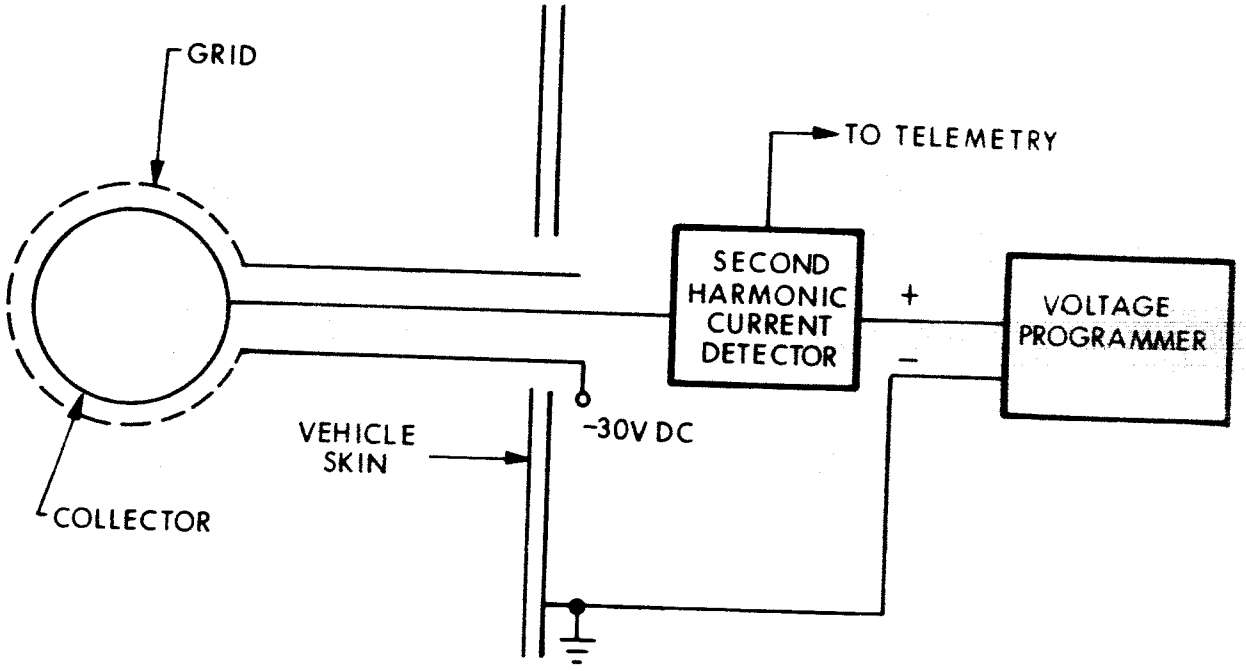

FIG. 5-2 BLOCK DIAGRAM OF A GRIDDED ANALYZER

peaks at energies corresponding to the various ion masses present; the area under the peak is related to the concentration ; and the width, to the ion temperature. This technique has been successfully used (in slightly modified form) on the satellite Ariel[8]. Resolution of the H^+, He^+, and O^+ peaks is readily achieved.

3. INSTRUMENT SPECIFICATION (see Fig. 5-4)

Dimensions: Sensor: 4" diameter; boom mounted
Electronics: 4" x 6" x 6"

Weight: 5 pounds

Power: 3 watts at 28 volts

Thermal: $-30^{\circ}C$ to $+60^{\circ}C$

Data: 200 bits/minute continuous

Mounting: Sensor boom mounted to clear spacecraft

Preferred Orbit: 1000 nautical miles modified sun synchronous or highly elliptical

---

[1] M. Nicolet, J. Geophys. Res., 66, p. 2263 (1961)

[2] W.B. Hanson, J. Geophys. Res., 67, p. 183 (1962)

[3] R.E. Bourdeau, J.L. Donley, E.C. Whipple, and S.J. Bauer, J. Geophys. Res., 67, p. 467 (1962)

[4] A.P. Willmore, R.L.F. Boyd, and P.J. Bowen, Proc. Int. Conf. Ionosphere, 1962, Inst. of Physics and the Physical Society, London, p. 317, 1963

[5] H.A. Taylor, Jr., L.H. Brace, H.C. Brinton, and C.R. Smith, J. Geophys Res., 68, p. 35339 (1962)

[6] D.L. Carpenter, J. Geophys. Res., 67, p. 3345 (1962)

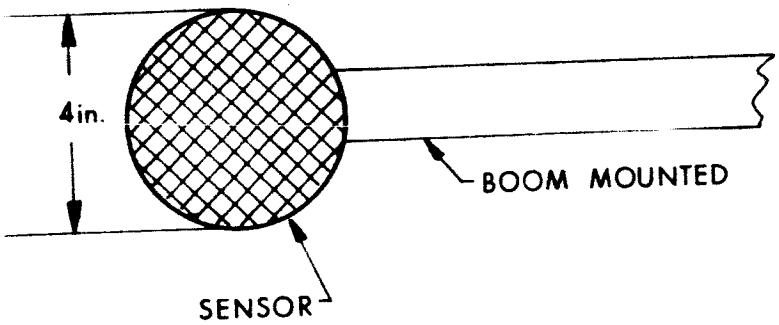

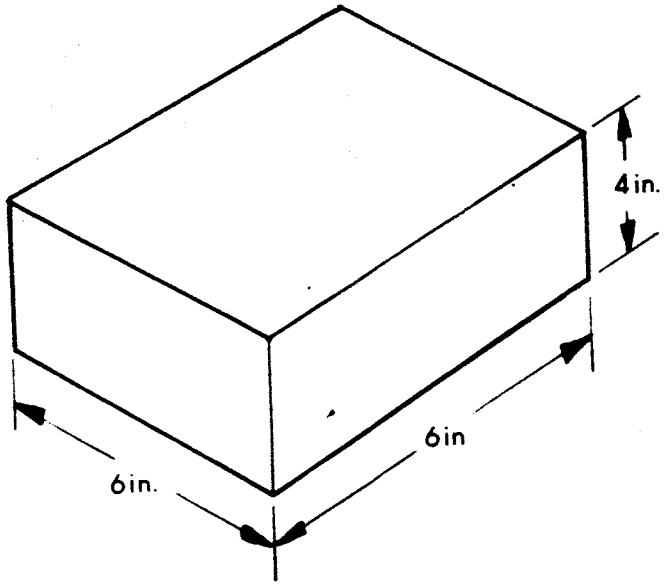

ELECTRONICS

FIG. 5-4 SKETCH OF COMPOSITION OF UPPER IONOSPHERE INSTRUMENT

VI

PLANETOLOGY

1. BACKGROUND

The planetology program is concerned with the condensed material of the solar system: Planets (including earth), moons, asteroids, comets, meteorites, and related objects.

The experiments considered do not pertain to the entire discipline of planetology but were concentrated in the areas of investigation related to the earth, the moon, and micrometeoroids.

EXPERIMENT VI-A

PHOTON EMISSION FROM DARK AREAS OF THE MOON

1. DESCRIPTION OF EXPERIMENT

This experiment is designed to detect and measure light emitted from the dark area of the moon, especially in the UV and IR regions that are inaccessible to earth-based instruments.

Of particular interest is the luminescence sometimes observed during lunar eclipses and the bright spots photographed recently at Pic du Midi by Kopal and Rackham.[1]

To date, the only lunar emissions that have been studied have been the visible luminescence and the IR thermal emission.

2. DESCRIPTION OF INSTRUMENT

2.1 Detectors

The instrument consists of two detectors--one for the UV and one for the IR--each provided with a collecting lens. The UV detector is a photomultiplier with a CsTe cathode and sapphire window which is insensitive for $\lambda > 3{,}000$ Å but responds at shorter wavelengths to ~1,450 Å. The IR detector is a PbS cell with an inherent long-wave limit of 1.3 μ and a short-wave limit set by a filter at 0.7 μ.

As seen from the vicinity of the earth, the whole area of the moon is never dark except during a total solar eclipse; even then, the disc is surrounded by the bright solar corona. The data from a simple photometer aimed at the moon would, therefore, be ambiguous because there would be no discrimination between light originating in the dark area and the reflected sunlight from the bright crescent (or corona during an eclipse). If the photometer is given a scanning motion, however, the time sequence of the readings will enable the data to be interpreted.

---

[1] Sky and Telescope 27, pages 140-141, 1964

The scanning motion will be carried out by means of mirrors placed in the optical system of the detectors. This method requires little power, and the instrument will be completely self-contained.

Neither the photomultiplier nor the PbS cell have stable responsivities, so it will be necessary to include a calibration system. For the PbS cell, the calibration source is a small tungsten lamp operated at reduced voltage. For the photomultiplier, a stable source of UV is needed. A capacitor charged to a carefully regulated voltage of some value near 100 V will periodically be discharged through an argon glow lamp to produce pulses of ultraviolet radiation of constant magnitude.

The lens for the IR region is made of Irtran glass; for the UV region, a sapphire lens transmitting to about 1,450 Å will be used.

2.2 Electronics

The electronics consists of a power supply, signal amplifiers, a programmer, and a calibration system.

3. INSTRUMENT SPECIFICATIONS

Dimensions:	Box 6 by 3 by 2 inches
Weight:	~ 5 lbs
Power:	~ 2 watts, increasing to 3 watts during calibration
Data:	~ 20,000 bits/readout
Magnetic interference:	Instrument not sensitive to such effects; shielded to prevent interference with other systems.
Thermal:	$-20^{\circ}C$ to $+60^{\circ}C$
Mounting:	For maximum effectiveness requires a secondary scanning platform
Preferred Orbit:	Any

EXPERIMENT VI-B

EARTH ALBEDO

1. DESCRIPTION OF EXPERIMENT

This experiment is proposed to measure the albedo of the earth over a wide spectrum extending from the UV into the IR. The spectrum will be divided into three broad bands; in the UV, from ~ 2000 Å to 4000 Å, in the visual from 4000 Å to 7000 Å, and in the IR, from 7000 Å to 3.5 .

No spatial resolution will be attempted, that is, radiation will be accepted from the entire illuminated area of the earth. Since the orbit is polar with its normal pointed at the sun, the satellite will always view a "half-earth" by reflected sunlight, but a "full-earth" by self emission. The self emission will not confuse the results, however, because only ~ .03 percent of its energy is at wavelengths less than 3.5μ, the long-wave cutoff of the instrument.

2. DESCRIPTION OF INSTRUMENT

The instrument consists of three simple telescopes, each having a suitable detector located in the focal plane, as in Fig. 6-1. The three units are mounted in a cluster with their optic axes orthogonal to the spin vector, so that the earth is viewed at each revolution of the satellite (Fig. 6-2). The UV and visual telescopes have fused silica lenses and the IR telescope an Intran lens. The detector for the UV is an EOS UV-sensitive silicon diode. For the visual and IR regions, filtered PbS detectors will be used.

Albedo is by definition a relative quantity, hence, it will be necessary to compare the energy reflected from the earth with that received directly from the sun. This is accomplished by placing a polished bead in front of each lens, as shown in Figs. 6-1 and 6-2. The bead will flood the detector with a small amount of sunlight at

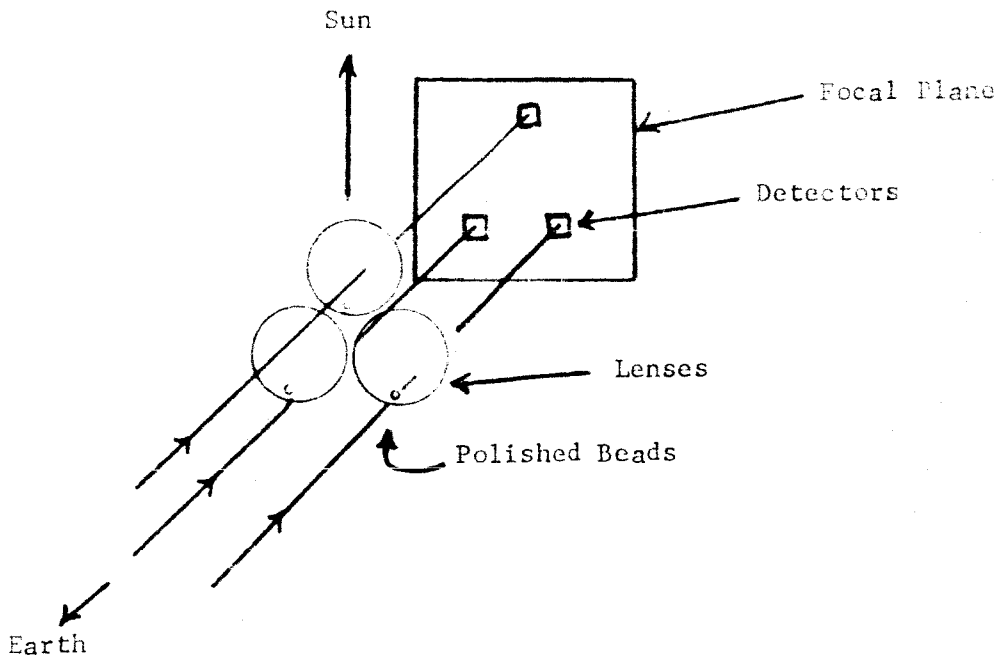

FIG. 6-1 Optical System

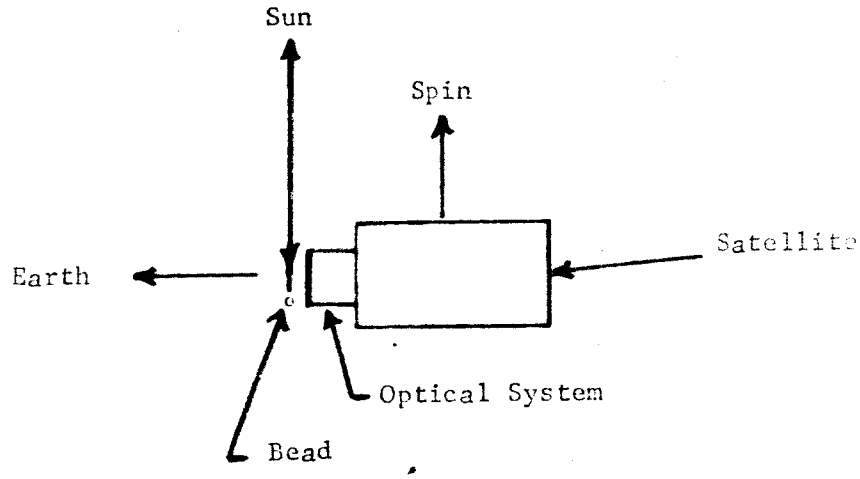

FIG. 6-2 Mounting of Instrument

all times, so that the output signal will be similar to the curve shown in Fig. 6-3. The albedo is found by taking the ratio of the lower signals, V_2 and V_1.

3. INSTRUMENT SPECIFICATIONS

Dimensions:	Optics - 6" diam x 6" long
	Electronics - 1" x 2" x 4"
Weight:	Optics - 1 lb., Electronics - 1 lb.
Power:	1 watt at 28 volts
Circuits:	3 amplifiers, detector biasing circuit, power supply, AD converter.
Thermal:	$-20^{\circ}C$ to $+60^{\circ}C$
Data:	500 bitts/orbit
Mounting:	90° to sun direction
Preferred Orbit:	Any

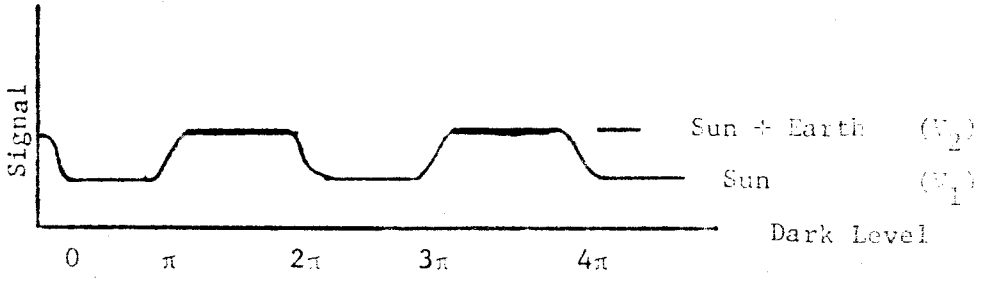

FIG. 6-3 Detector Signal

EXPERIMENT VI-C

ULTRAVIOLET AND INFRARED LUNAR ALBEDO

1. DESCRIPTION OF EXPERIMENT

The purpose of this experiment is to measure the albedo of the moon in the UV and IR regions of the spectrum to which the earth's atmosphere is opaque.

A spectroradiometer orbiting outside the atmosphere would be able to measure the reflected solar radiation without atmospheric interference.

Apart from instrument sensitivity, there is no theoretical short-wave limit to the spectral range, but the long-wave sensitivity must be restricted in order to avoid sensing the moon's self-emission. Fortunately, this is easy to do, owing to the large difference between lunar and solar temperatures. The maximum temperature of the lunar surface is $\sim 400^{\circ}K$, which gives $\lambda max = 7.2\mu$ and an energy at wavelengths less than 3.6μ of only 1 percent of the total emission. On the other hand, only 1 percent of the energy of sunlight is at wavelengths longer than 3.6μ so that, by taking this wavelength as the long-wave limit, the IR albedo could be found with small error.

The short-wave limit is set by the sensitivity of the UV sensors. Two factors act to prevent extending the measurements to extremely short wavelengths; first, the solar energy falls very rapidly for $\lambda < 0.3\mu$; and second, the lunar reflectance of short wavelengths can be expected to be very low. As a result, the reflected energy available to the sensor may be undetectable at wavelengths less than 0.2μ, although no definite limit can be set without further study.

2. INSTRUMENT DESCRIPTION

2.1 Detectors

The instrument will consist of a number of detectors determined by the desired spectral resolution. If only broad-band information were required, two filtered detectors would be sufficient--one in the IR and one in the UV. For the finer spectral detail desired, several detectors will be used and the spectral bands defined by narrow-band filters. Although a single detector provided with a filter wheel would accomplish the same purpose as a multi-detector system, it would require a moving part and is, therefore, not feasible.

Only one detector type is required to cover the range of wavelengths below 4,000 Å. This is the EOS UV-sensitive silicon cell which has high sensitivity to at least 450 Å, and good radiation resistance. It also has a highly stable responsivity so that in-flight calibration would not be necessary.

The IR sensor will be a PbS cell, which covers the range from 0.7 to 3.5 μ. These cells have good radiation resistance but do not have high calibration stability, hence an in-flight calibrator will be necessary. The calibrator would be a small tungsten lamp operating at reduced voltage for improved reliability and life.

Lenses are needed to define the field of view and to collect useful amounts of energy. For the IR region, the lenses will be made of Irtran glass. In the UV region, fused silica lenses are suitable to ~ 2,000 Å; but at shorter wavelengths it will be necessary to use materials such as LiF protected by a sapphire window, or to make the lens itself of sapphire.

2.2 Electronics

The electronics consists of a power supply, sensor amplifiers, a signal commutator (assuming sequential, rather than parallel, outputs), a programmer to control the signal switching and calibration functions.

3. INSTRUMENT SPECIFICATIONS

Dimensions:	Cylindrical can 6 in. diameter by 2 in. long (assumes 7 sensors, each provided with 1.75 in. diameter lens)
Weight:	~ 2 lbs
Power:	~ 2 watts, except during calibration cycle when it increases by ~ 1 watt
Magnetic:	Instrument not susceptible to magnetic interference. Will be shielded to prevent interference with other systems.
Thermal:	$-20^{\circ}C$ to $+60^{\circ}C$
Data:	~ 2000 bits/orbit
Mounting:	For maximum effectiveness requires secondary scan platform
Preferred Orbit:	Any

EXPERIMENT VI-D

PHYSICAL ANALYSIS OF MICROMETEOROIDS

1. DESCRIPTION OF EXPERIMENT

The following experiment has been designed to measure flux density, momentum, and velocity of micrometeoroids.

Micrometeoroids, submicrogram particles of interplanetary matter traveling through space with speeds as high as 70 km/sec, pose questions affecting all vehicles put into space. For example, prolonged exposure to these very small projectiles leads to gradual erosion of the vehicles' outer surface. The particles also cause damage to solar cells and optical instruments. Micrometeoroid storms may prove to be a serious hazard to men operating on the exterior of vehicles such as manned space stations. Certainly, the study of micrometeoroids is a matter of great practical importance, as well as purely scientific interest.

Visual, photographic, and radar tracking of meteors along with various methods of studying meteoritic material reaching the earth's surface, make it possible to formulate a physical theory of meteors. At present, however, these methods of observation are only useful for registering particles with masses larger than 10^{-4} gram. Certainly, the greatest value of these studies is in establishing design parameters for more complete and accurate instrumentation.

The instrument described in this document was developed by Electro-Optical Systems, Inc. for Mr. Paige Burbank, of Manned Spacecraft Center, under Contract NAS9-2787 and consists of a small system of integrated components. By approaching the problem in this manner, no single measurement need be compromised for attainment of another. Furthermore, each component, founded on basic engineering principles, can be accurately calibrated and utilized for direct measurement of particle characteristics. By employing two major components the system will measure flux density, momentum, and both scalar and vector components of velocity of the particles.

2. DESCRIPTION OF INSTRUMENTATION

The instrument consists essentially of a modified ballistic pendulum for particle momentum measurements and a system of thin capacitive foils to determine velocity of the micrometeoroid. Once these two quantities are known, the mass and energy of the particle may be calculated. Large area sounding boards are employed in the instrument system for measurement of radiation flux density. A schematic diagram of the instrument is given in Fig. 6-4. A detailed description of each component is presented below.

2.1 The Ballistic Pendulum

The true ballistic pendulum represents a classical device for determination of projectile momentum. To apply this principle optimally to micrometeoroids in a gravity-free environment, a spring-loaded pendulum is adopted. The theory is best expounded by summarizing appropriate equations. The conservation of momentum when a particle of mass m collides inelastically with a pendulum of mass M is expressed by the relation

$$MV = mv \qquad (1)$$

where V = velocity of pendulum after impact

v = velocity of micrometeoroid before impact.

The initial kinetic energy of the pendulum, after impact, is completely transferred to the spring at maximum deflection. That is

$$1/2\ MV^2 = 1/2\ kX^2 \qquad (2)$$

where k = the spring constant

X = the total deflection of the pendulum.

Equations 1 and 2 can be solved simultaneously for the momentum mv of the micrometeoroid. The result is

$$mv = X\sqrt{Mk} \qquad (3)$$

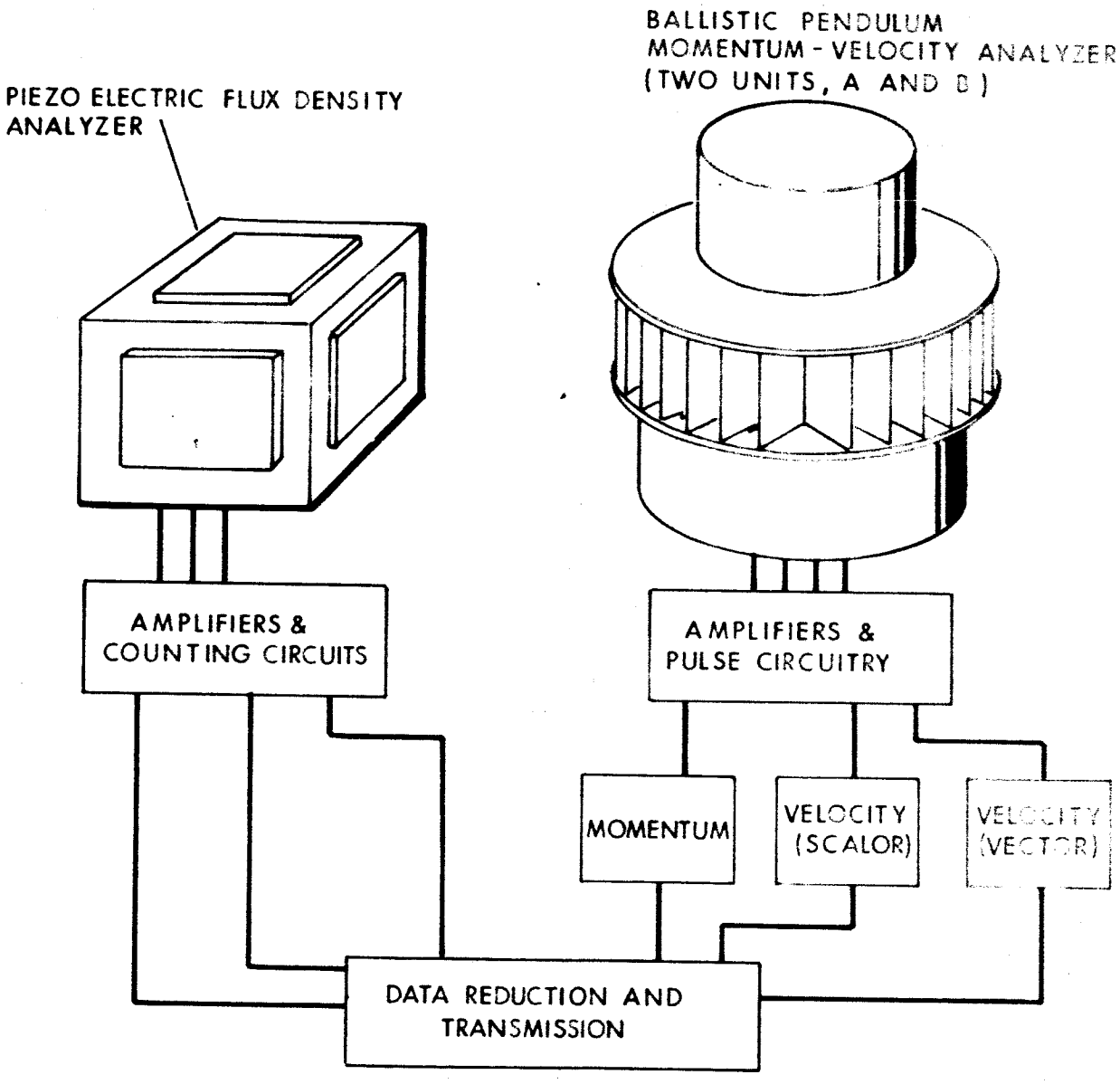

FIG. [illegible] SCHEMATIC DIAGRAM OF MICROMETEOROID INSTRUMENT

[illegible]

19589

We see from Eq. 3 that the deflection of the pendulum is directly proportional to the momentum of the particle. The constant of proportionality involves both the mass of the pendulum and the spring constant of the fiber. Each of these quantities may be measured very accurately in the laboratory.

2.2 Velocity Measurement

The ballistic pendulum is utilized not only for momentum determination but also for the measurement of velocity. It is shown in Fig. 6-5 that the pendulum consists of a particle absorber with a concentric outer ring or bumper. The radial distance between the outer edge of the core and apron represents the transit interval for particle time of flight measurement. By using this scheme, any momentum that might be lost when the particle pierces the outer apron is transferred to the pendulum; thus, accuracy of momentum determination is preserved.

The penetration detectors consist of thin capacitive foils, the first forming the outer apron, the second wrapped around the core of the pendulum. When a suitable voltage is applied across each capacitor, penetration during a hypervelocity event causes a momentary pulse in the electrical circuit. Following the event, the capacitor heals almost instantaneously and the system is ready for the next penetration. Knowledge of the time interval between two consecutive pulses and the distance of separation between the capacitors enables one to find the velocity of the particle.

2.3 The Flux Counter

The flux counter consists of a large-area, ultra-sensitive microphone. Electronic circuitry for this omnidirectional device consists of amplifiers, counters, and an appropriate storage mechanism. Time correlation is planned for the counter and the velocity-momentum detector. At selected times, the information will be transmitted to receivers on earth.

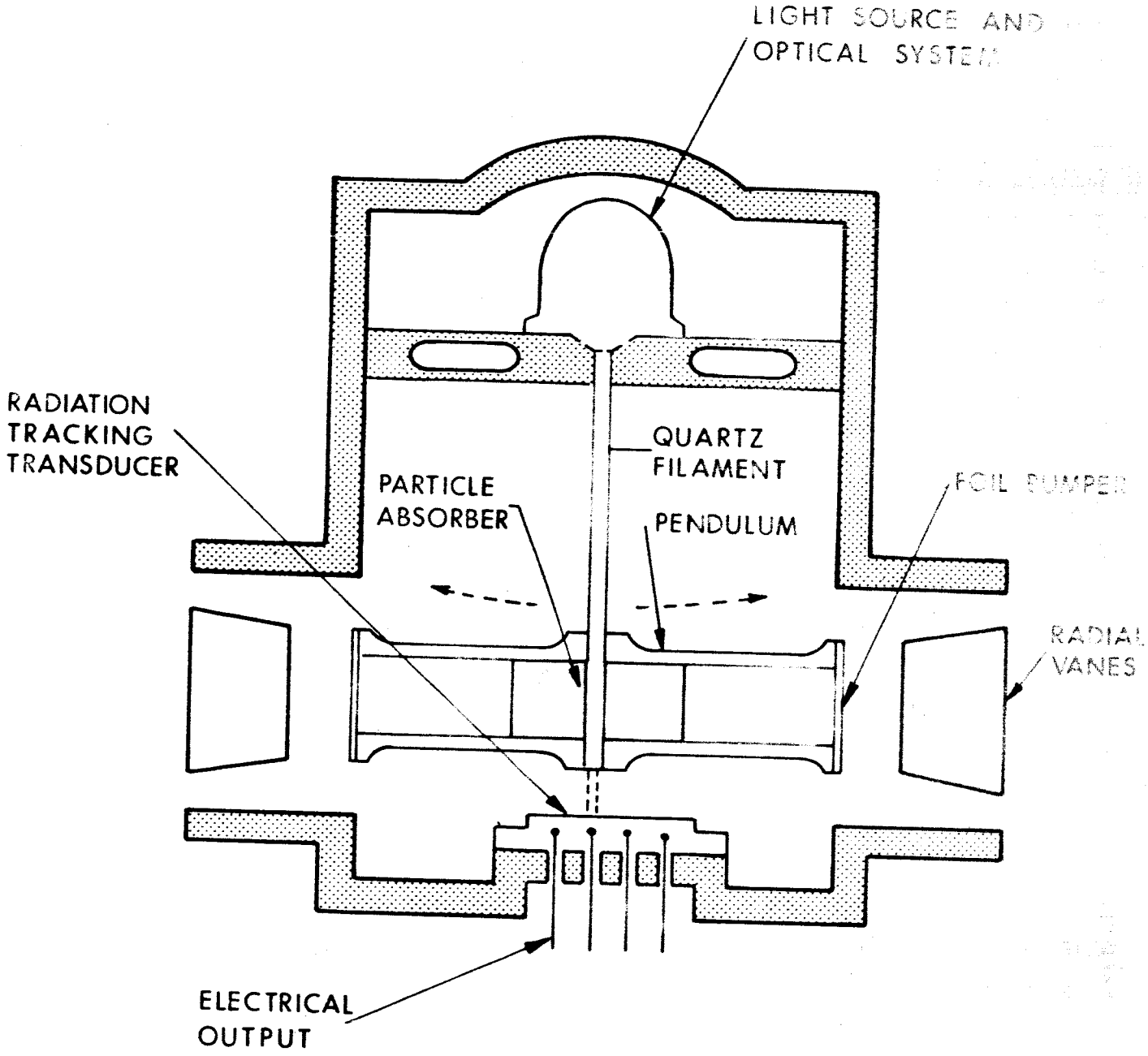

FIG. 6-5 BALLISTIC PENDULUM

3. INSTRUMENT SPECIFICATIONS

The dimensions of the instrument are such that it will fit into a cylinder 10 inches high by 10 inches in diameter. For optimum operation, a 360^{o} viewing port is required.

Input voltage required is 28 V; power requirement, exclusive of data conditioning and transmission, is 2 W. Contribution to the magnetic field of the spacecraft (however small) may be minimized by appropriate shielding.

Transmission requirement will be approximately 10 bits/second.

EXPERIMENT VI-E

EFFECT OF HYPERVELOCITY IMPACTS ON STRUCTURAL SURFACES

1. DESCRIPTION OF EXPERIMENT

1.1 Introduction

The experiment about to be described measures the results of micrometeoroid impacts on spacecraft structures. Briefly, micrometeoroids are small particles of matter traveling through space at "hypervelocity" speeds. They are encountered either as sporadic events or in regularly occurring individual showers. Recent investigations utilizing rocket- and satellite-based detectors have provided sufficient data for the formulation of a cumulative mass-distribution curve and an approximate model of the dynamic properties of micrometeoroids. More experimentation is needed, however, to ascertain the effect of hypervelocity impacts on structural surfaces such as the skin of a spacecraft. This information is basic to the design of all satellites, and especially of manned vehicles operating in a micrometeoroid environment.

A variety of detectors have been developed and flown, with varying amounts of success. These include capacitive-puncture type sensors, microphone impact detectors, fracture-gauge impact detectors, erosion gauges, and photocell-puncture type detectors. Several of these types of detectors will be considered in the proposed program. Looking ahead, however, the large area requirements resulting from present studies suggest pressurized cell and capacitive-puncture type detectors which are readily adaptable to this specific situation.

1.2 Micrometeoroid Properties

The average cumulative-mass distribution curve for interplanetary dust is reproduced in Fig. 6-6.

A summary of micrometeoroid properties pertinent to this discussion is presented in Table VI-1. With reference to Table VI-1, the flux density has been extracted from the cumulative-mass distribution curve,

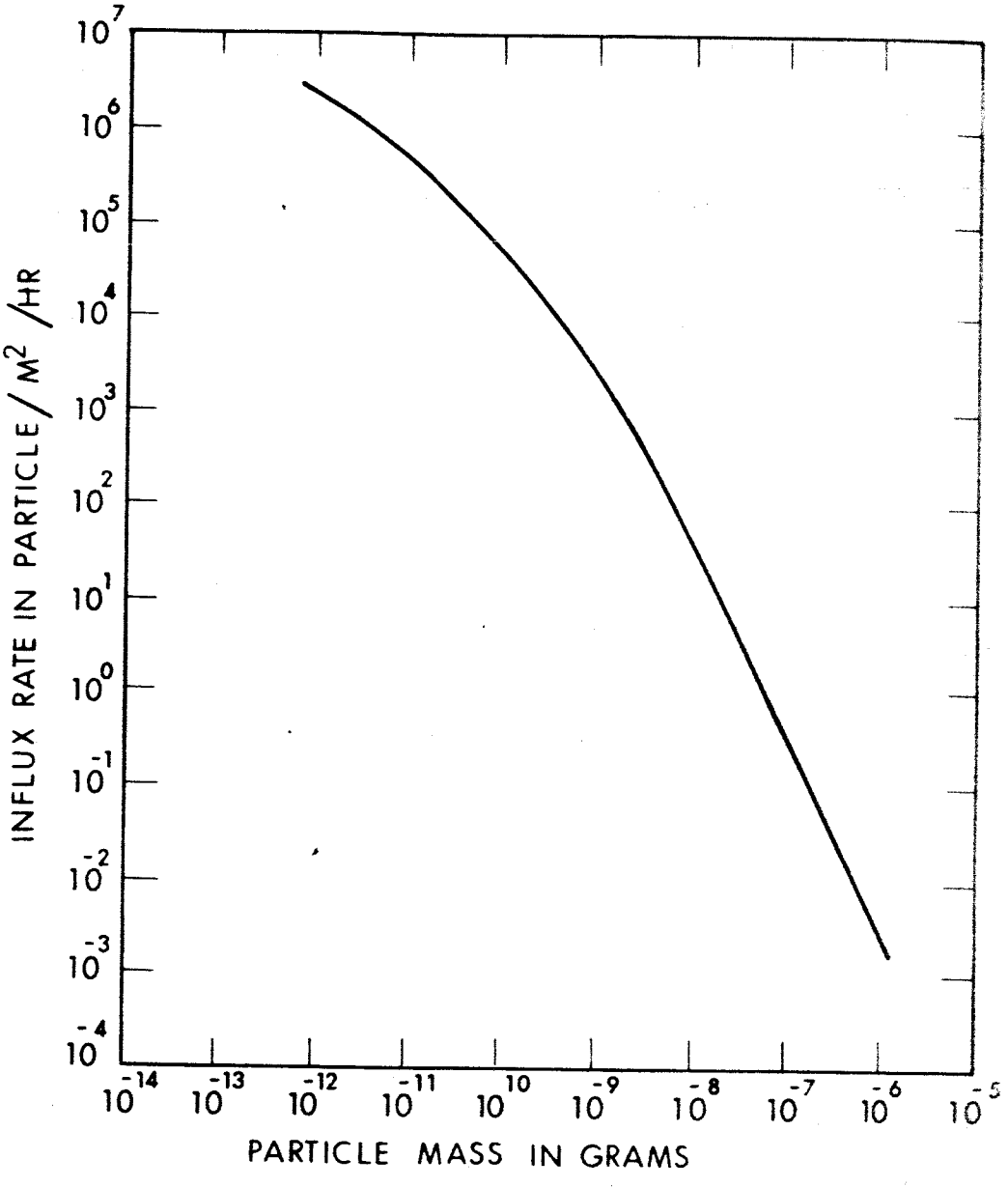

FIG. 6-5 AVERAGE CUMULATIVE-MASS DISTRIBUTION OF [illegible]
DUST NEAR THE EARTH (ADOPTED FROM [illegible]
ACADEMY OF SCIENCES, A. J. J. [illegible]

TABLE VI-1 MICROMETEOROID PROPERTIES AND DETECTOR TYPE

Mass (grams)	Impacts per m^2/hr	Impacts per m^2/yr	Area Required For 10 Impacts per m^2/yr	Approx. Depth of Penetration in Aluminum (mils)	Capacitive Detector	Pressure Cell Detector
10^{-12}	2×10^{6}	17.5×10^{9}			A	
10^{-11}	3×10^{5}	26.4×10^{8}		0.1		
10^{-10}	3×10^{4}	26.4×10^{7}	0.4×10^{-7}			
10^{-9}	10^{3}	8.8×10^{6}	1.1×10^{-6}		↑	
10^{-8}	2×10^{1}	17.5×10^{4}	0.6×10^{-4}	1.0	B	↑
10^{-7}	3×10^{-1}	26.4×10^{2}	0.4×10^{-2}		↑	
10^{-6}	2×10^{-3}	17.5	0.6		C	↓
10^{-5}	10^{-4}	8.8×10^{-1}	11.4	10.0	↑ D	

and the sensor area requirements are based upon a minimum density of 10 impacts per year in each mass range. The approximate depth of penetration in aluminum is also indicated. Various types of detectors will be required to cover the full range of particle sizes, as indicated in the last two columns of Table VI-1. A detailed discussion of the sensors is presented in the following sections.

2. DESCRIPTION OF INSTRUMENTATION

Experimental objectives of the proposed program are listed below in the order of their importance:

1. Penetration rate variation with distance from the earth
2. Impact rate variation with distance from the earth

The primary objective--penetration rate variation with distance from the earth--suggests the use of either pressurized cells with several different wall thicknesses, or the use of large-area capacitive detectors. To realize the advantages of both detector types a combination of the two is recommended for the primary sensor system. Each instrument is described below.

2.1 Capacitive Sensors

In general, the capacitive sensors consist of large-area parallel plate capacitors with the electrodes separated by a thin layer of dielectric material. It is well known that penetration of the charged capacitive sandwich by a hypervelocity particle causes an instantaneous discharge and subsequent healing so that the capacitor is ready for the next event.

The advantages of this type of sensor speak for themselves. Sampling area can be made large for interception of a broad particle-mass range. The capacitive sensor has a long life and, by fabricating in electrically independent segments, high reliability. It is ideally suited to material studies since the specimen electrodes may be formed with a variety of metals of varying thickness.

A major disadvantage of the capacitive sensor is the occurrence of erroneous outputs due to spurious electron discharges. That is, electrons intercepted by the sensor during the course of its mission accumulate in the dielectric. When the imposed potential exceeds the dielectric strength, a discharge occurs which is erroneously recorded as a hypervelocity event. Identification and elimination of unwanted spurious discharges may be achieved through the use of anticoincidence type detectors, radiation monitoring systems or through the use of special discrimination circuits.

2.2 Pressurized Cells

The pressurized cell is an excellent sensor for penetration experiments. In general, the detector consists of pressurized hermetically-sealed zones on the satellite shell with walls of various materials exposed to the micrometeoroid flux. Shell thickness and, hence, depth of penetration is selected on the basis of experimental requirements. The puncture of any particular wall is signaled by a bellows switch located within the cell. In the past, a mixture of nitrogen and helium has been successfully used for the pressurizing medium. The Explorer 16 Micrometeoroid Satellite employed pressurized cells with a minimum shell thickness of 0.001 inch.

Advantages of a pressurized cell are many. Principally, it has a high reliability, is not subject to erroneous results due to noise (such as often occurs with microphone detectors) or to spurious electron discharge (a major drawback of the capacitive system). Although reasonably large sensor areas (several square feet) can be deployed, the pressurized cell array does not have the large-area potential of the capacitive sensor. It is also difficult to produce very thin (fraction of a mil) cell walls--which limits the sensitivity of this device to particles greater than about 10^{-7} grams.

3. INSTRUMENT SPECIFICATIONS

The contemplated system consists of a combination of capacitive detectors and pressurized cells. It is visualized that the large-area capacitive sensors will be mounted on retractable structures and deployed in space, whereas the pressurized cells will be permanently mounted flush with the satellite shell.

3.1 Capacitive Detectors

It is convenient to divide the capacitive detectors into four categories. They are described below.

Category A. This detector unit is designed for detection of penetration by particles of mass less than 10^{-9} grams. With reference to Fig. 6-6, the detector consists essentially of two capacitors mounted on a substrate. Electrode material and thickness are selected in such a manner that penetrations of the first, but not of the second, capacitor are indicative of the desired mass range. Particles penetrating both capacitors are deemed larger than 10^{-9} grams and are not counted. Aluminum 0.3 mil thick has been shown as the specimen electrode. Other metals of appropriate thickness may be used. With reference to Table VI-1, it is seen that the area of the detector may be very small (a few square inches) for the required number of hits during a 1-year lifetime.

Category B. This detector is designed for penetration by particles in the mass range 10^{-9} to 10^{-7} grams. A schematic cross section is given in Fig. 6-8. Except for the thickness of the outer electrode, it is identical to the Category A detector. Again, only particles penetrating the first, but not the second, capacitor are counted. With reference to Table 1, an area of a few square inches is seen to be sufficient for the desired number of hits during a 1-year mission.

Category C. This capacitive detector is designed for penetration by particles whose masses lie in the range 10^{-6} to 10^{-7} grams. As in the earlier cases, two capacitors are used to separate the large particle penetrations from the range of particles desired. In the case of this

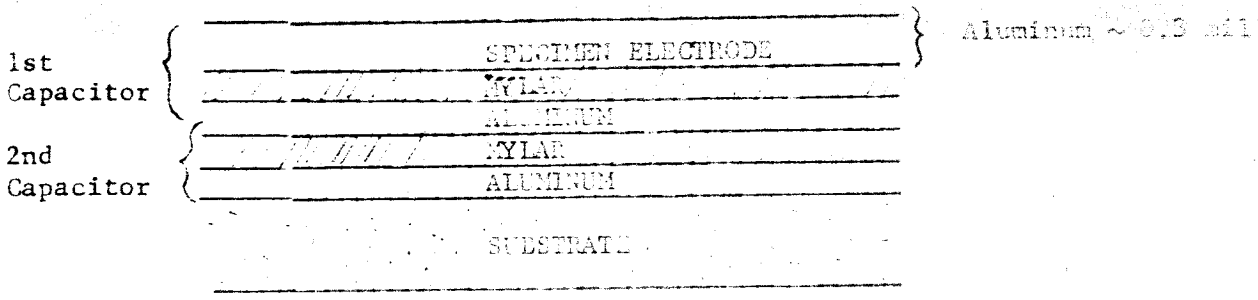

FIG. 6-7 CAPACITIVE SANDWICH, CATEGORY A DETECTOR, PARTICLE MASS ~ 10^{-9} gm

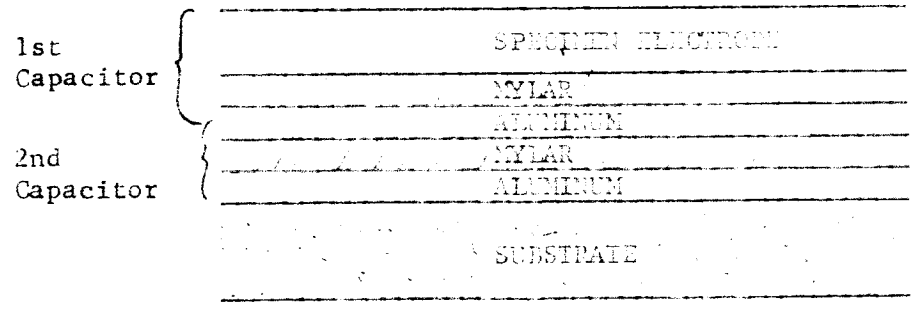

FIG. 6-8 CAPACITIVE SANDWICH, CATEGORY B DETECTOR, PARTICLE MASS 10^{-9} TO 10^{-7} gms

the thickness of the outer electrode will be approximately 3.5 mils. With reference to Table VI-1, the necessary area of the detector is approximately 7 square feet. This is sufficient to ensure at least 10 penetrations during a 1-year lifetime. It is contemplated that the capacitors will be laminated on styrofoam panels of about 1 square foot each.

To prevent misleading results due to spurious electron discharge, a third, very thin (0.25 mil) capacitive sandwich is included as the outermost detector. Coincident discharge in the outer two detectors may thus be used as the criteria for a counted hit. The detector is depicted in Fig. 6-9.

Category D. Due to the exponential nature of the mass distribution curve, the increase in sensor area for a statistically significant number of hits becomes a critical consideration for particles of mass greater than 10^{-6} grams. It is apparent that in the planning of this satellite the desire for a broad range of penetration must be tempered by the cost of deploying large surface areas. Preliminary studies indicate a minimum necessary deployable surface area of 100 square feet.

The Category D detector is illustrated in Fig. 6-10. Except for its large area and greater specimen-electrode thickness, it is similar to the Category C detector. A thin outer capacitive sandwich has been included for elimination of erroneous results, due to spurious electron discharge, by coincidence detection. For the case of an aluminum outer electrode, the metallic thickness is 10 mils. The detector is intended for a mass range 10^{-6} to 10^{-5} grams.

3.2 Pressurized Cell Detectors

Since pressurized cells are not amenable to large area deployment, they will be mounted on the spacecraft bus flush with the outer surface. Each unit in the array consists of a pressurized hermetically-sealed semi-cylindrical cell. Approximately 5 square feet of detector area is recommended.

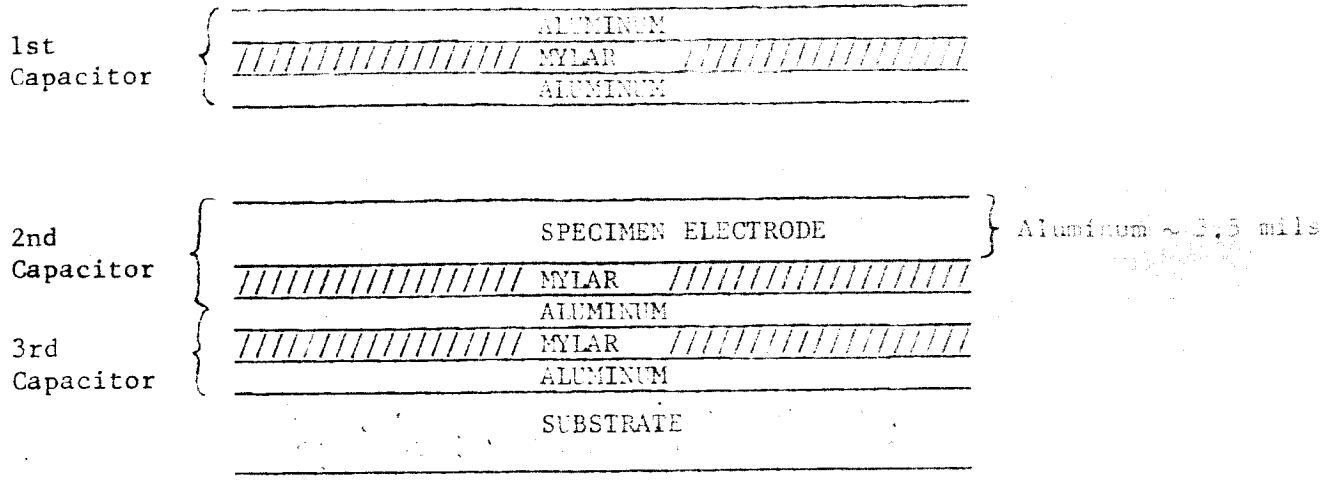

FIG. 6-9 CAPACITIVE SANDWICH, CATEGORY C DETECTOR, PARTICLE MASS 10^{-7} TO 10^{-6} gms. (FIRST CAPACITOR FOR COINCIDENCE DETECTION)

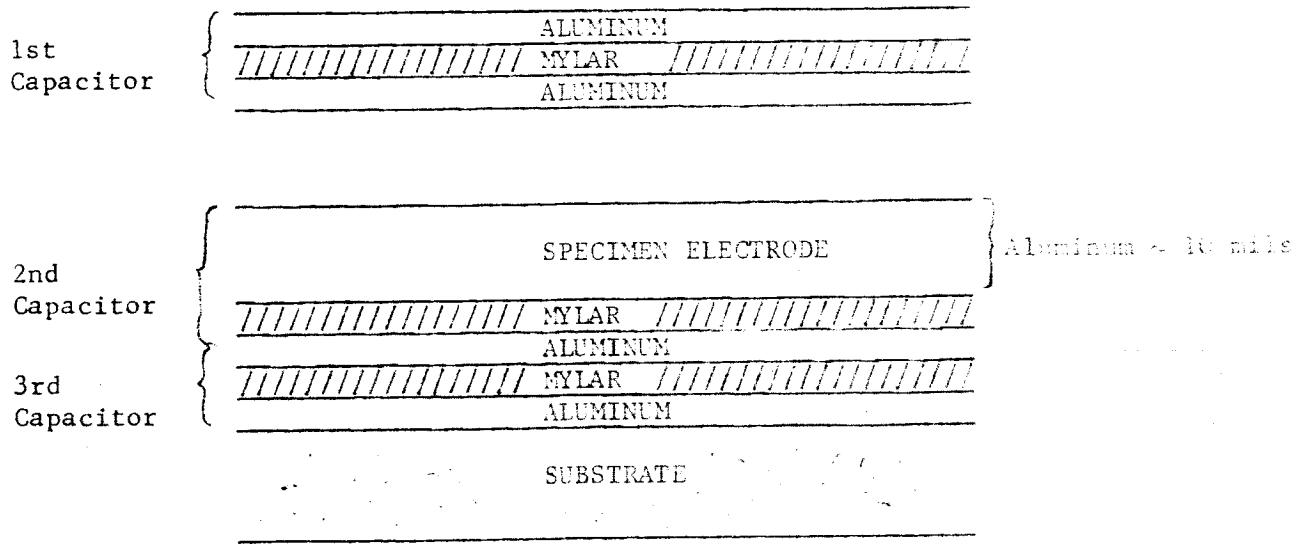

FIG. 6-10 CAPACITIVE SANDWICH, CATEGORY D DETECTOR, PARTICLE MASS 10^{-5} ATO 10^{-6} gms. (FIRST CAPACITOR FOR COINCIDENCE DETECTION)

Several combinations of cell wall material and thickness can be used. With reference to Table VI-1, it is noted that surface area restrictions limit the large particle investigations to about 10^{-6} grams, and minimum thickness considerations (about 1 mil) provide a lower limit for particle mass of 10^{-8} grams. For the case of stainless steel, the wall thickness should not exceed 2 mils, whereas it may be as great as 6 mils for aluminum.

3.3 Instrument System and Electronics

A schematic diagram of the instrument system configuration is shown in Fig. 6-11. The pressurized cells are mounted on the bus flush with the vehicle skin. A total of 32 cells is employed with an exposed surface area of 6 square feet. Category A and B capacitive sandwiches are mounted on the under side of the instrument panels. The total exposed area of these detectors if 750 square inches. Structural and packaging considerations permitting, the Category C detector may be mounted on the under side of the solar panel.

It is anticipated that the pressurized cells will contain helium gas at about 10 psi over atmospheric pressure so that the pressure switch would be closed on the ground, thereby providing a check prior to launch. The switch would open if the pressure in the cell dropped to about 5 psi. The weight of each cell is 0.14 lbs, hence for 32 cells the total weight is 4.5 lbs. An additional 15 lbs of mounting hardware, plugs, and wiring will be required. Approximately 1 volt of electrical potential will be required for the pressure switches with almost negligible power requirement.

The weight of the Category A and B detector system, including hardware mounting, wire and plugs, is less than 5 lbs. This figure is approximately 10 lbs for the Category C detector. The electrical requirements for the capacitive detector system is 45 volts with negligible power requirements.

The electronic package for the entire system will consist of appropriate trigger circuits, counters and storage. It will weigh approximately 3 lbs and require less than 1 watt of electrical power.

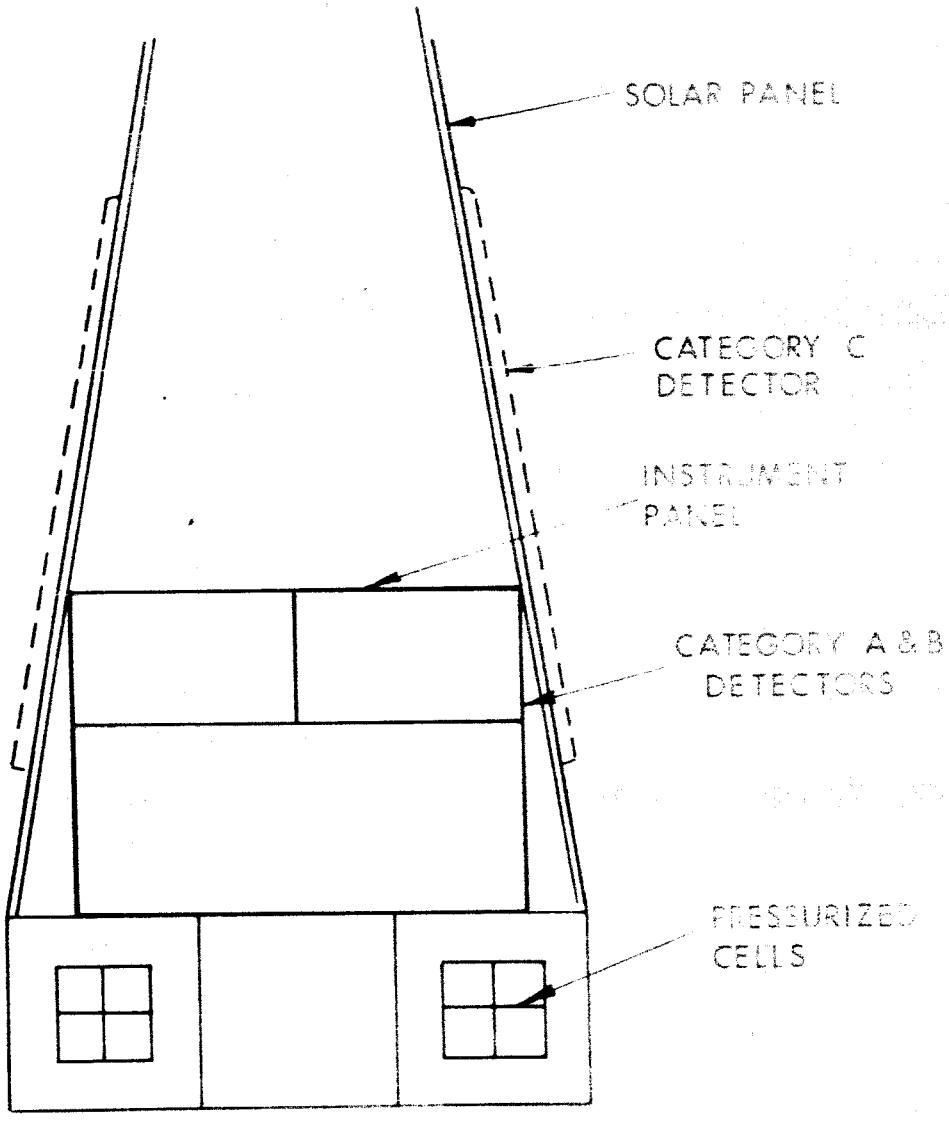

FIG. 6-11 SCHEMATIC DIAGRAM OF [illegible]

EXPERIMENT VI-F

CHEMICAL ANALYSIS OF CARBONACEOUS METEOROIDS

1. DESCRIPTION OF EXPERIMENT

1.1 Introduction

The following sections describe an experiment involving in-situ analysis of carbonaceous meteoroids.

Recent studies of carbonaceous chondrites collected on earth have disclosed similarities between their mass spectra and that of terrestrial hydrocarbons. These results have been interpreted as evidence for the biological origin of meteoritic compounds. However, many sources of possible contamination of museum specimens reduce the possibility of drawing absolute conclusions. Chemical analysis of uncontaminated samples during a space flight mission is thus a necessity, an almost absolute ingredient to the current experimental program.

1.2 Carbonaceous Chondrites

Meteoroids are particles of matter traveling through space at hypervelocity speeds. Although their collective mass may reach millions of tons, the proponderence of particles lies in the range 10^{-12} to 10^{-6} grams. It has been found that most meteoroids fall into two general classes: the stones and the irons. In the stony samples, or aerolites, elements are distributed in much the same ratio as they have been found on earth. Oxygen, silicon, magnesium, and iron predominate. The iron meteoroids, or siderites, however, are usually about 90 percent iron and up to eight percent nickel.

An important subgroup of stony meteoroids are called chondrites because they contain small round bodies, or chondrules. These chondrules consist of the magnesium-iron silicates, olivine and pyroxene. A special variety of chondrites which contained carbonaceous matter were discovered in 1834. An excellent description of these meteorites by Brian Mason[1] is summarized below.

[1] Brian Mason, "Organic Matter from Space", Scientific American, Vol. [illegible], No. 2, p. 43, March 1963

Unlike other meteorites, the carbonaceous chondrites are usually black, friable objects. They are characterized by the presence of an appreciable amount of carbonaceous material other than free carbon. In 1961 a group of investigators discovered a variety of complex hydrocarbons in a carbonaceous meteorite. They found sufficient resemblance between these compounds and those formed on earth by living things to propose the possibility that the meteorite contained products of extraterrestrial life. The volatile fraction of the organic material consisted largely of saturated hydrocarbons (compounds in which all the available bonds on the carbon atoms are occupied by hydrogen atoms). Such compounds are common in ancient terrestrial sediments and petroleum. Mass-spectrometric analysis of solid particles and distillates identified types of compounds, including paraffins and cyclic hydrocarbons, and showed the relative abundance of compounds of different molecular weights in each group. The investigators found similarities between these mass spectra and those of the hydrocabrons in butter and other material of known biological origin.

A serious drawback to all investigations of carbonaceous meteorites collected on the earth's surface is the possible presence of terrestrial contaminants. According to Brian Mason, many of the carbonaceous chondrites are highly porous. As they enter the atmosphere from the near vacuum of space, they must have "breathed in" air and minute floating organisms. Also, the particles may lie on the ground for some time before they are picked up, and then they are generally passed through many hands before reaching a museum collection. In the museum, the meteorites are subject to contamination not only by local bacteria, spores and pollen, but also by exotic organisms carried in with other collections from worldwide sources. Certainly, it would be remarkable <u>not</u> to find a variety of terrestrial microorganism in them.

In summary, the possible existence of extraterrestrial life has been enhanced by promising evidence found in carbonaceous meteorites. Thus far, however, all experimental results have been downgraded to some extent due to terrestrial contamination. The need for further investi-

studies is necessary before present experimental results can be completely assessed. Pertinent consideration to qualitative analysis of meteorites in the aerospace environment will form the remainder of this discussion.

2. DESCRIPTION OF INSTRUMENTATION

2.1 General

The instrument contemplated for in-situ analysis of meteoroids consists essentially of a target plate and a mass spectrometer. Geometric arrangement of these components will permit vaporized particle constituents resulting from meteoroid impact with the target to be sampled and analyzed by the mass spectrometer. In the case of a manned flight laboratory, the mass spectrogram will be available immediately to the crew so that appropriate modification to experimental procedure can be made.

2.2 Target Area

Of the 700 or so meteorites that have been collected after having been seen to fall, only some 20 are carbonaceous chondrites. It is likely, though, that the true abundance of carbonaceous chondrites may be considerably greater since they are very difficult to recognize and are often quickly destroyed by weathering. Hence this ratio, which we shall adopt, should be considered as a minimum.

The average cumulative mass distribution curve for micrometeoroids is given in Fig. 6-6. With reference to this figure it is observed that a target area of 10 sq cm will result in approximately 100 impacts per hour of particles whose mass is 10^{-10} gram or larger. Using the ratio 20/700 for carbonaceous particles, we can expect a minimum of 14 hydrocarbon analysis per hour.

It should be noted that this calculation is based on data for near earth vicinity. For interplanetary flights in deep space, the result may be reduced by a factor of 10^4 or greater.

2.3 Particle Vaporization

It is worthwhile, at this point, to demonstrate that the meteoroid will completely vaporize as a result of hypervelocity impact with the instrument target plate. Since the heat of vaporization of iron is many times that of the hydrocarbon constituents, we select that element for a worse-case analysis.

Iron has a melting point of 1535°C and boils at 3000°C. The specific heat is 0.16 at 1000°C, hence the heat of vaporization is approximately 480 cal/gm or very nearly 2×10^6 joules/kg. The energy E of a meteoroid is given by

$$E = 1/2MV^2 \text{ joules}$$

or

$$E/M = 1/2V^2 \text{ joules/kg}$$

Particle speed lies in the range 10 km/sec to 70 km/sec. For an average speed of 30 km/sec we have

$$E/M = 1/2(30 \times 10^3)^2 = 450 \times 10^6 \text{ joules/kg}$$

which is $450 \times 10^6 / 2 \times 10^6$ or 225 times the energy actually required.

It should be pointed out that the energy released at impact is insufficient for constituent ionization and electron bombardment must be utilized in the mass spectrometer.

2.4 Mass Spectrometer

Many different types of mass spectrometers are available for adaption to space flight instrumentation. These include magnetic deflection, cycloidal focusing, Bennett R.F., the Omegatron, and time-of-flight mass spectrometers. Certain aspects of the time-of-flight mass spectrometer make it especially attractive for this application. It is a lightweight, rugged instrument with reported resolution as high as 1 part in 1000 at all masses. The device has been used with good results in meteorite studies at California Institute of Technology.

In the non-magnetic time-of-flight mass spectrometer, both the electron beam and ion beam are pulsed and all ions with the same charge receive the same energy. The ion bunch created at the beginning of each

cycle is accelerated into a field-free drift space between the source and the detector. Since these ions have a mass-dependent velocity, the lightest ions reach the detector first and are followed in succession by ions of heavier mass. Since no mass scanning is used, the ion signal amplifier needs a wide bandwidth to avoid widening the individual ion peaks and thereby reducing resolution. An ion selector grid system may be placed near the detector. The grid is excited once each cycle, and only ions gaining this extra energy can pass a repeller grid, thus eliminating the wide bandwidth requirements on the amplifier.

3. INSTRUMENT SPECIFICATIONS

A conceptual design of the flight analyzer is given in Fig. [illegible]. The target plate consists of a hemispherical shell of hardened steel. The cylindrical time-of-flight analyzer is positioned on a radius in such manner that the ion source is approximately in the center of the shell. A rigid boom from the spacecraft replaces one of the secondary panels and supports the device and permits a 2π steradian field of view.

It is estimated that the flight instrument will require [illegible] watts of electrical power and the total weight is approximately [illegible] lbs.

VII

BIOSCIENCE

The experiments considered in this discipline placed requirements on the configuration, data handling, telemetry and environmental control subsystems of the spacecraft which is beyond their capabilities in the present configuration. Therefore, no bioscience experiments are contained in the catalog.